ISSN 1408-7073

RMZ – MATERIALS AND GEOENVIRONMENT

PERIODICAL FOR MINING, METALLURGY AND GEOLOGY

RMZ – MATERIALI IN GEOOKOLJE

REVIJA ZA RUDARSTVO, METALURGIJO IN GEOLOGIJO

RMZ-M&G, Vol. 59, No. 1 pp. 1–98 (2012)

Ljubljana, July 2012

Historical Rewiev

More than 90 years have passed since in 1919 the University Ljubljana in Slovenia was founded. Technical fields were joint in the School of Engineering that included the Geologic and Mining Division while the Metallurgy Division was established in 1939 only. Today the Departments of Geology, Mining and Geotechnology, Materials and Metallurgy are part of the Faculty of Natural Sciences and Engineering, University of Ljubljana.

Before War II the members of the Mining Section together with the Association of Yugoslav Mining and Metallurgy Engineers began to publish the summaries of their research and studies in their technical periodical Rudarski zbornik (Mining Proceedings). Three volumes of Rudarski zbornik (1937, 1938 and 1939) were published. The War interrupted the publication and not untill 1952 the first number of the new journal Rudarsko-metalurški zbornik - RMZ (Mining and Metallurgy Quarterly) has been published by the Division of Mining and Metallurgy, University of Ljubljana. Later the journal has been regularly published quarterly by the Departments of Geology, Mining and Geotechnology, Materials and Metallurgy, and the Institute for Mining, Geotechnology and Environment.

On the meeting of the Advisory and the Editorial Board on May 22nd 1998 Rudarsko-metalurški zbornik has been renamed into "RMZ - Materials and Geoenvironment (RMZ -Materiali in Geookolje)" or shortly RMZ - M&G.

RMZ - M&G is managed by an international advisory and editorial board and is exchanged with other world-known periodicals. All the papers are reviewed by the corresponding professionals and experts.

RMZ - M&G is the only scientific and professional periodical in Slovenia, which is published in the same form nearly 50 years. It incorporates the scientific and professional topics in geology, mining, and geotechnology, in materials and in metallurgy.

The wide range of topics inside the geosciences are wellcome to be published in the RMZ -Materials and Geoenvironment. Research results in geology, hydrogeology, mining, geotechnology, materials, metallurgy, natural and antropogenic pollution of environment, biogeochemistry are proposed fields of work which the journal will handle. RMZ - M&G is co-issued and co-financed by the Faculty of Natural Sciences and Engineering Ljubljana, and the Institute for Mining, Geotechnology and Environment Ljubljana. In addition it is financially supported also by the Ministry of Higher Education, Science and Technology of Republic of Slovenia.

Editor in chief

Table of Contents – Kazalo

Original Scientific Papers – Izvirni znanstveni članki

Preliminary notes – Predhodne objave

Review papers – Pregledni članki

Particle swarm based batch filling scheduling

Načrtovanje polnjenja šarž z uporabo rojev delcev

Miha Kovačič[1, 2, *], Božidar Šarler[2]

[1]ŠTORE STEEL, d. o. o., Štore, Slovenia
[2]Laboratory for Multiphase Processes, University of Nova Gorica, Nova Gorica, Slovenia

*Corresponding author. E-mail: miha.kovacic@store-steel.si

Received: December 1, 2011 **Accepted:** March 21, 2012

Abstract: ŠTORE STEEL Ltd faces a problem of production of a huge amount (approximately 1 400) of different steel compositions in a relatively small quantities (approximately 15 t). This production is performed in batches of predetermined quantities (50–53 t). The purpose of this paper is to present the methodology for optimizing the production of predetermined steel grades in predetermined quantities before a customer's set deadline in such a way as to reduce the non-planned and ordered quantities with the date before the deadline and minimize the number of batches. The particle swarm method was used for the optimization. The results of the research have been used in practice since 2006 with reducing the non-planned and ordered quantities from 17.17 % up to 10.12 % since then.

Izvleček: ŠTORE STEEL, d. o. o., se spopada s problemom majhnih naročil (v povprečju 15 t) ter z izdelavo ogromne količine različnih kvalitet jekla (več kot 1 400). Jeklo se izdeluje v šaržah (50–53 t). V članku je predstavljena metodologija za optimiranje izdelave načrtovanih kvalitet in količin jekla v predvidenem roku z namenom, da se zmanjša odlita načrtovana količina jekla, kjer je dobavni rok daljši, kot je določen, ter nenačrtovana količina jekla. Optimizacija je bila izvedena z uporabo rojev delcev. Rezultati raziskave so uporabljeni v praksi od leta 2006, ko sta se v letu 2007 odlita načrtovana količina jekla, kjer je dobavni rok daljši, kot je bil določen, ter nenačrtovana količina jekla zmanjšali iz 17,17 % na 10,12 %.

Original scientific paper

Key words: steelmaking, continuous casting, steel grade, work orders, scheduling, optimization, particle swarm optimization
Ključne besede: jeklarstvo, kontinuirano odlivanje, kvaliteta jekla, delovni nalogi, načrtovanje, optimizacija, optimizacija z uporabo rojev delcev

Introduction

The steelmaking and casting represent basic steel production operations and play a primary role in the downstream steel production. The optimization of the casting batch planning according to the different requirements for chemical composition, ordering dates, casting quantities, etc., is an extremely challenging task. The complexity of batch planning increases with the number of different steel grades and customers' orders.

There is a lack of descriptions of batch filling scheduling in the open literature. Probably the most plausible reasons for this are the non-tendency of manufacturers to expose their well-understood heuristics in order to form production schedules, and the different technology and hardware equipment specifics.[1–3] On the other hand, there are plenty of publications on casting technology and physical modeling available[4–9] at the present.

One of the principal problems in steel production scheduling,[2] consists of determining the scheduling of operations to be performed on molten steel at the production stage from the steelmaking to the continuous casting. A theoretical basis of the time dependent batch scheduling is by the best of the authors' knowledge presented only in.[10, 11] Similarly,[12] explores the scheduling problem between the production and the transportation in a steelmaking shop, in order to minimize the completion time. Paper[13] deals with the schedules for casting of different casting moulds from a number of heats, and[14] deals with the scrap charge optimization problem according to its chemical composition in secondary steel production. The last reference is most probably most relevant with respect to the batch filling scheduling, discussed in the present paper.

To a great extent, at ŠTORE STEEL Ltd. work orders scheduling and related issues have been traditionally carried out by a highly skilled expert human scheduler. The particle swarm method was considered for generation of batch filling schedules in the present paper. During optimization the particles 'fly' intelligently in the solution space and search for optimal batch filling schedules according to the strategies of the particle swarm algorithm. Many different work order schedules were obtained during the optimization.

Work orders scheduling

ŠTORE STEEL Ltd. owns a small (200 000 t per year) flexible steel plant and is one of the best-known producers of flat spring steel in Europe. The company is producing more than 80 steel grades with more than 1 400 different customer-specific chemical compositions.

Customer can order hot rolled or cold finished bars. Purchasing department forwards the order to quality department where customers' delivery terms have been checked. After aproving the delivery conditions the order is processed by production planning department wher technology and delivery deadline is discused. After approving the technology and delivery deadline the purchasing department calculates the prices.

The production planning department assures the working orders for all steps in production chain which starts in the steel plant.

In the steel plant, scrap iron is melted in a 60 t capacity electric arc furnace. The liquid steel is then poured into the ladle (ca. 53 t), which a crane transports to a subsequent ladle furnace, where manganese, chromium, molybdenum, nickel, vanadium and other alloying elements are added to the steel in order to meet the chemical quality requirements.

The molten steel is cast into square billets of dimensions 140 mm or 180 mm in a continuous caster. The billets are reheated afterwards and the steel bars of various shapes and dimensions are manufactured by means of hot rolling and finally according to customers' orders, heat treated, peeled, drawn or grinded.

The production of steel at ŠTORE STEEL Ltd. is usually deliberately cast for a pool of 384 customers. The mean cast quantity is 14.32 t (standard deviation 23.77 t). Due to the constraints posed by the production, some extra cast steel is produced on top of the ordered cast quantity. This is denoted as a non-planned cast quantity.

Structure of the work order

The work orders for batch processing are generated based on the customers' orders. A typical structure of work orders is presented in Table 1.

The work order number is a sequential number. The cover quality prescription and the work order chemical limitations define the chemical composition of the related batch.

Each quality prescription has also its own steelmaking technology (i.e. times, temperatures, sampling, purging, oxygen activities). There are, in general,

Table 1. Work order example

Work order number: 0001019			
Cover quality prescription code	Chemical limitations in mass fractions, *w*/%		
732.59.2	*w*(C)/% = 0.52–0.54; *w*(P)/% = 0.015(max.) *w*(Sn)/% = 0.02 (max.); *w*(As)/% = 0.04(max.)		
Quality prescription code	Customer order code	Ordered quantity t	Delivery date
732.54.2	0000855022	25	30. 1. 2009
732.01.0	0000937001	3.5	8. 11. 2009
732.59.2	0000855007	1.5	30. 1. 2009
732.59.2	Non-planned cast quantity	23	

two groups of steelmaking technologies: the first, for the extra-machinability steels[15], where the batch weight is 50 t, and the second, for the other steel qualities, where the batch weight is 53 t. In the extra-machinability steelmaking technology, the molten steel in the ladle is more reactive, so the molten steel quantity (batch weight) should be smaller.

Tables 2, 3 and 4 show three sample quality prescriptions (732.00.1, 732.59.2, 732.54.2) and their calculated chemical limits. Chemical limitations are calculated according to the quality prescriptions limits and simple rules presented in Figures 1 and 2. If the chemical aim value for the chemical element is prescribed in the quality prescription, it means that the ladle furnace operator has to obtain the exact chemical weight percentage of the element. The internal minimum and maximum are prescribed according to the technology procedure. The batch satisfies the customer's chemical requirements if the chemical weight percentage is within the customer's limits (minimum and maximum). The customers' set chemical limitations are because of the technology limitations and rules converted to internal composition limits in order to assure the customer set specifications. The briefly described rules dictate that the in plant chemical limitations are narrower than the set customers' chemical limitations.

In fact, all three of the quality prescriptions presented, fit into the chemical composition of 50CrV4 (W. NR. 1.8159) spring steel. For example, at the moment there are 53 quality prescriptions for 50CrV4 steel existing in the company, and it is not possible to chemically combine all of them.

Table 2. Quality prescription 732.01.0 and its calculated chemical limits (minimum and maximum)

Quality prescription 732.01.0						Calculated chemical limits	
Element	Customer minimum	Internal minimum	Aim	Internal maximum	Customer maximum	Quality prescription limits – minimum	Quality prescription limits – maximum
	w/%	*w*/%	*w*/%	*w*/%	*w*/%	*w*/%	*w*/%
C	0.47	0.50		0.53	0.55	0.47	0.55
Si	0.15	0.20		0.35	0.40	0.15	0.40
Mn	0.70	0.80		1.00	1.10	0.70	1.10
P				0.015	0.025	0	0.025
S				0.020	0.025	0	0.025
Cr	0.90	1.00		1.10	1.20	0.90	1.20
Mo				0.05	0.08	0	0.08
Ni				0.25	0.30	0	0.30
Al		0.010	0.011	0.015	0.100	0.010	0.015
Cu				0.25	0.40	0	0.40
V	0.10	0.14		0.17	0.20	0.10	0.20
Sn				0.030		0	0.030
As						0	100
N						0	100

Table 3. Quality prescription 732.54.2 and its calculated chemical limits (minimum and maximum)

Quality prescription 732.54.2						Calculated chemical limits	
Element	Customer minimum	Internal minimum	Aim	Internal maximum	Customer maximum	Quality prescription limits – minimum	Quality prescription limits – maximum
	w/%	*w*/%	*w*/%	*w*/%	*w*/%	*w*/%	*w*/%
C	0.49	0.50		0.52	0.54	0.49	0.54
Si	0.20	0.20	0.34	0.35	0.40	0.20	0.40
Mn	0.90	0.91		1.00	1.10	0.90	1.10
P				0.015	0.015	0	0.015
S				0.015	0.015	0	0.015
Cr	0.90	0.91		1.00	1.20	0.90	1.20
Mo				0.04	0.08	0	0.08
Ni				0.10	0.20	0	0.20
Al	0.010	0.010	0.011	0.015	0.025	0.010	0.025
Cu				0.25	0.25	0	0.25
V	0.10	0.11		0.14	0.20	0.10	0.20
Sn				0.015		0	0.015
As				0.035	0.040	0	0.040
N						0	100

Table 4. Quality prescription 732.59.2 and its calculated chemical limits (minimum and maximum)

Quality prescription 732.59.2						Calculated chemical limits	
Element	Customer minimum *w*/%	Internal minimum *w*/%	Aim *w*/%	Internal maximum *w*/%	Customer maximum *w*/%	Quality prescription limits – minimum *w*/%	Quality prescription limits – maximum *w*/%
C	0.51	0.52	0.52	0.55	0.55	0.52	0.55
Si	0.25	0.25	0.34	0.35	0.40	0.25	0.35
Mn	0.95	1.00	1.00	1.10	1.10	1.00	1.10
P				0.015	0.020	0	0.020
S				0.008	0.008	0	0.008
Cr	1.05	1.10	1.10	1.20	1.20	1.10	1.20
Mo				0.05	0.06	0	0.05
Ni				0.20	0.20	0	0.20
Al		0.010	0.011	0.015	0.040	0.010	0.015
Cu				0.25	0.25	0	0.25
V	0.10	0.15	0.16	0.18	0.25	0.15	0.18
Sn				0.025		0	0.025
As						0	100
N				0.016		0	0.016

Table 5. Batch chemical limitations

	Quality prescription 732.01.0 limits *w*/%		Quality prescription 732.54.2 limits *w*/%		Quality prescription 732.59.2 limits *w*/%		Batch chemical limitations *w*/%	
Element	Minimum	Maximum	Minimum	Maximum	Minimum	Maximum	Minimum	Maximum
C	0.47	0.55	0.49	0.54	0.52	0.55	0.52	0.54
Si	0.15	0.40	0.20	0.40	0.25	0.35	0.25	0.35
Mn	0.70	1.10	0.90	1.10	1.00	1.10	1.00	1.10
P	0	0.025	0	0.015	0	0.020	0	0.015
S	0	0.025	0	0.015	0	0.008	0	0.008
Cr	0.90	1.20	0.90	1.20	1.10	1.20	1.10	1,2
Mo	0	0.08	0	0.08	0	0.05	0	0.05
Ni	0	0.30	0	0.20	0	0.20	0	0.20
Al	0.010	0.015	0.010	0.025	0.010	0.015	0.010	0.015
Cu	0	0.40	0	0.25	0	0.25	0	0.25
V	0.10	0.20	0.10	0.20	0.15	0.18	0.15	0.18
Sn	0	0.030	0	0.015	0	0.025	0	0.015
As	0	100	0	0.040	0	100	0	0.040
N	0	100	0	100	0	0.016	0	0.016

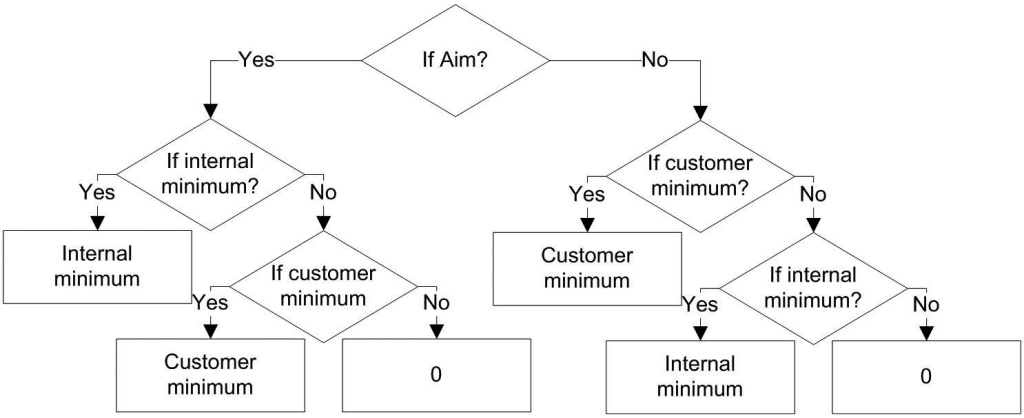

Figure 1. The rules for defining quality prescription minimum limit

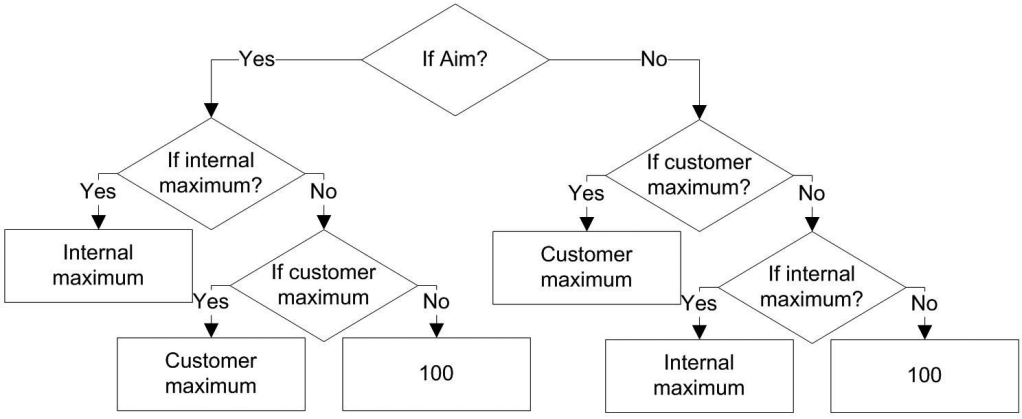

Figure 2. The rules for defining the quality prescription maximum limit

According to the selected customers' orders and their quality prescriptions (732.00.1, 732.59.2, 732.54.2), it is possible to easily calculate the batch chemical limitations (Table 5), based on the rules in Figure 1 and 2.

The logic for defining the cover quality prescription is as follows: The quality prescription with the highest number of chemical elements limitations among the selected work order quality prescriptions is defined as the cover quality prescription. In such case, the ladle operator uses the technology prescribed according to the cover quality prescription and adjusts the steelmaking technology according to the required chemical composition. In case of a customer order for the extra-machinability steels between the work order quality prescriptions, its quality prescription automatically becomes a cover quality prescription.

PARTICLE SWARM BATCH SCHEDULING

At the beginning of the batch scheduling, a grouping based on the ordered quantities is performed. The ordered quantities are divided into groups with similar chemical composition. The ordered quantity fits into the group if there are one or more ordered quantities with similar chemical composition (similar quality prescriptions) existing in the group.

After the grouping of the ordered quantities the particle swarm method was used for batch filling scheduling.[15]

The "particle" structure is conditioned by the problem's nature – consecutive events – the batch is cast consecutively. The biggest problem is in dealing with the batch filling schedule – organism evaluation.

BATCH FILLING SCHEDULES AS PARTICLES

The batch filling schedules are in fact the work order sequences and can be presented as sequence of batches with ordered quantities (Figure 3). Figure 3 shows the customer's ordered quantities cast within 4 batches. The ordered quantity 3 is cast within 3 batches, the ordered quantity 4 within 2 batches, and all other ordered quantities within one batch. The non-planned cast quantity can be observed in the last batch – batch 4.

Hence, the organism in Figure 3 can be written down as a sequence: Ordered quantity 1 - Ordered quantity 2 - Ordered quantity 3 - Ordered quantity 4.

The principal problem is to form the batch filling sequence according to the customers' ordered cast quantities, quality prescriptions, delivery dates, and possible additional rules.

FORMATION AND EVALUATION OF WORK ORDERS

The deadline must be defined in terms of the delivery date for ordered quantities. This means that all quantities

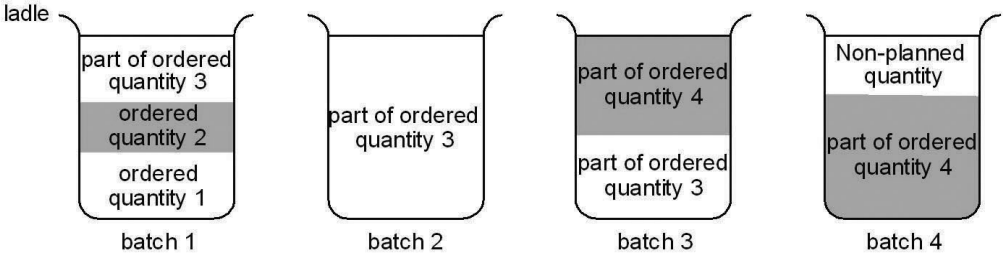

Figure 3. Work order schedule – the organism

should be cast in terms of that delivery date. The batch weight is defined according to the steelmaking technology – for extra-machinability steels, the batch weight is 50 t and for the other steel qualities the batch weight is 53 t.

From the ordered quantities pool the individual ordered quantities are added to the work order until the batch weight is reached. If the last added quantity exceeds the batch weight, which usually happens, the partial quantity is added to one or more consecutive work orders. The rule is that the partial quantities are added to the consecutive work order only when they exceed 5 %. Small orders of up to 5 t should not be split between the batches, i.e. to be cast within one batch.

For each ordered quantity, the chemical composition is compared to the quality prescriptions for the added quantity as well. In the event that the chemical composition does not fit the chemical prescriptions of the added quantities, the actual work order is filled with the non-planned quantity and the quantity is added to the consecutive work order (orders), which is filled according to the previously mentioned guidelines.

The work orders for quantities with a delivery date beyond the defined deadline are automatically abandoned.

The evaluation of the work order schedule consists of the following three parts:

O_1 The number of additional ordered quantities, where the ordered quantities are not cast within one batch (for instance, as seen in , we have to cast the ordered quantity 3 into 2 additional batches, and the ordered quantity 4 in one additional batch, so the total number of additional ordered quantities parts, where the ordered quantities are not cast within one batch is, in this case, 3)

O_2 Non-planned cast quantities in tons, and

O_3 All the customers' quantities in tons with the delivery date ahead of the deadline.

For the proper evaluation of optimum solution, weights were also used: $w_1 = 4$, $w_2 = 1$ and $w_3 = 1$ for each evaluation part (O_1 – number of additional ordered quantities parts, O_2 – non-planned cast quantities, and O_3 – all the customers' quantities in tons with the delivery date ahead of the deadline). The weights were selected according to the expert scheduler's advice and the preliminary test runs. The respective evaluation function can be simply written as:

$$f_e = w_1 \cdot O_2 + w_2 \cdot O_2 + w_3 \cdot O_3 \qquad (1)$$

THE PARTICLE SWARM OPTIMIZATION

The problem is set in a discrete space, so the most important issue in applying particle swarm optimization successfully is to develop an effective "problem mapping" and "solution generation" mechanism. If these two mechanisms are devised successfully, it is possible to find good solutions for a given optimization problem in acceptable time.

The particle swarm optimization used can be described in three following steps:[15]

1. Let initialization iterative generation be $k = 0$, initialization population size p_{size}, the termination iterative generation, *Maxgen*. Give birth to p_{size} initializing particles. Calculate each particle's fitness value of initialization population, and let first generation p_i be initialization particles, and choose the particle with the best fitness value of all the particles as the p_g (g_{Best}).
2. Every $p_{i,k}$ and $p_{g,k}$ crossover can get two child particles, compare them and let smaller fitness value particle be final child of predecessors. Using equation (2) obtains "flying" velocity v_i particles, then utilizing equation (3) randomly permutating N particles of them. And using equations (4) and (5) with the same method gives birth to the next generation particles x_i. If the fitness value is better than the best fitness value p_i (p_{Best}) in history, let current value as the new p_i (p_{Best}). Choose the particle with the best fitness value of all the particles as the p_g (g_{Best}). If k = *Maxgen*, go to Step 3, or else let $k = k + 1$; go to Step 2.
3. Put out the p_g.

The changing of the particles' velocities is presented by following equations:

$$v_{i,k+1} = p_{i,k} \otimes p_{g,k}, \tag{2}$$

$$\left(v_{r1}, v_{r2}, ..., v_{rN}\right)_{k+1} = P\left(v_{r1}, v_{r2}, ..., v_{rN}\right), \tag{3}$$

$$x_{i,k+1} = x_{i,k} \otimes v_{i,k+1}, \tag{4}$$

$$\left(x_{r1}, x_{r2}, ..., x_{rN}\right)_{k+1} = P\left(x_{r1}, x_{r2}, ..., x_{rN}\right), \tag{5}$$

where k represents the iterative generation number, and r ($1 \le r \le p_{\text{size}}$) is random integer which denotes permutating particle, and $\otimes$ is crossover denotation which denotes two particles making crossover operator. $P(v_r)$, $P(x_r)$ mean mutating particle v_r and x_r. The termination criterion for the iterations is determined according to whether the max generation (10 000).

For each final work orders schedule 100 independent runs were performed.

In the presented algorithm, each particle of the swarm shares mutual information globally and benefits from the discoveries and previous experiences of all other colleagues during the search process. The algorithm requires only primitive and simple mathematical operators, and is computationally inexpensive in terms of both memory requirements and time.

Results of the scheduling

In order to demonstrate the methodology, real data from production in October 2009 were used. There were 196 ordered quantities with an average quantity of 21.66 t (standard deviation 37.45 t). Table 6 enlists the quality prescription quantities (46 different quality prescriptions) and their calculated chemical limits within 196 orders. The deadline chosen was 31. 10. 2009.

From the quality prescription enlistment (Table 6), 29 ordered quantities groups can be established (Table 7) based on rules defined in section Formation and evaluation of work orders.

In order to make the presentation more clear, let us take a closer look at the batch filling scheduling of the largest group – group 23. Group 23 presents, in general, 50CrV4 (W. NR. 1.8159) spring steel. But we must state again that it is not possible to chemically combine all of them. For instance, we cannot cast within one batch orders with quality prescription 732.66.0 with 732.12.5 or 732.13.5, quality prescription 732.18.1 with 732.59.2 or 732.54.2 (Table 6). In group 23 there are 113 customer orders, with a total amount of 1699.239 t, with an average ordered quantity of 15.0375 t, and with 52 orders within the deadline.

The simulated swarm scheduled the group 23 with the following results:

- number of additional ordered quantities parts: 9
- non-planned cast quantities: 10.517 t
- customer quantities with the delivery date ahead of the deadline: 37.230 t
- number of work orders: 19.

The best batch filling schedule was obtained in the 6758-th generation (the generation 0 is a randomly generated generation). For clearer understanding, only the first five successive work orders of the best work order schedule are presented in the following tables (Tables 8–12).

It is possible to notice that the customer order 901000085507 is present at work order 0001020 (Table 8) and 0001021 (Table 9) – so the order is processed within two batches and thus has an additional part. The best solution is obtained, as mentioned before, when the ordered quantity is cast within one batch.

Table 6. Quality prescription quantities in October 2009 and their calculated chemical limits

Quality Prescription code	Steel quality	Ordered Quantity [t]	C w/%	Si w/%	Mn w/%	P w/%	S w/%	C w/%
108.15.0	44MnSiVS6	30.192	0.42-0.47	0.5-0.7	1.3-1.6	MAX 0.035	0.02-0.035	MAX 0.25
108.33.0	38MnVS5	121.5	0.35-0.4	0.5-0.7	1.2-1.5	MAX 0.035	0.045-0.06	0.15-0.25
108.70.1	38MnVS6 (extra machinability)	18.944	0.41-0.44	0.3-0.5	1.1-1.4	MAX 0.035	0.03-0.035	0.15-0.25
127.11.5	61SiCr7	83.841	0.57-0.65	1.6-1.8	0.7-1	MAX 0.02	MAX 0.015	0.25-0.4
140.11.1	CSN 15230.3[1]	18.038	0.24-0.34	0.17-0.37	0.4-0.8	MAX 0.035	MAX 0.035	2.2-2.5
193.31.0	27MnCrB5	18.352	0.25-0.3	0.15-0.35	1-1.4	MAX 0.035	MAX 0.035	0.3-0.6
193.52.0	30MnB5	26.374	0.27-0.3	0.1-0.3	1.05-1.2	MAX 0.035	MAX 0.035	MAX 0.3
193.54.0	28MnCrB7-2	53.872	0.26-0.28	0.15-0.25	1.68-1.78	MAX 0.03	0.02-0.04	0.48-0.53
503.14.0	St 37-2	4.019	0.14-0.17	0.15-0.5	0.4-1.4	MAX 0.035	MAX 0.035	MAX 0.3
503.31.1	RSt 37-2	97.65	0-0.08	0-0.08	0.28-0.45	MAX 0.02	MAX 0.02	
516.17.1	Cm45	13.616	0.43-0.48	0.15-0.35	0.6-0.7	MAX 0.035	0.02-0.035	0.17-0.23
523.00.0	C75	46.176	0.7-0.8	0.15-0.35	0.6-0.8	MAX 0.045	MAX 0.045	MAX 0.3
524.11.0	C70	0.918	0.65-0.75	0.25-0.35	0.8-0.9	MAX 0.02	MAX 0.02	0.2-0.3
615.12.0	C22E	30.251	0.16-0.19	MAX 0.1	0.3-0.4	MAX 0.015	MAX 0.015	MAX 0.2
623.32.0	70MnVS4	218.093	0.69-0.72	0.15-0.25	0.8-0.9	MAX 0.015	0.06-0.07	0.1-0.2
625.13.1	C50	105.08	0.5-0.53	0.2-0.35	0.8-0.9	MAX 0.03	0.015-0.02	0.23-0.3
635.36.5	C35R	23.088	0.36-0.39	0.2-0.4	0.65-0.8	MAX 0.03	0.02-0.035	0.2-0.3
636.11.1	C45	515.41	0.47-0.5	0.2-0.35	0.7-0.8	MAX 0.035	0.02-0.025	0.24-0.29
705.13.3	SAE 1141[2]	54.6	0.39-0.43	0.2-0.3	1.4-1.55	MAX 0.03	0.08-0.092	MAX 0.3
711.00.1	41Cr4	26.869	0.38-0.45	0.2-0.4	0.6-0.9	MAX 0.035	MAX 0.035	0.9-1.2
711.14.0	41Cr4	15.333	0.38-0.45	0.2-0.4	0.6-0.9	MAX 0.035	MAX 0.035	0.9-1.2
718.70.2	16MnCr5 (extra machinability)	55.388	0.14-0.19	0.2-0.4	1-1.3	MAX 0.035	0.02-0.035	0.8-1.1
724.24.0	42CrMo4	38.438	0.38-0.45	0.15-0.4	0.6-0.9	MAX 0.035	0.02-0.035	0.9-1.2
732.01.0	50CrV4	150.341	0.47-0.55	0.15-0.4	0.7-1.1	MAX 0.025	MAX 0.025	0.9-1.2
732.03.0	51CrV4	9.709	0.47-0.55	0.15-0.4	0.7-1.1	MAX 0.025	MAX 0.025	0.9-1.2
732.12.5	51CrV4	67.113	0.51-0.54	0.2-0.35	1-1.1	MAX 0.015	MAX 0.015	1.1-1.2
732.13.5	51CrV4	141.563	0.51-0.56	0.2-0.35	1-1.2	MAX 0.015	MAX 0.015	1.1-1.25
732.18.1	51CrV4	5.661	0.47-0.51	0.15-0.4	0.7-0.85	MAX 0.025	MAX 0.025	0.9-1
732.19.1	51CrV4	11.485	0.51-0.55	0.15-0.4	0.85-0.95	MAX 0.025	MAX 0.025	0.95-1.1
732.20.2	51CrV4	58.785	0.51-0.55	0.15-0.4	0.9-1.1	MAX 0.025	MAX 0.025	1.05-1.2
732.21.2	51CrV4	27.675	0.52-0.54	0.2-0.35	0.95-1.1	MAX 0.025	MAX 0.025	1.1-1.2
732.24.4	50CrV4	69.967	0.47-0.55	0.2-0.4	0.7-1.1	MAX 0.035	MAX 0.035	0.9-1.2
732.26.2	51CrV4	17.263	0.51-0.54	0.2-0.35	0.9-1.05	MAX 0.02	MAX 0.015	1-1.1
732.27.3	51CrV4	31.69	0.51-0.55	0.15-0.4	0.95-1.1	MAX 0.025	MAX 0.025	1.1-1.2
732.54.2	51CrV4	636.408	0.49-0.54	0.2-0.35	0.9-1.1	MAX 0.015	MAX 0.015	0.9-1.2
732.59.2	50CrV4	427.379	0.52-0.55	0.25-0.35	1-1.1	MAX 0.02	MAX 0.008	1.1-1.2
732.62.0	50CrV4	6.83	0.47-0.55	0.2-0.4	0.7-1.1	MAX 0.02	MAX 0.01	0.9-1.2
732.66.0	51CrV4	37.37	0.47-0.5	0.2-0.4	0.7-1.1	MAX 0.035	MAX 0.035	0.9-1.2
741.33.3	15CrNiS6	4.144	0.12-0.17	0.15-0.4	0.4-0.6	MAX 0.035	0.02-0.035	1.4-1.7
775.13.0	23MnNiMoCr5-4	25.693	0.21-0.24	0.15-0.25	1.25-1.4	MAX 0.02	MAX 0.012	0.5-0.6
779.27.1	16MnCrS5	414.9	0.14-0.17	0.2-0.35	1-1.1	MAX 0.035	0.02-0.03	0.8-0.9
779.71.4	16MnCrS5 (extra machinability)	40.848	0.17-0.19	0.15-0.3	1-1.1	MAX 0.025	0.03-0.035	0.9-1
780.10.0	20MnCrS5	52.8	0.2-0.23	0.15-0.25	1.3-1.4	MAX 0.025	0.02-0.03	1.2-1.3
780.13.2	20MnCr5	138.45	0.17-0.22	0.2-0.35	1.1-1.4	MAX 0.03	0.015-0.035	1-1.3
781.00.1	18CrNiMo7-6	17.997	0.15-0.21	0.2-0.4	0.5-0.6	MAX 0.035	MAX 0.035	1.5-1.8
781.18.1	19CrNiMo7-6	228.75	0.15-0.17	0.2-0.35	0.52-0.62	MAX 0.03	0.018-0.025	1.55-1.65

[1] Czech State Norm [2] Society of Automotive Engineers standard

M *w*/%	Ni *w*/%	Al *w*/%	Cu *w*/%	V *w*/%	Sn *w*/%	As *w*/%	N *w*/%
MAX 0.07	MAX 0.25	0.016-0.03	MAX 0.25	0.1-0.13	MAX 0.03		
MAX 0.08	MAX 0.3	0.02-0.038	MAX 0.25	0.08-0.13	MAX 0.03		0.015-0.018
MAX 0.08	0.15-0.25	0.01-0.03	MAX 0.3	0.13-0.15	MAX 0.03		0.011-0.02
MAX 0.08	MAX 0.3	0.015-0.025	MAX 0.25	MAX 0.1	MAX 0.02		
MAX 0.05	MAX 0.2	0.02-0.035	MAX 0.25	0.1-0.2	MAX 0.03		
MAX 0.05	MAX 0.2	0.02-0.035	MAX 0.25	MAX 0.05	MAX 0.03		
MAX 0.08	MAX 0.3	0.02-0.035	MAX 0.4	MAX 0.1	MAX 0.02		
MAX 0.1	MAX 0.3	0.02-0.05	MAX 0.25	MAX 0.1	MAX 0.02		MAX 0.012
MAX 0.08	MAX 0.3	0.02-0.035	MAX 0.4	MAX 0.1	MAX 0.03		MAX 0.009
		0.015-0.025				MAX 0.012	
MAX 0.07	MAX 0.25	0.01-0.05	MAX 0.25	MAX 0.05	MAX 0.03		
MAX 0.08	MAX 0.3	0.02-0.1	MAX 0.4	MAX 0.1	MAX 0.03		
MAX 0.05	MAX 0.2	0.015-0.05	0.05-0.25	MAX 0.1	MAX 0.03		
MAX 0.1	MAX 0.2	0.02-0.035	MAX 0.2	MAX 0.05	MAX 0.03		
MAX 0.06	MAX 0.2	MAX 0.03	MAX 0.25	0.14-0.15	MAX 0.03		0.013-0.016
MAX 0.08	0.15-0.24	0.02-0.035	MAX 0.25	MAX 0.1	MAX 0.03		0.008-0.013
MAX 0.08	MAX 0.3	0.02-0.03	MAX 0.25	MAX 0.1	MAX 0.03		
MAX 0.08	0.15-0.2	0.02-0.035	MAX 0.25	MAX 0.1	MAX 0.03		0.008-0.013
MAX 0.08	MAX 0.3	0.015-0.02	MAX 0.3				
MAX 0.08	MAX 0.3	0.02-0.1	MAX 0.4	MAX 0.1	MAX 0.03		
MAX 0.08	MAX 0.3	0.02-0.1	MAX 0.4	MAX 0.1	MAX 0.03		
MAX 0.08	MAX 0.3	0.02-0.1	MAX 0.4	MAX 0.1	MAX 0.03		MAX 0.015
0.15-0.3	MAX 0.25	0.02-0.045	MAX 0.25	MAX 0.1	MAX 0.03		
MAX 0.08	MAX 0.3	0.01-0.015	MAX 0.4	0.1-0.2	MAX 0.03		
MAX 0.08	MAX 0.3	0.01-0.015	MAX 0.4	0.1-0.2	MAX 0.03		
MAX 0.08	MAX 0.2	0.01-0.015	MAX 0.25	0.1-0.2	MAX 0.02	MAX 0.04	
MAX 0.08	MAX 0.2	0.01-0.015	MAX 0.25	0.1-0.2	MAX 0.02	MAX 0.04	
MAX 0.08	MAX 0.25	0.01-0.04	MAX 0.25	0.1-0.25	MAX 0.025		
MAX 0.08	MAX 0.25	0.01-0.04	MAX 0.25	0.1-0.25	MAX 0.025		
MAX 0.08	MAX 0.25	0.01-0.04	MAX 0.25	0.1-0.25	MAX 0.025		
MAX 0.07	MAX 0.2	0.01-0.015	MAX 0.25	0.12-0.2	MAX 0.025		
MAX 0.05	MAX 0.2	0.01-0.015	MAX 0.25	0.1-0.2	MAX 0.03		MAX 0.012
MAX 0.04	MAX 0.2	0.01-0.015	MAX 0.25	0.11-0.15	MAX 0.025		
MAX 0.08	MAX 0.25	0.01-0.04	MAX 0.25	0.1-0.25	MAX 0.025		
MAX 0.08	MAX 0.2	0.01-0.015	MAX 0.25	0.1-0.2	MAX 0.02	MAX 0.04	
MAX 0.06	MAX 0.2	0.01-0.015	MAX 0.25	0.15-0.18	MAX 0.025	MAX 0.016	
MAX 0.08	MAX 0.2	0.01-0.015	MAX 0.25	0.1-0.2	MAX 0.03		MAX 0.012
MAX 0.08	MAX 0.3	0.01-0.015	MAX 0.25	0.1-0.25	MAX 0.03		MAX 0.012
MAX 0.08	1.4-1.7	0.02-0.1	MAX 0.25	MAX 0.1	MAX 0.03		MAX 0.013
0.5-0.6	1-1.1	0.02-0.05	MAX 0.25	MAX 0.1	MAX 0.02		MAX 0.012
MAX 0.05	MAX 0.15	0.02-0.03	MAX 0.25	MAX 0.1	MAX 0.03		MAX 0.013
MAX 0.07	MAX 0.15	0.02-0.03	MAX 0.28	MAX 0.1	MAX 0.02		0.01-0.012
0.07-0.1	0.15-0.25	0.02-0.03	MAX 0.25	MAX 0.1	MAX 0.03		0.008-0.012
MAX 0.1	MAX 0.35	0.02-0.05	MAX 0.25	MAX 0.1	MAX 0.02		
0.25-0.35	1.4-1.7	0.02-0.1	MAX 0.4	MAX 0.1	MAX 0.03		
0.25-0.35	1.42-1.52	0.02-0.03	MAX 0.25	MAX 0.1	MAX 0.03		

Table 7. Ordered quantities groups

Ordered quantities groups #	Quality prescriptions within the group	Number of customer orders	Ordered quantities [t]
1	108.15.0	2	30.192
2	108.33.0	2	121.5
3	108.70.1	1	18.944
4	127.11.5	14	83.841
5	140.11.1	3	18.038
6	193.31.0	2	18.352
7	193.52.0	4	26.374
8	193.54.0	1	53.872
9	503.14.0	8	4.019
10	503.31.1	7	97.65
11	516.17.1	1	13.616
12	523.00.0	1	46.176
13	524.11.0	1	0.918
14	615.12.0	1	30.251
15	623.32.0	2	218.093
16	625.13.1	2	105.08
17	635.36.5	1	23.088
18	636.11.1	3	515.41
19	705.13.3	2	54.6
20	711.00.1, 711.14.0	3	42.202
21	718.70.2	3	55.388
22	724.24.0	2	38.438
23	732.01.0, 732.03.0, 732.12.5, 732.13.5, 732.18.1, 732.19.1, 732.20.2, 732.21.2, 732.24.4, 732.26.2, 732.27.3, 732.54.2, 732.59.2, 732.62.0, 732.66.0	113	1699.239
24	741.33.3	1	4.144
25	775.13.0	2	25.693
26	779.27.1	1	414.9
27	779.71.4	4	40.848
28	780.10.0, 780.13.2	3	191.25
29	781.00.1, 781.18.1	6	246.747

Table 8. The first work order (out of 19) from the best batch filling schedule

Work order number: 0001020			
Cover quality prescription code	Chemical limitations		
732.54.2	/		
Quality prescription code	Customer order code	Ordered quantity [t]	Delivery date
732.54.2	901000085507	53	30.10.2009

Table 9. The second work order (out of 19) from the best batch filling schedule

Work order number: 0001021			
Cover quality prescription code	Chemical limitations		
732.54.2	w(C)/% = 0.51–0.54; w(Cr)/% = 1.05–1.2; w(Al)/% = 0.015–0.025		
Quality prescription code	Customer order code	Ordered quantity [t]	Delivery date
732.20.2	901000086002	3.148	9.11.2009
732.01.0	901000087902	5.765	8.11.2009
732.54.2	901000085507	44.087	30.10.2009

Table 10. The third work order (out of 19) from the best batch filling schedule

Work order number: 0001022			
Cover quality prescription code	Chemical limitations		
732.59.2	w(Al)/% = 0.015–0.04; w(N)/% = 0.012 (max.)		
Quality prescription code	Customer order code	Ordered quantity [t]	Delivery date
732.01.0	901000093717	16.639 t	31.10.2009
732.20.2	901000087401	5.535 t	31.10.2009
732.01.0	901000093711	5.698 t	31.10.2009
732.01.0	901000093712	11.1 t	31.10.2009
732.20.2	901000086001	5.594 t	31.10.2009
732.62.0	901000094102	6.83 t	31.10.2009
732.59.2	901000084801	1.604 t	2.11.2009

Table 11. The fourth work order (out of 19) from the best work order schedule

Work order number: 0001023			
Cover quality prescription code	Chemical limitations		
732.59.2	w(C)/% = 0.51–0.54; w(P)/% = 0.015 (max.); w(Al)/% = 0.01–0.025; w(Sn)/% = 0.02 (max.); w(As)/% =0.04 (max.)		
Quality prescription code	Customer order code	Ordered quantity [t]	Delivery date
732.01.0	901000093718	5.683	31. 10. 2009
732.54.2	901000090501	31.909	30. 10. 2009
732.03.0	901000090401	9.709	31. 10. 2009
732.59.2	901000093101	5.594	31. 10. 2009
732.59.2	Non-planned cast quantity	0.105	

Table 12. The fifth work order (out of 19) from the best work order schedule

Work order number: 0001024			
Cover quality prescription code	Chemical limitations		
732.54.2	w(C)/% = 0.52–0.54!; w(P)/% = 0.015 (max.) w(Sn)/% = 0.02 (max.); w(As)/% = 0.04 (max.)		
Quality prescription code	Customer order code	Ordered quantity [t]	Delivery date
732.54.2	9010000873/1	45.028	30.10.2009
732.54.2	9010000855/21	3.337	30.10.2009
732.24.4	9010000883/10	4.635	30.10.2009

As a remark: in work order 0001023 (Table 12), we can notice that the optimal batch weight (53 t) is not achieved – non-planned cast quantity is 0.105 t, which is practically insignificant. Usually this quantity is added to one or more ordered quantities (within 5 % of ordered quantity).

Conclusions

The present paper deals with improving of the batch filling scheduling by using the particle swarm algorithm. The scheduling problem was divided into the following subsequent steps:

- grouping of ordered quantities according to the chemical composition,
- work order representation and evaluation, and finally,
- particle swarm based search for optimal batch filling schedule.

The batch filling scheduling strategy has been implemented in ŠTORE STEEL Ltd. as follows:

1. The period up to 2006: Only the expert knowledge of the batch scheduler was used. The non-planned and ordered quantities with the date ahead of the deadline presented 17.17 % of the total production in 2005.
2. The period after 2006: The particle swarm based search has been used to globally optimize the proper combination of the batches in order to reduce the non-planned and ordered cast quantities with the date ahead of the deadline, and to minimize the number of batches. The non-planned and the ordered quantities with the date ahead of the deadline, presented 10.12 % of the total production in 2006, and 10.12 % of the total production in 2007. This was enhanced to 16.22 % in 2008, and 32.70 % in 2009. The reasons for the increase lie in the off-standard ordered quantities due to the global economic crisis, and not in the deficiency of the represented algorithm.

These quantities would be of course much higher in case of using the expert knowledge only.

References

[1] Broughton, J. S., Mahfouf, M., Linkens, D. A. (2007): A Paradigm for the Scheduling of a Continuous Walking Beam Reheat Furnace Using a Modified Genetic Algorithm. *Materials and Manufacturing Processes*, Vol. 22, 607–614.

[2] Pacciarelli, D., Pranzo, M. (2004): Production scheduling in a steelmaking-continuous casting plant. *Computers and Chemical Engineering*, Vol. 28, 2823–2835.

[3] Kovačič, M., Šarler, B. (2009): Application of the genetic programming for increasing the soft annealing productivity in steel industry. *Materials and Manufacturing Processes*, Vol. 24, 3, 369–374.

[4] Verlinden, B., Driver, J., Samajdar, I., Doherty, R. D. (2007): *Thermo-mechanical Processing of Metallic Materials*, Elsevier, Amsterdam.

[5] Gheorghies, C., Crudu, I., Teletin, C., Spanu, C. (2009): Theoretical Model of Steel Continuous Casting Technology, *Journal of Iron and Steel Research*, International, Vol. 16, No. 1, 12–16.

[6] Janik, M., Dyja, H. (2004): Modelling of three-dimensional temperature field inside the mould during continuous casting of steel, *Journal of Materials Processing Technology*, 157–158, 177–182.

[7] Thomas, B. G., Najjar, F. M. (1991): Finite element modelling of turbulent fluid flow and heat transfer in continuous casting, *Applied Mathematical Modelling*, Vol. 15, No. 5, 226–243.

[8] Wen-hong, L., Zhi, X., Zhen-ping, J., Biao, W., Zhao-yi, L., Guang-lin, J. (2008): Dynamic Water Modeling and Application of Billet Continuous Casting, *Journal of Iron and Steel Research, International*, Vol. 15, No. 2, 14–17.

[9] Kolenko, T., Jaklič, A., Lamut, J. (2007): Development of a mathematical model for continuous casting of steel slabs and billets. Mathematical and Computer Modelling of Dynamical Systems: *Methods, Tools and Applications in Engineering and Related Sciences*, Vol. 13, No. 1, 1744–5051.

[10] Mendez, C., A., Cerda, J., Grossmann, I., E., Harjunkoski, I., Fahl, M. (2006): State-of-the-art review of optimization methods for short-term scheduling of batch processes. *Computers and Chemical Engineering*, Vol. 30, 913–946.

[11] Azizoglu, M., Webster, S. (2001): Scheduling a batch processing machine with incompatible job families. Computers & Industrial Engineering, Vol. 39, 325–335.

[12] Tanga, L., Guanb, J., Huc, G. (2010): Steelmaking and refining coordinated scheduling problem with waiting time and transportation consideration. *Computers & In-*

dustrial Engineering, Vol. 58, No. 2, 239–248.

[13] DEB, K., REDDY, A., R., SINGH, G. (2009): Optimal Scheduling of Casting Sequence Using Genetic Algorithms. *Materials and Manufacturing Processes*, Vol. 18, No. 3, 409–432.

[14] RONGA, A., LAHDELMAB, R. (2008): Fuzzy chance constrained linear programming model for optimizing the scrap charge in steel production. *European Journal of Operational Research*, Vol. 186, No. 3, 953–964.

[15] ZHIGANG, L., XINGSHENG, G., BIN, J. (2008): A novel particle swarm optimization algorithm for permutation flow-shop scheduling to minimize makespan, *Chaos, Solitons and Fractals*, Vol. 35, 851–861.

Study of process parameters on Al-7.0 % Si-0.45 % Mg alloy cast trough strain induced melt activation technique

Študija procesnih parametrov v zlitini Al-7,0 % Si-0,45 % Mg, uliti s tehniko aktivacije taline z deformacijo

Ashok Sharma[1,*], S. K. Gupta[1] & Madhulika Srikanth[2]

[1]Department of Metallurgical and Materials Engineering, Malaviya National Institute of Technology Jaipur-302017, India
[2]Wichita State University, Kansas, USA

*Corresponding author. E-mail: ashok.mnit12@gmail.com

Received: December 7, 2011 Accepted: July 27, 2012

Abstract: The effect of process parameters on microstructure evolution of semi-solid Al-7 % Si-0.45 % Mg alloy produced by strain induced melt activation (SIMA) process were investigated. Predeformation of 20 %, 30 %, and 40 % were used by hot working at 380 ºC. After predeformation the samples were heated to a temperature above the solidus and below the liquidus point and maintained in the isothermal conditions at three different temperatures (580 °C, 590 °C and 600 °C) for varying time (10 min, 20 min, and 30 min). It was found that increased predeformation reduced the soaking time to obtain globular α_{Al} grains. It was observed that strain induced predeformation and subsequently melt activation has caused the globular morphology of α_{Al} grains.

Izvleček: Raziskan je bil vpliv procesnih parametrov na razvoj mikrostrukture kašaste zlitine Al-7 % Si-0,45 % Mg, proizvedene s tehniko aktivacije taline z deformacijo (SIMA). Uporabljene so bile preddeformacije 20 %, 30 % in 40 % pri vročem preoblikovanju na 380 °C. Vzorci so bili po preddeformaciji segreti na temperaturo, večjo od temperature solidusa ter manjšo od likvidusa, ter vzdrževani v konstantnih razmerah pri treh različnih temperaturah (580 °C, 590 °C in 600 °C) različno dolgo (10 min, 20 min in 30 min). Ugotovljeno je bilo, da večja preddeformacija zmanjša čas predgretja za dosego globularnih zrn α_{Al}. Razvidno je bilo, da preddeformacija in posledično aktivirana talina povzročata globularno morfologijo zrn α_{Al}.

Original scientific paper

Key words: Al-Si alloy, semi-solid, SIMA, microstructure, globular α_{Al}
Ključne besede: zlitina Al-Si, kašasto stanje, SIMA, mikrostrukture, globularni α_{Al}

Introduction

Light weight structural materials, especially Al-alloys, play an important role in achieving vehicle weight reduction and improving fuel economy in the automotive industry. Liquid metal high pressure die-casting (HPDC) currently satisfies the bulk of the automotive industry's needs in this regard. Last two decades have seen a rise in the consumption of Al-alloys in car and in light weight truck market. Growing demands for improved quality and weight reduction, however, have been driving the development of new processing technologies. Problems inherently associated with liquid metal HPDC have resulted in enhanced interest in semi-solid metal (SSM) casting processes.[1]

Semi-solid processing can be done in two ways namely: Rheocasting and Thixocasting.[1, 2] Shaping of materials in the semi-liquid state includes both casting and deformation processes. The critical volume fraction of liquid phase, which allows the material to maintain its shape, is the criterion for the distinction between casting and forming processes. The volume fraction of liquid phase is a function of temperature in the range between solidus and liquidus. The research, which has been carried out in recent years, has proved that deformation of materials with the presence of a liquid phase exhibits some abilities, which are not attainable in conventional metal forming. These processes are referred to in the literature as forming in mushy state or forming in semi-liquid state or thixoforming.[3, 4] The basic principle of these processes is deformation at temperatures between solidus and liquidus points. However, the alloy has to be prepared before deformation in a special way, so that it has a very fine spherical microstructure. The low melting temperature phase should be located at the grain boundaries. Such a microstructure is called thixoforming microstructure. As one of the SSM processes, the strain induced melt activation (SIMA) process is adapt to produce the semi-solid Al and Mg based alloys.[5] SIMA has been reported to obtain near equiaxed grain structures by deformation followed by a heat treatment in the semi-solid region. Liquid phase is located at high angle grain boundaries and alloy achieves a microstructure consisting of almost spherical solid particles. These particles are separated by a low melting-temperature liquid phase. Size of these particles depends on;

- chemical composition of the alloy, which determined the solidus–liquidus temperature interval
- microstructure at the beginning of melting
- heating rate below the solidus
- and holding time in the semi-liquid state

Kirkwood[6, 7] suggested that recrystallization of a previously deformed specimen in the semi-solid isothermal process is the main reason of this modification. In the study, the effect of predeformation rate, as well as holding time and temperature at semi-solid state on the microstructural characteristics of A356 specimens were investigated.

Materials and methods

The alloys were cast in the form of rectangular strips of size 250 mm × 15 mm × 10 mm. The experiment consisted of mainly three stages.

In stage 1, Al - 7 % Si - 0.45 % Mg alloy was prepared according to conventional melting and casting procedure. The mass fraction 0.2 % of Al-5Ti-1B master alloy was also added into the melt for grain refinement of α_{Al} phase. The ingot was cut breadth wise to get samples of length 25 mm.

In stage 2, the samples were mechanically worked with the help of a forging press and a rolling mill. The present alloy under investigation has relatively high Si content which decreases ductility at room temperature, hence warm working was used instead of cold working. Later, the samples were heated to 380 °C and a reduction of 20 % to 40 % was given in the incremental steps of 10 %. Initial reduction up to 10 % was done by forging and the remaining amount of reduction was done by rolling.

In the last stage, the worked samples were given heat treatment in an electric resistance furnace. The temperature was in the freezing range which was varied from 580 °C to 600 °C in the incremental steps of 10 °C, the soaking time was 10 min, 20 min, and 30 min. After this the samples were quenched in water. The quenched samples were taken for microstructural study. The specimens were polished by standard metallographic practice and etched with the Keller's reagent to reveal the microstructure.

Results and Discussion

Effect of predeformation, temperature and holding time

Advantages of thixoforming process are due to the mechanism of deformation, which is different than in the conventional metal forming. Due to a

localization of the liquid phase at grain boundaries, the plastic deformation involves sliding along the boundaries and rotations of grains. This mechanism of deformation involves low yield stress, as the workability of the alloy increases significantly.[8]

There exists an optimum for the required amount of predeformation which results in the occurrence of recrystallization. It is important to consider that after predeformation, the density of vacancies and dislocations increases, which increases the atomic diffusion capacity on reheating. In specimens with a little amount of predeformation, the density of the vacancies and dislocations is low, which results in a low atom diffusion rate. However, when sufficient amount of predeformation is exerted to the alloy, the final semi-solid microstructure may have equiaxed morphology by diffusion of the eutectic melted phase into the high stress containing regions of the dendrites.[8]

Figure 1a shows optical photo-micrograph of conventionally cast Al-7 % Si-0.45 % Mg alloy where α_{Al} dendrites can be seen along with the eutectic mixture. Figure 1b shows 30 % predeformation which clearly exhibits heavily oriented α_{Al} dendrites in the direction that was vertical to the hot working direction.

During plastic deformation of samples, internal strain energy is stored in the form of dislocation multiplication, elasticity stress and vacancies, which provide the driving force for recovery and recrystallization. The energy increases with the degree of predeformation which promote the morphological

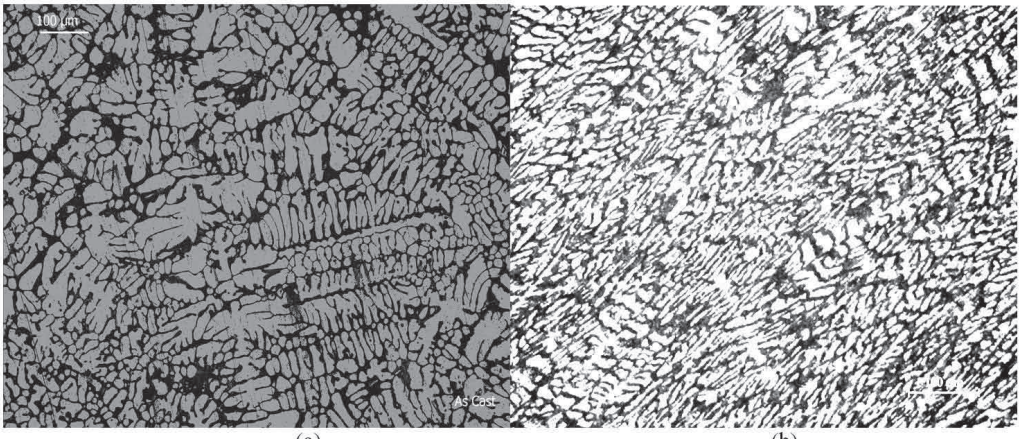

Figure 1. Optical micrographs of cast Al-7 % Si-0.45 % Si alloy (a) as cast and (b) at 30 % predeformation

transition from dendritic to globular structure.

Figure 2 (a&b) shows representative microstructures of cast alloy heat treated at 580 ºC and 600 ºC for 10 min. at varying predeformation of 20 % and 40 % respectively. The microstructures consist of α_{Al} grains, liquid phase and the entrapped liquid inside the α_{Al} grains. The experimental results show the effect of predeformation and temperature at 10 min of holding time on α grain size and morphology Figure 2 (a&b). The adjoining grain coalesces and coarsens quickly at 580 ºC. In other words, coalescence and coarsening occurs in the stage of low liquid fraction. However, with an increase of isothermal temperature to 600 ºC, the large α grains coarsen continuously and the small grains melts gradually as shown in Figure 2b. Where it could be observed that with increase in temperature and predeformation, the amount of semi - solid particles reduce and the size of α_{Al} grains increase, solid volume fraction lowers down and shape of the grains becomes more globular (average aspect ratio of around 0.8). The average α_{Al} grain size increases from 40 μm to 60 μm. The particles with large curvature show lower melting point at the protuberant part. Due to this the protuberant part of the solid particles melts, which makes the solid particles more globular.[8] This is known as the Gibbs-Thompson effect. It is clear that the high semi-solid isothermal temperature reduces the volume fraction of solid and accelerates the spherical evolution of the solid particles (Figure 2b). At temperatures higher than the eutectic temperature, the eutectic phase dissolves completely and the atoms diffuse to the α_{Al} grains due to increasing of the diffusion capacity and the solubility

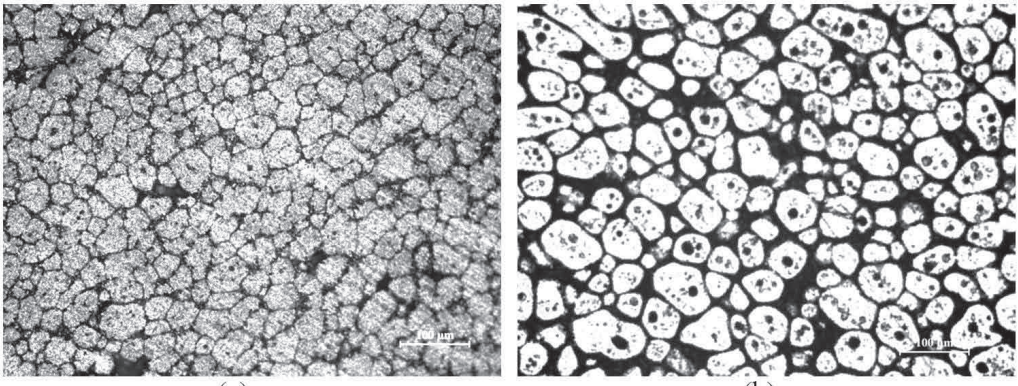

(a) (b)

Figure 2. Optical micrographs of Al- % Si-0.45 % Mg alloy at 10 min holding time at (a) 20 % predeformation and 580 ºC (b) 40 % predeformation and 600 ºC

of the elements in α_{Al} at higher temperatures. Since the secondary arms are small, they coarsen, combine and disappear when the eutectics between them is melted completely. Entrapped liquid[7] is also observed inside the α_{Al} grains. It is also observed that coalescence of complex shaped grains results in large liquid entrapment as shown in Figure 2b. When the isothermal holding temperature is increased, the ability of atomic mobility increased, which promotes coalescence ripening.

Figure 3(a–c) shows representative microstructures of 30 % predeformed alloy heated treated to 590 °C for 10 min, 20 min and 30 min. On comparing the microstructures of Figure 3 (a–c) it can be seen that there is coarsening as well as deviation from globularity as the holding time increases i.e. with increase in holding time α_{Al} solid particles loose their globularity and become irregular and large (Figure 3b&c). With the increasing the isothermal holding time, coalescence ripening does an effect on

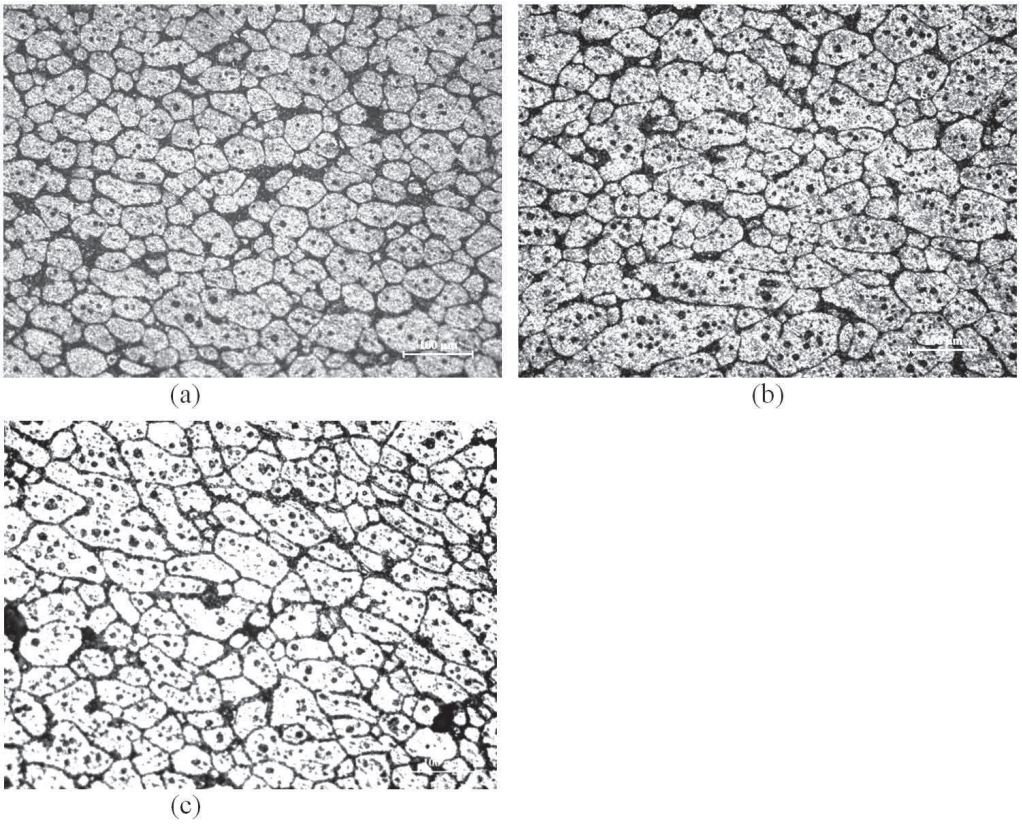

Figure 3. Optical micrographs of cast Al-7 % Si-0.45 % Mg alloy at 30 % predeformation and 590 ºC with varying holding time (a) 10 min (b) 20 min and (c) 30 min

the average size of the solid particles and allow the particles to grow larger. As time passes from 10 min to 30 min, the total number of grains decreases however, volume fraction of α_{Al} (the grain constitution) is constant.

Coalescence and Ostwald ripening mechanisms[9] play an important role to increase the average size of the α_{Al} particles. The coarsening mechanism is the coalescence of α_{Al} grains, which occurs between adjoining grains at low liquid fraction. Liquid content plays an important role in kinetics of coalescence since it defines the number of solid necks between grains. It has been shown that the coalescence frequency is proportional to the number of adjacent grains. Therefore, coalescence is expected to occur at early stages of heating or in high fraction solid in the semi-solid regime where the number of necks per grain is relatively high and grains are discrete.

Ostwald ripening involves the growth of larger α_{Al} particles at the expense of smaller α_{Al} particles, and it is governed by the Gibbs–Thompson effect. This effect changes the chemical potential of solutes at the particle/liquid interface, depending on the curvature of the interface.[16] The lowering of interfacial energy between the solid phase and liquid phase supplies the driving force for grain coarsening. The larger grain gradually becomes spheroidal to lower the solid/liquid interfacial energy. Ostwald ripening is active at higher liquid fraction, in which α_{Al} grain continuously coarsen and the small grain gradually melts. According to the LSW theory[18] third power diameter of α grain is proportional to holding time;

$$D^3 = Kt + D_0^3$$

where D and D_0 are the final and initial grain sizes respectively is the initial size of a solid phase particle; and t is the holding time measured from the moment when annealing temperature is reached; K is a coarsening rate constant.

The isothermal holding time, temperature and degree of predeformation have effects on the average size and degree of spheroidization of α_{Al} particles of semi solid slurry.

Conclusion

High semi-solid heat treatment temperature make the α_{Al} particles more globular. However, the solid fraction reduces. Size of the particles grow larger due to coarsening. Higher soaking time also causes coarsening of α_{Al} particles and globularity is also lost. The whole microstructure evolution process of SIMA processed Al-7 % Si-0.45 % Mg alloy can be divided in to two steps: first is recovery, recrystalli-

zation and partial melting and second is sheroidizing and grain coarsening as holding time increases.

References

[1] Fleming, M. C. (1991): Behaviour of Metal in Semi-solid State, Metall. Trans., 22A, pp. 957–981.

[2] Sirong, Y., Dongcheng, L., Kim, N. (2006): Microstructure Evolution of SIMA Processed Al 2024 Alloy; Mater. Sci. Engg. A, 420, p. 165–170.

[3] Shrikanth, Mandhulika, Sharma, Ashok (2009): In pursuit of Advanced Technologies- Semi-Solid Metal Processing; Foundry May/ June, pp. 75–83.

[4] Pandya, Divyesh Y., Shrikanth, Mandhulika, Sharma, Ashok (2008): The Effect of Strain Induced Melt Activation (SIMA) on properties of Al-7Si-0.4Mg alloy; Presented in International conference ALUCAST 2008 (Theme - Die Casting Industry in Pursuit of Excellence), 11–14 Dec. (2008) Chennai, pp. 93–97.

[5] Young, K. P., Kyonka, C. P., Courtois, F.: Fine Grain Metal Compositions. United States patent 4415374, p. 1983.

[6] Kirkwood, D. H. (1994): Semi-Solid Metal Processing; Int. Mater. Rev., Vol. 39, p. 173–189.

[7] Kirkwood, D. H., Sellars, C. M., Elias-Boyed, L. G.: Thixotropic materials. European patent.0305375 B1, p. 1992.

[8] Bolouri, A., Shahmiri, M., Cheshmeh, E. N. H. (2010): Microstructural evolution during semi-solid state strain induced melt activation process of aluminum 7075 alloy , Trans. of Non Ferrous Met. Soc. of China, Vol. 20, pp. 1663–1671.

[9] Yalin, L., Miaoquan, L., Young, N., Xingcheng, L. (2008): Microstructure and Element Distribution During Partial Remelting of An Al- 4 Cu- Mg Alloy; Jr. of mat. Engg. & performance, Vol. 17, No. 1, pp. 25–29.

Investigation of ironing process depending on applied tool materials and coatings

Preiskava procesa stanjševalnega vleka v odvisnosti od uporabljenih materialov za orodja in prevleke

Dragan Adamović[1], Vesna Mandić[1,*], Milan Terčelj[2], Milentije Stefanović[1], Miroslav Živković[1]

[1]Faculty of Mechanical Engineering in Kragujevac, s. Janjic 6, 34000 Kragujevac, Serbia
[2]University of Ljubljana, Faculty of Natural Sciences and Engineering, Aškerčeva 12, SI-1000 Ljubljana, Slovenia

*Corresponding author. E-mail: mandic@kg.ac.rs

Received: March 7, 2012 **Accepted:** April 24, 2012

Abstract: Friction has significant influence, both on geometrical, kinematic and dynamic conditions of metals forming execution and on tool life; in that way, it influences the continuity of production. One of the methods for enabling the reduction of friction resistance (and in that way the influence on product quality) is the selection of properties of outer layers of the tool. Unlike machine elements, where it is possible to select a wide range of contact couples materials, in the case of ironing process one of contact couples elements – strained material – is determined in advance. The only thing that can be changed here, in certain limits, is tool material (die and punch) or various thermochemical procedures can be applied, as well as hard coatings etc., by which chemical content of surface layers is changed. In this paper, we will present the experimental results obtained by modelling ironing process by application of proper technological lubricants, use of anti-adhesion coatings on tools (coating TiN and hard coating Cr), selection of suitable type of tool materials (tool steel, hard metal) etc. The obtained results indicate that friction resistance can be reduced to a large extent, which will also minimize tool wear.

Izvleček: Trenje ima velik vpliv tako na geometrijske, kinematične in dinamične pogoje preoblikovanja kovin kot tudi na trajnostno dobo orodij

Preliminary notes

in s tem tudi na kontinuiteto proizvodnje. Ena od metod, ki omogoča zmanjšanje trenjskega upora (s tem tudi vpliva na kvaliteto izdelka), je prava izbira površinskih plasti orodja. Nasprotno od strojnih elementov, ki jih lahko izbiramo iz širokega nabora materialov, pa je pri postopku stanjševalnega vleka eden od materialov, ki je v kontaktu, to je materal, ki se preoblikuje, določen vnaprej. Z določenimi omejitvami lahko pri stanjševalnemu vleku spreminjamo material, iz katerega je narejeno orodje (matrica in pestič), ali pa uporabimo različne termokemijske postopke, kot tudi trde prevleke itd., pri katerih se kemijska sestava površinskih plasti spreminja. V tem prispevku so prikazani eksperimentalni rezultati, ki so bili dobljeni pri modeliranju postopka stanjševalnega vleka z uporabo ustreznih tehnoloških maziv, z uporabo prevlek, ki so protiadhezijske (oplaščanje TiN in trda prevleka Cr), z izbiro ustreznih materialov za orodja (orodno jeklo, trdnina) itd. Dobljeni rezultati nakazujejo, da je mogoče bistveno zmanjšati trenje in s tem tudi obrabo orodja.

Key words: ironing, coatings, friction, wear, tools
Ključne besede: stanjševalni vlek, prevleke, trenje, obraba, orodja

Introduction

High intensity of tool wear in metal forming (MF) is the reason why tool life problem is getting the increasing attention. Together with the advancement of tool wear process, which mainly reflects the change of dimensions and form, the product quality deteriorates, and the obtained products have major dimensional deviations, worse surface quality and even visible errors in the form of notches and nodes. [1] Tool life also influences the reliable functioning of the machines or forming systems. Frequent replacements of tools lead to unavoidable standstill of machines which also influences productivity decrease, and therefore the production costs. Tool wear process is very complex, and, and tool fracture can be caused by several reasons which act together. Tool wear process is influenced not only by friction appearance, but also by other processes, such as: fatigue (thermal and mechanical), corrosion and oxidation. Therefore, tool wear for MF will be the result of the superposition of all physical processes which act upon the tool; consequently it will be more intense than it would have been if it were influenced only by friction process course.[2]

In tools intended for cold MF, the following types of wear are dominant:

- adhesive,
- abrasive and
- fatigue (crumbling).

However, abrasive wear is considered as the significant process which determines tool life for MF.

Intensive tool wear in ironing processes results from the fact that the entire work surface of the tool is in constant contact with the material being formed. From that reason, wear intensity is higher when compared with other tools. Wear cases for this kind of tools can be divided into following types:[3]

- adhesive wear which manifests as the appearance of adhesive particles ("bulges"),
- micro and macro cracks,
- crumbling and
- the appearance of material loss in the form of ring, which is the effect of abrasive wear.

The most influential type of wear for this kind of tools is the appearance of so called annular damage on work (conic) surface for compression, which eliminates the conditions for normal forming and causes the appearance of additional friction resistance and significant increase of drawing force.[1]

Such mechanism of tool wear is the consequence of material flow kinetics and distribution of pressures in cone for compression. The material being compressed achieves the largest straining in the entrance cone zone, which is why the highest unit pressures are created there. Furthermore, all impurities, oxides etc. remain on work edges at the entrance into the cone tool part; those impurities can act as abrasives which cause abrasive wear characterised by high intensity; therefore the contact of partly formed material of released oxide and tool material occurs in the central part of the cone.

The increase of tool life for MF can be accomplished by:[3]

- replacement of tool steels used so far with materials with better resistance properties, which are also much more expensive,
- application of properly selected methods of surface forming which enable the obtaining of desired surface layer properties, especially higher resistance to wear,
- application of suitable technological lubricants.

The deficit of alloying elements and, particularly, their high price are the reasons why high-alloyed steels are applied only in special cases and for heavily loaded tool elements. That is why effective and efficient increase of tool durability can be accomplished by surface forming. By using this solution for the problem of short durability of productive tools, friction and wear processes, as well as processes of fatigue, oxidation and corrosion are mainly localised on surface layers, so they are

the only ones required to have higher resistance to wear, thermal fatigue, oxidation, corrosion etc.; thus, it is not necessary that the entire tool has those properties.

In the course of searching for optimal properties of surface layers, nowadays we have at our disposal several forming methods which enable accomplishment of useful contact couples properties. In addition to the mechanical forming where the improvement of tribological properties is achieved, mainly, as the result of increase of outer layers hardness (e.g. pressing procedures), in other cases one of the important goals of surface forming is the change of chemical content (e.g. by enriching with ingredients, such as: carbides Cr, carbides B, nitrides Al, Ti, Cr, Mo, V etc.) due to which a significant increase of resistance to abrasive wear is accomplished. It has been determined, as the result of many investigations, that finely-dispersed hard phases (e.g. carbides, nitrides etc.) are the most resistant to abrasive wear.[4]

Galvanic forming represents a special group of surface layers modifications. It includes the procedures such as: hard chromium-coating, phosphating etc.[5]

Coating obtained by hard chromium-coating is characterised by relatively high hardness (1000–1200 HV), as well as by characteristic grid which represents natural canals for lubrication. The result of such surface layers forming is the significant increase of resistance to wear.

With the aim of obtaining good tribological properties, both at room and at increased temperature, plasma technologies were developed which involve applying coatings of hard soluble metals such as: Cr, W, Co, Ti or their compounds TiN, TiC etc.[6]

The group of methods for surface forming which are also worth the attention also includes also electro-polishing and chemical polishing. The result of polishing is the removal of defective surface layers made at preceding forming (e.g. forming by cutting) and new surface layers are obtained which are characterised by significantly less roughness and lower or very low levels of their own stresses. Surface layers obtained as the result of these processes are characterised by considerably smaller friction coefficient, increase of resistance to abrasive wear and to corrosion.[7]

Experimental investigations

Experimental investigations in this paper were conducted on the original model of ironing, which is characterised by a double sided simulation of the contact zone with the punch and die.[8]

This model enables realization of the high contact pressures and respects the physical and geometrical conditions of the real process (die and punch materials, topography of the contact surfaces, the die cone angle (α) etc.). The scheme of the mentioned model is shown in Figure 1.

The dies are placed in holders, where the left hand holder is fixed and the right hand holder is moving together with the die. The punch consists of the body 3 and the front 4, which are mutually connected by the pickup with the strain gauges 5.

The bent strip of thin sheet 7, in the U shape, (test-piece) is being placed on the "punch". The strip is being acted upon by "dies" 2 with force F_D. Test-piece is passing (sliding) between dies, by the action of the force F_{ir} on the punch front, when the sample wall is being ironed. During passing through, the external surface of the sample is sliding along the die surface, which is inclined for an angle α, while the internal surface of the sample is sliding over the plates 6, which are fixed to the punch body.

The device was made with the possibility for an easy substitution of the contact – pressure elements (die 2 and plates 6), easy cleaning of the contact zones and convenient placing of samples.

Plates 6 and dies 2 can be made of various materials, as well as with various

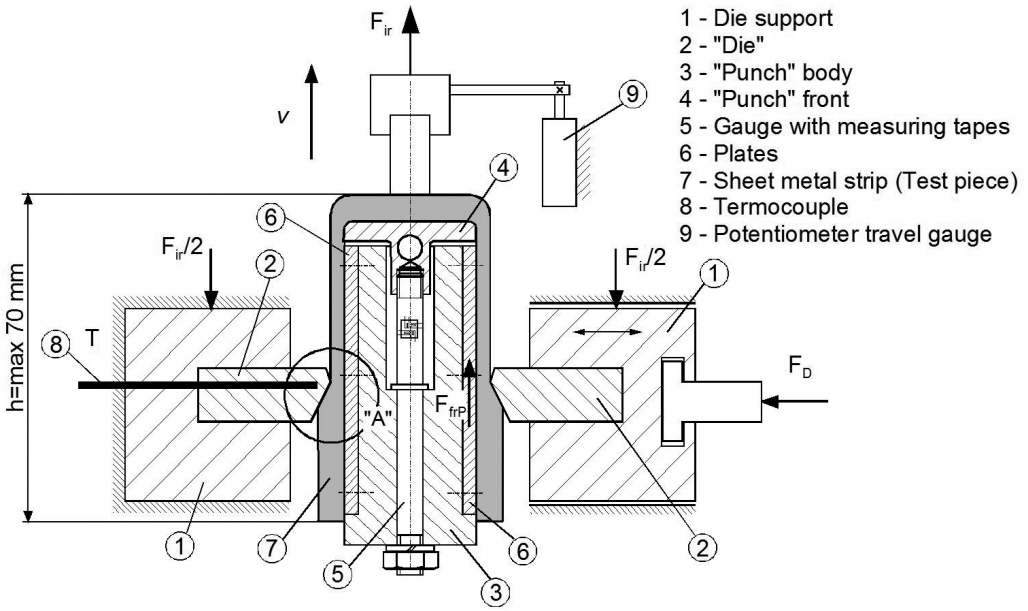

Figure 1. Scheme of model used in this paper

roughnesses, while dies can have various slope angle α.

The total ironing force F_{iz} represents the sum of the force of friction between punch and work piece, F_{trI} and force which acts upon the test piece bottom F_z, i.e.:

$$F_{iz} = F_{trI} + F_z \tag{1}$$

Force F_{iz} is measured on the device itself, and the friction force on the punch side F_{trI} is registered by means of gauge with measuring bands.

The friction coefficient on the punch side, taking into account that it changes according to *Coulomb*'s law, can be calculated on the basis of the following expression:

$$\mu_I = \frac{F_{trI}}{2 \cdot F_D}, \tag{2}$$

and friction coefficient on die side by the expression:

$$\mu_M = \frac{F_{iz} \cdot \cos\alpha - 2 \cdot F_D \cdot \sin\alpha}{F_{iz} \cdot \sin\alpha + F_D \cdot \cos\alpha}, \tag{3}$$

Knowing the dependency of forces F_{iz} and F_{trI} on sliding path h, it is possible to determine the friction coefficients (μ_M and μ_I) in function of sliding path on the basis of previous expressions.

On the mentioned device it is also possible to simulate consecutive (multi-phase) ironing, when one sample is passing between the contact pairs several times.

The device for ironing is installed on a special machine for thin sheet testing ERICHSEN 142/12.

For experimental investigations in this paper, the low carbon steel sheet, tempered by aluminium, Č0148P3 (WN: 1.0336; DIN: DC 04 G1/Ust 4, Ust 14) was chosen. It belongs into a group of high quality sheets aimed for the deep drawing and it has properties prescribed by standard SRPS EN 10130:2004.

For the die and punch material, the alloyed tool steel (TS) Č4750 (WN: 1.2601; DIN17006: X165CrMoV12; EN: X 160 CrMoV 12 1) was selected, while one set of dies was made of the hard metal. In order to improve the surface, a certain number of dies and of punches – their working surfaces – were coated by chromium (Cr) or titanium nitride (TiN). In experiments, pairs of dies and punches made of the same materials were always used, e.g., D-TS/P-DS or D-TS + Cr/P-TS + Cr, with exception of the hard metal die, which was always used with the punch made of tool steel.

The special attention was devoted to material characteristics in the sheet rolling direction (0°), since the tested

Table 1. Properties of tools and test piece materials

		Material	Mechanical properties
Tool	Die (D)	TS* TS + Cr plate TS + TiN plate HM**	TS Hardness 60÷63 HRC HM Hardness 1200 HV30
	Punch plate (P)	TS* TS + Cr plate TS + TiN plate	
Test-piece		Č0148P3 (WN: 1.0336; DIN: DC 04 G1/Ust 4) Thickness: 2.0 mm width: 18.6 mm	R_p = 186.2 MPa R_m = 283.4 MPa A_{80} = 37.3 % n = 0.2186 r = 1.31915
* - TS – Tool steel, Č4750 (DIN17006: X165CrMoV12) ** - HM – Hard metal, WG30 (DIN4990: G30)			

samples were cut in that way, (SRPS C.A4.002:1986) which was applied using specimens in rolling direction. Material characteristics for test-piece were determined. Values are shown in Table 1. Tests have been performed under laboratory conditions (v = 20 mm/min, T = 20 °C).

Results and discussion

The investigations performed on tribo-model of the ironing process made it possible to estimate the influence of surface tool layers (die and punch) on the progression of ironing process (drawing force, friction coefficient on die and punch, wall tension stress etc.).

The change of mean value of drawing force in dependence on blank holding force at various surface states of the tool is given in Figure 2. The increase of blank holding force leads to the increase of the mean value of drawing force similarly for all the states. Application of both the tool without coating (TS) and with chromium coating (TS + Cr) leads to similar values of drawing force, which are somewhat smaller than the ones obtained by tools with coating TiN (TS + TiN) and hard metal (HM). These results suggest somewhat lower compatibility between tools, both with the coating TiN and hard metal with mild steel sheets, compared to the tools with Cr coating and tool steel. Using the tool with TiN coating on the surface of mild steel sheets led to the small scratches at first, which sometimes grew into rough cuts on the metal sheet surface. The higher forming degree there was (bigger holding force and bigger angle of die gradient), the more frequently those rough cuts appeared on the metal sheet

surface. This can be also confirmed by greater differences in mean ironing force in those conditions.

The change of mean value of drawing force in dependence on die gradient angle, when tool material is the parameter, is given in Figure 3. Drawing force increases with the increase of die gradient angle. At smaller die cone angles, that increase is more intensive than at bigger angles.

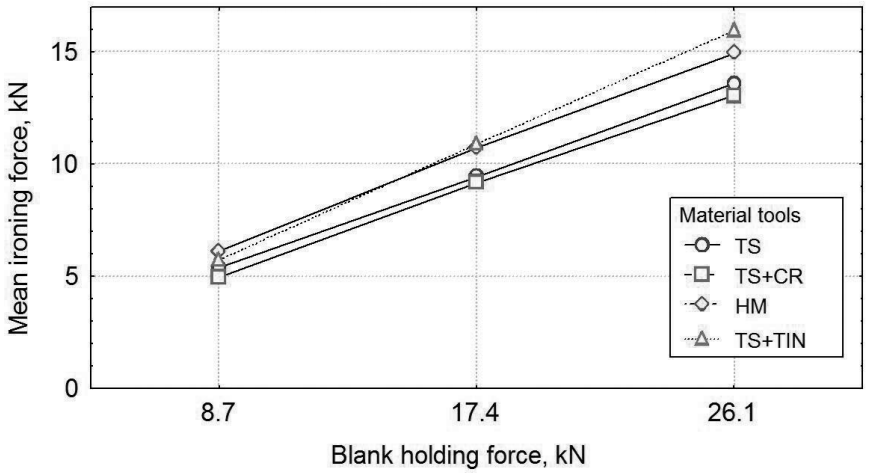

Figure 2. The change of mean value of drawing force in dependence on blank holding force at various tool materials

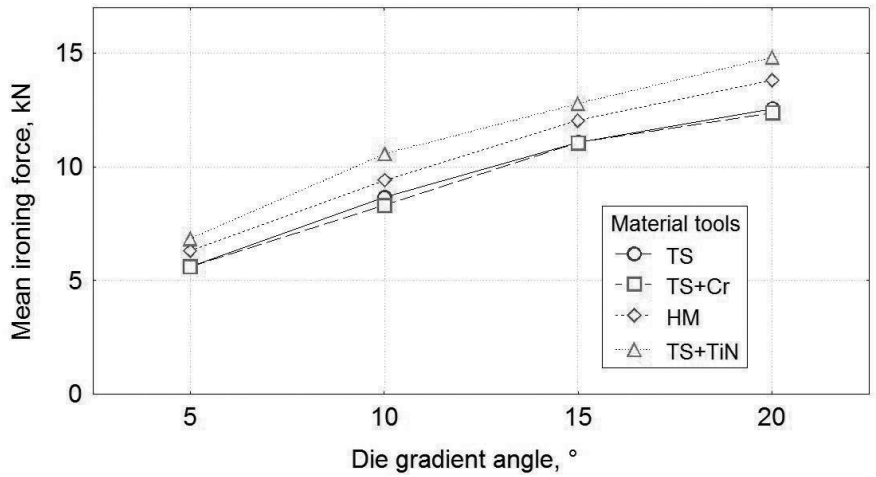

Figure 3. The change of mean value of drawing force in dependence on die gradient angle for various tool materials

Mean values of drawing force for various tool materials are given in Figure 4. The tool with hard chromium coating (TS + Cr) proved to be the best (the smallest value of drawing force). Somewhat worse results were obtained by using the tool of alloyed tool steel (TS), hard metal (HM) and coating TiN (TS + TiN), respectively.

Figure 5 shows the change of friction coefficient on die side in dependence on blank holding force and die gradient angle at various tool materials. The smallest friction coefficient was obtained by using the tool with hard chromium coating at all angles of die gradient. Somewhat higher values were obtained with alloyed tool

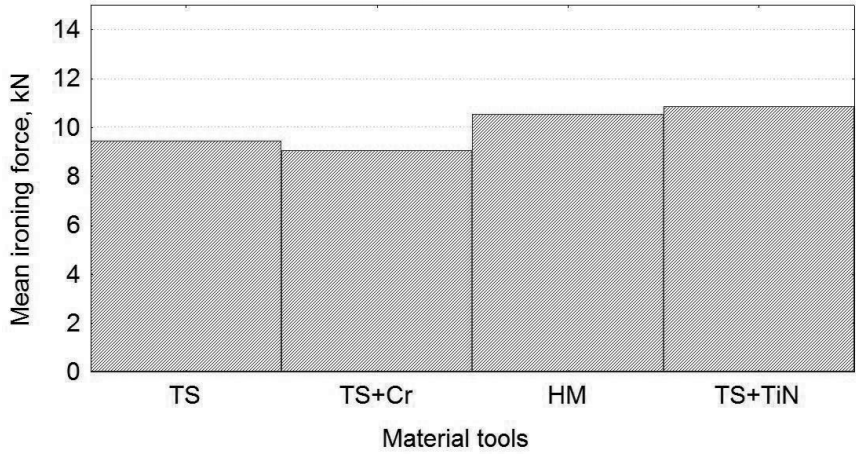

Figure 4. Mean value of drawing force for various tool materials

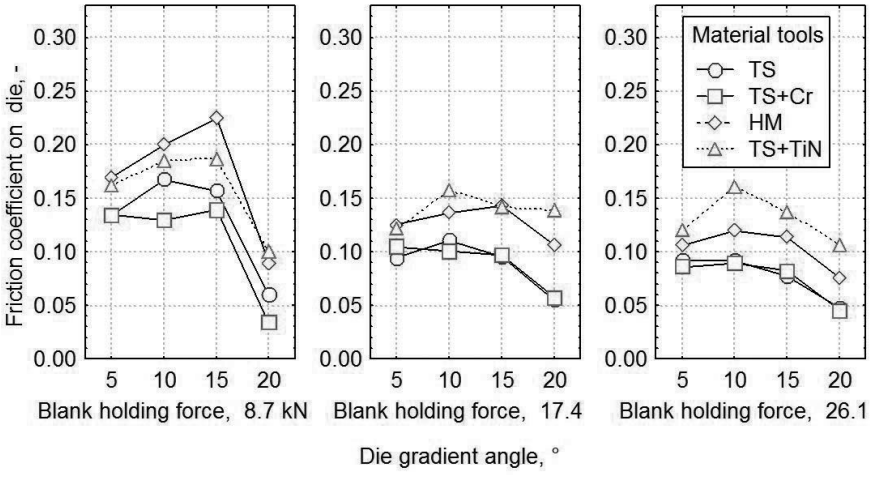

Figure 5. Change of friction coefficient on die in dependence on die gradient angle and blank holding force for various tool materials

steel, and the highest values were obtained with tools of hard metal and titan-nitride coating. Changes in friction coefficient values on the die side varied a lot, from very low values of 0.05, up to significantly higher ones of 0.23.

The examples of change of friction coefficient on die side on sliding path at ironing with various tool coatings are given in Figure 6. Instability and higher friction coefficient on the slide path indicate to the occasional impairment of contact conditions.

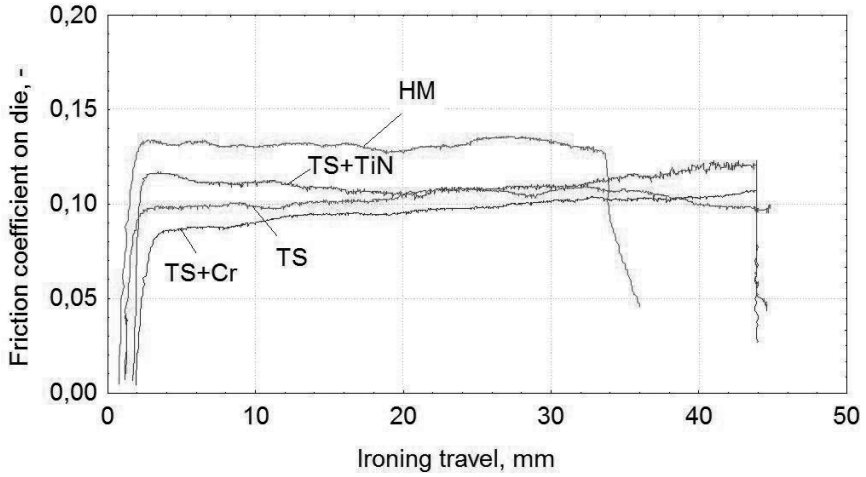

Figure 6. Friction coefficient for various tool materials

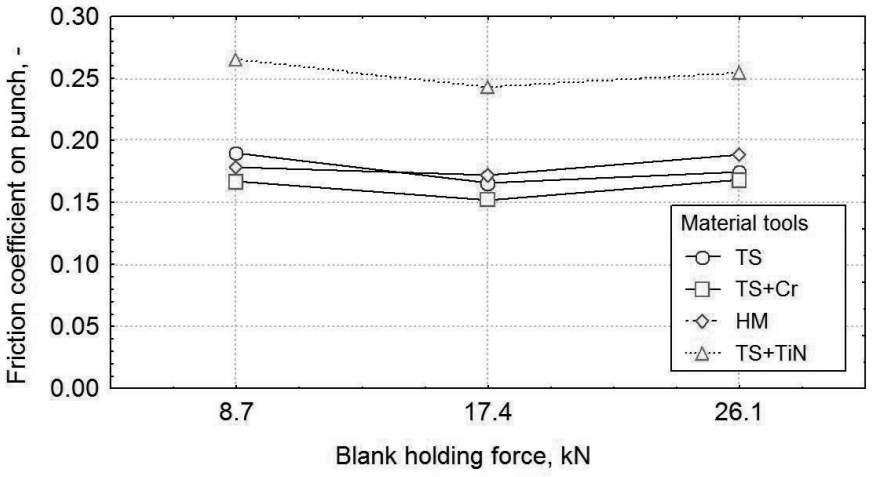

Figure 7. Chang of friction coefficient on punch in dependence on blank holding force at various tool materials

The change of friction coefficient on punch in dependence on blank holding force, for various tool materials, is shown in Figure 7. For steel samples, for all tool materials, friction coefficient will decrease in the beginning, with the increase of blank holding force, and then it will start increasing with further increase of blank holding force. The highest value of friction coefficient is obtained by using the tool with titan nitride coating (TiN).

The influence of tool material on friction coefficient on punch at various die gradient angles is shown in Figure 8.

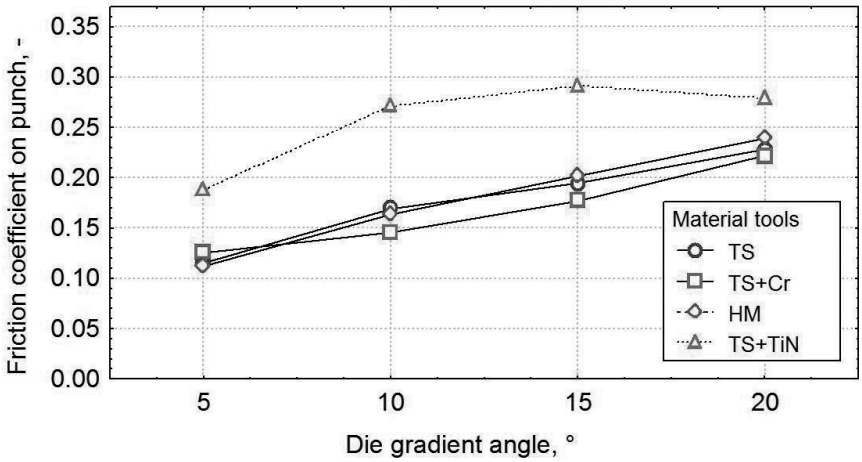

Figure 8. The change of friction coefficient on punch in dependence on die gradient angle at various tool materials

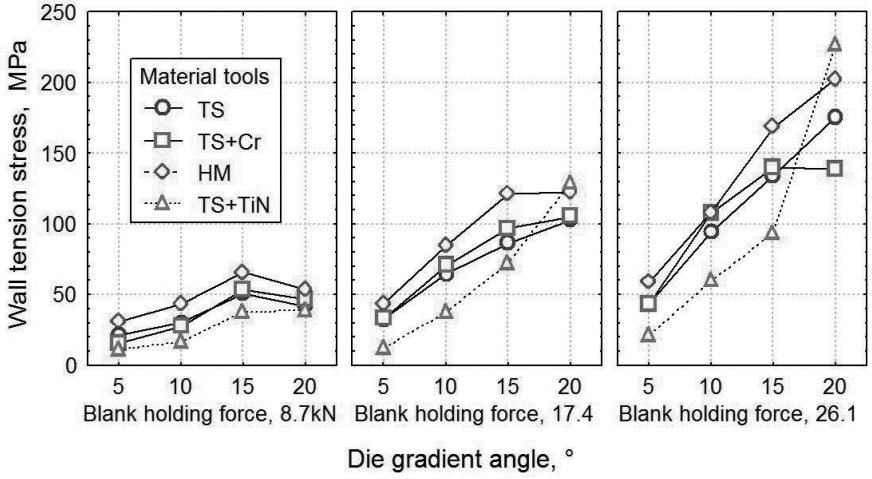

Figure 9. Change of wall tension stress independence on die gradient angle and blank holding force for various tool materials

By using the tool of tool steel (TS), with chromium coating (TS + Cr) and hard metal (HM) at the increase of angle α, friction coefficient constantly increases and that connection is almost linear. The values for TS and HM are almost identical, which is understandable, because the tool is marked with HM, i.e. HM/TS, i.e. Punch plate is made of tool steel. The tool with hard titan nitride coating (TS + TiN) gives significantly higher values of friction coefficient.

Figure 9 shows the change of wall tension stress in dependence on die gradient angle and blank holding force for various tool materials. The smallest values of wall tension stress are obtained with tools with TiN coating, and the highest values are obtained with tools of HM. Regarding aluminium alloy samples, the smallest wall tension stress is obtained by using the tool of alloyed tool steel (TS), and the largest one is obtained with tool of hard metal (HM).

The specified diagrams show that at small blank holding forces, with the increase of die gradient angle above 15°, the decrease of wall tension stress occurs. At larger blank holding forces and larger die gradient angles, stress differences become more significant compared with the ones obtained at small blank holding forces and small die gradient angles.

Contrary to the friction of die side which is damaging and which needs to be as low as possible, the friction of the punch is useful and its increase to a certain value is well justified. Higher values of the friction coefficient on the punch side lead to the decrease of wall tension stress, and in this way to the increased possibility of forming without damaging the material. According to all abovementioned, we can say that higher values of friction coefficient on the punch side, obtained using punch-tool with TiN coating were more beneficial than other conditions of punch surface.

Conclusions

One of the methods which enable the reduction of friction resistance (and in that way the influence on product quality) is the selection of properties of tool surface layers. However, it should be emphasised that, unlike machine elements for which it is possible to select the a wide range of contact couples materials, in the case of MF process, one of the contact couple elements – strained material – is determined in advance. The only thing that can be changed, in certain limits, is the tool material or various procedures of thermo-chemical forming, galvanisation etc. can be applied, which change the chemical content of surface layers.

The device presented in this paper can be used to assess the behavior of tool surface layers, dies and punch for ironing. It is sensitive enough for comparative examinations of compatibility between different types of ironing tools with formed metal sheet.

Through comparative examination of tool, die and extruder, made of tool steel (TS), tool steel with Cr coating (TS + Cr), hard metal (HM) and tool steel with titanium nitride (TS + TiN) during the ironing of mild steel, following conclusions were reached:

- The lowest ironing force was obtained while using the tool with Cr coating (TS + Cr). Using tool steel (TS), extrusion force was somewhat higher (about 5 %), whilst using hard metal (HM) led to even higher values (about 16 %). The tool with hard coating (AC + TiN) had the lowest compatibility. Obtained ironing force was about 20 % higher compared to the force obtained from the tool with hard Cr coating.
- Besides its dependence on the other parameters of forming process (angle of die gradient, forming degree, type of lubricant, roughness of the tool surface, etc), change in friction coefficient, both on the die and punch, also depends on condition of the tool surface layers and it is completely adequate to the change of ironing force.

Acknowledgements

The part of this research is supported by Ministry of Education and Science, Republic of Serbia, Grant TR32036 and TR34002.

References

[1] Avitzur, B. (1983): *Handbook of Metal-Forming processes*, JOHN WILEY & SONS Inc., New York, 1983.

[2] Karlsson, P., Gaard, A., Krakhmalev, P., Bergstrom, J. (2010): *Galling resistance and wear mechanisms for cold work tool steels in lubricated sliding against high strength stainless steel sheets*, Proceedings of the 4th International Conference on Tribology in Manufacturing Processes (ICTMP 2010), Nice, France, June 13th – 15th, 2010, 673–679.

[3] Dohda, K., Kawai, N. (1990): *Compatibility Between Tool Materials and Workpiece in Sheet-Metal Ironing Process*, J. Tribology, Volume 112, Issue 2, 1990., 275–282.

[4] Gierzynska, M. (1983): *Tarcie* zużycie *i smarowanie w obrobce plastycznej metali*, WNT, Warszawa.

[5] Pesch, P. (2003): *Performance of Hard Coated Steel Tools for Steel Sheet Drawing*, Journal of Surface and Coatings Technology, Vol. 163–164, pp. 739–746.

[6] Dohda, K. (1990) *Tribological prop-*

erties of thin hard coatings used in metal forming, Proceedings of the Japan International Tribology Conference, Nagoya, pp 1973–1980.

[7] Lindvall, F., Bergstrom, J., Krakhmalev, P., Bay, N. (2010): *The Influence of Grinding and Polishing Procedure of Tool Steels in Sheet Metal Forming*, Proceedings of the 4th International Conference on Tribology in Manufacturing Processes (ICTMP 2010), Nice, France, June 13th – 15th, 603–613.

[8] Adamovic, D. (2002): *Conduct of materials in contact at processes of plastic forming with high working pressures*, Doctoral thesis, The Faculty of Mechanical Engineering, Kragujevac, (in Serbian).

Contribution of Mn content on the pressure dose properties

Prispevek vpliva deleža Mn na lastnosti tlačnih doz

Jožef Medved[1], Tomaž Godicelj[2], Stanislav Kores[1], Primož Mrvar[1] & Maja Vončina[1,*]

[1]University of Ljubljana, Faculty of Material Science and Engineering, Department of Materials and Metallurgy, Aškerčeva 12, SI-1000 Ljubljana, Slovenia
[2]Talum d.d. Kidričevo, Tovarniška cesta 10, 2325 Kidričevo, Slovenia

*Corresponding author. E-mail: maja.voncina@omm.ntf.uni-lj.si

Received: May 28, 2012 **Accepted:** July 17, 2012

Abstract: For the pressure dose manufacture electrolytic aluminium and its alloys are used. With the purpose of improvement of the material properties and production rationalization, the optimal composition of the alloy must be achieved to reach good formability and mechanical properties with the best exploitation of the material.

The aim of this work was to analyse the properties of three alloys according the AA standard: 1050, 3002 and 3003 which are used in dose production. The investigation was made using computer simulation of phase equilibrium with Thermo-Calc program, optic and electron microscopy and technological testing. The Mn content in mentioned alloys influences the phase equilibrium as the content of the phases on base of Mn increases, increases the strength properties and raises the recrystallization threshold. Inclusions are at the longitudinal courses always longitudinal distributed (course of the impact extrusion) and of polyedric shape; on the bottom of the pressure dose (Pos.1), the inclusions can be found in bigger heaps. The results show that the hardness, deformation pressure and crack pressure increase with the increasing Mn content in the alloy.

Izvleček: Za izdelavo tlačnih doz se uporablja elektrolizni aluminij in njegove zlitine. Za izboljšanje lastnosti materiala in racionalizacije izdelave je treba zagotoviti optimalno sestavo zlitine tako, da bi dosegli dobre preoblikovalne in mehanske lastnosti ob čim manjši potrebni količini materiala.

Preliminary notes

Namen dela je bila analiza lastnosti treh zlitin po AA-standardih 1050, 3002 in 3003, ki se uporabljajo za izdelavo tlačnih doz. Preiskave zlitin so obsegale računalniško simulacijo faznih ravnotežij s programom Thermo-Calc, optično in elektronsko mikroskopijo ter tehnološke preizkuse. Delež Mn v obravnavanih zlitinah vpliva na fazno ravnotežje s povečanjem deleža faz na osnovi Mn, vpliva na povišanje trdnostnih lastnosti in rekristalizacijskega praga. Vključki so pri vzdolžnih smereh vedno vzdolžno razporejeni (smer protismernega stiskanja) ter poliedrične oblike, na dnu tlačnih doz (Poz.1) pa se vključki nahajajo v večjih skupkih. Rezultati so pokazali, da se trdota, deformacijski tlak ter razpočni tlak povečujejo z naraščajočo koncentracijo Mn v zlitini.

Key words: Al-Mn alloys, slugs, thermodynamics, mechanical properties
Ključne besede: Al-Mn zlitine, rondelice, termodinamika, mehanske lastnosti

Introduction

AA 3XXX aluminium alloys find wide applications in the transportation, food, beverage and packaging industries. In these applications, control of the plastic anisotropy of the sheet is of great importance in order to ensure the formability of the final product and to reduce the waste of the material resulting from earing behaviour.[1] Conventionally, aluminium sheet is mainly produced by the direct chill (DC) cast technology. Continuous cast (CC) technology, a new technology, however provides both energy and economic savings while reducing environmental emissions that are more and more urgent issues in today's environment. Compared with DC cast technology, CC technology also takes advantage of high productivity.[2, 3]

Al-Mn alloys, known also as AA 3XXX series, distinguish good formability, corrosion resistance, good weldability and relatively good mechanical properties which make them very wanted alloys.[4] It is often used in a shape of plates and lamellas; they can be extruded or forged whereas their uses are limited.[5]

Slugs are used for the production of aluminium packaging tubes with or without membrane and for aerosol cans. Slugs are round, with or without a hole, surface treatment is tumbled or sandblasted, they can be flat or domed. Once punched, the slugs must go through an annealing process. Slugs and discs are produced from continuously cast and rolled narrow strip. The surface of the slugs must be smooth without obvious cracks.[6]

The type, size and distribution of dispersoids formed during solidification and cooling and during the homogenization process is of great importance.[7, 9] It has strong influences on the deformation behaviour, recrystallization behaviour and mechanical properties of non-heat-treatable 3xxx aluminium alloys. A better understanding of the precipitation behaviour of dispersoids is crucial to the optimization of the chemical compositions, homogenization processes and mechanical properties of the alloys. During annealing at 450 °C, two types of dispersoids precipitate in the alloy. They were identified as a thin elongated $Al_{12}Mn$ phase with a body centred cubic (bcc) structure and an equiaxed plate-shaped or needle shaped[5] Al_7Mn phase with an orthorhombic structure. Both $Al_{12}Mn$ and orthorhombic Al_7Mn dispersoids precipitate in binary 3003 alloy during annealing at temperatures lower than 550 °C. Since both phases are metastable, during annealing at higher temperatures, Al_6Mn dispersoids precipitate as a stable phase. When there were trace levels of Fe and Si impurities in 3009 alloy, in addition to $Al_{12}Mn$ phase, hexagonal α-Al(Mn,Fe)Si phase[8] or plane cubic α-AlMnSi phase[9, 10] was found to precipitate in the alloy. The addition of alloying elements in 3XXX alloys has strong influence on the precipitation behaviour. Fe and Si greatly decrease the solubility of Mn in solid solution and accelerate the precipitation rate. Addition of Cu can also enhance the decomposition of the supersaturated solid solution. Fe favours the precipitation of $Al_6(Fe,Mn)$,[11] while Si favours the precipitation of cubic α-phase, $Al_{12}Mn_3Si$ or $Al_{12}(Fe,Mn)_3Si$ (when Fe is also present) in the alloy. α-Al(Mn,Fe)Si dispersoid, which is considered to be incoherent with the matrix, is a very important phase in 3xxx alloys.[12, 13]

Materials and methods

As an entry material for the production of pressure dose, the slugs of 52.7 mm diameter and 8.6 mm of thickness were used. Three series of pressure doses were made from three various alloys: 1050, 3002 and 3003.

The production process of pressure dose is composed from seven following steps (Figure 1):
(1) impact extrusion → (2) annealing (280 °C) → *(3) interior protection* (140 °C) → *(4) drying of base colour* (200 °C) → *(5) printing → (6) drying of lacquer* (170 °C) → *(7) forming of cupola*

After each of these seven steps, five specimens were taken for further investigations. After the sampling, the specimens were systematically marked.

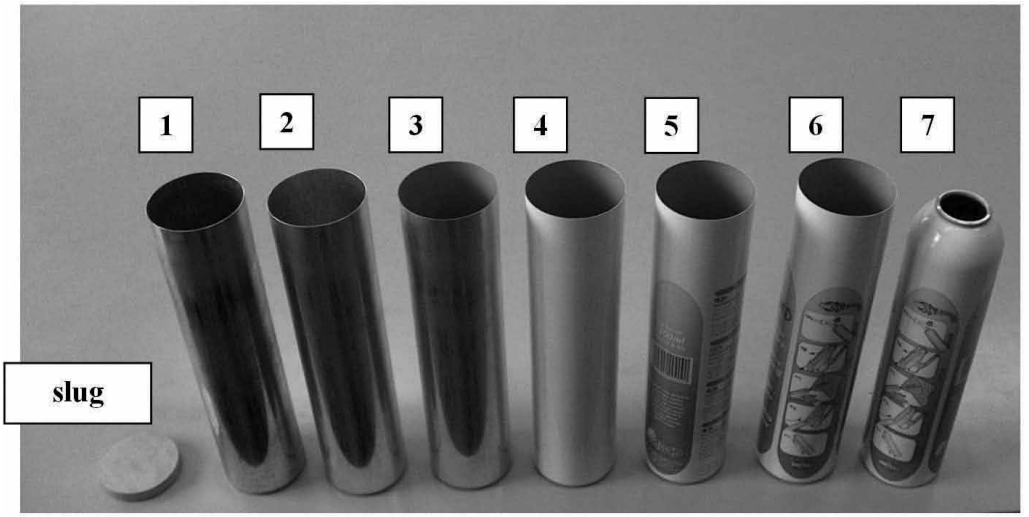

Figure 1. Specimens from the production process of pressure dose

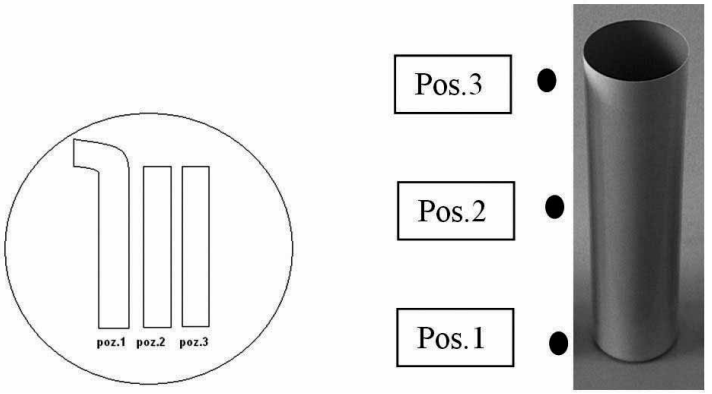

Figure 2. Sampling from the pressure dose

For each composition, the chemical analysis and computer simulation of thermodynamic equilibrium solidification with determination of equilibrium phase composition at room temperature using Thermo-Calc program and database COST507 were made.

Sample preparation for the microscopy

The samples for the microstructure analysis were taken from three places (samples from 1−7): from the bottom longitudinal to the forming course, at the place where the crossing of bottom to the wall was captured (pos.1), 1 cm from the top in a transversal course (pos.3) and longitudinal course (pos.2) according to the course of forming (Figure 2). Sample 0 represents the microstructure of a slug.

Optic microscope OLYMPUS BX61 equipped with video camera DP70 and analySIS 5.0 program was used for the microstructure analysis and the scanning electron microscope JEOL 5610 with EDS electron microanalyzer SUPERPROBE 73 enabled phase analysis.

The hardness was measured using the Brinell test. The test for the determination of deformation and crack pressure was made on a special equipment, that through the fluid causes the pressure from the inside walls of the pressure dose. The pressure is measured with the manometer. When the dose cracks, the manometer senses the swing at otherwise constant pressure increase. The bottom is under higher load as the walls, so it is thicker and in concave shape. It is necessary that the bottom undergoes under the pressure and goes from concave to convex shape, which is detected as a swing on the manometer. At least 12 bar is demanded for the bottom resistance on the plastic deformation. Furthermore, the crack pressure is detected as a sudden drop of pressure on the manometer. At least 18 bar is demanded for the pressure strength of the pressure dose. The cracks always appear on the upper side of the dose in a longitudinal course because of the texture of the crystal grains.

Results and Discussion

Chemical analyses of slugs of all three alloys were conducted in the laboratory for quality control of Talum d.d. company and are presented in Table 1.

Computer simulations of thermodynamic equilibrium solidification, equilibrium phase diagram (Figure 3) and equilibrium phase concentration at room temperature were made using Thermo-Calc program for all investigated alloys. For input data the results from the chemical analyses were used (Table 1).

The mass percent of inclusions (Al_6(FeMn) and AlMnSi) is with increasing Mn-content which hardens the alloy (Figure 4).

At room temperature, according to the equilibrium calculation, for the 1050 alloy, the primary phase α_{Al} is composed from 99.99 wt. % Al and the phase Al_6(FeMn) is composed from 74.47 wt. % Al, 15.50 wt. % Fe and 10.02 wt. %

Table 1. Chemical composition of investigated alloys in mass fractions, wt. %

Alloy	Si	Fe	Mn	Zn	Ti	Rest
1050	0.0913	0.2515	0.0016	0.0089	0.0066	99.61
3002	0.0726	0.2159	0.2945	0.0085	0.0545	99.35
3003	0.1917	0.5577	1.0037	0.0087	0.0066	98.21

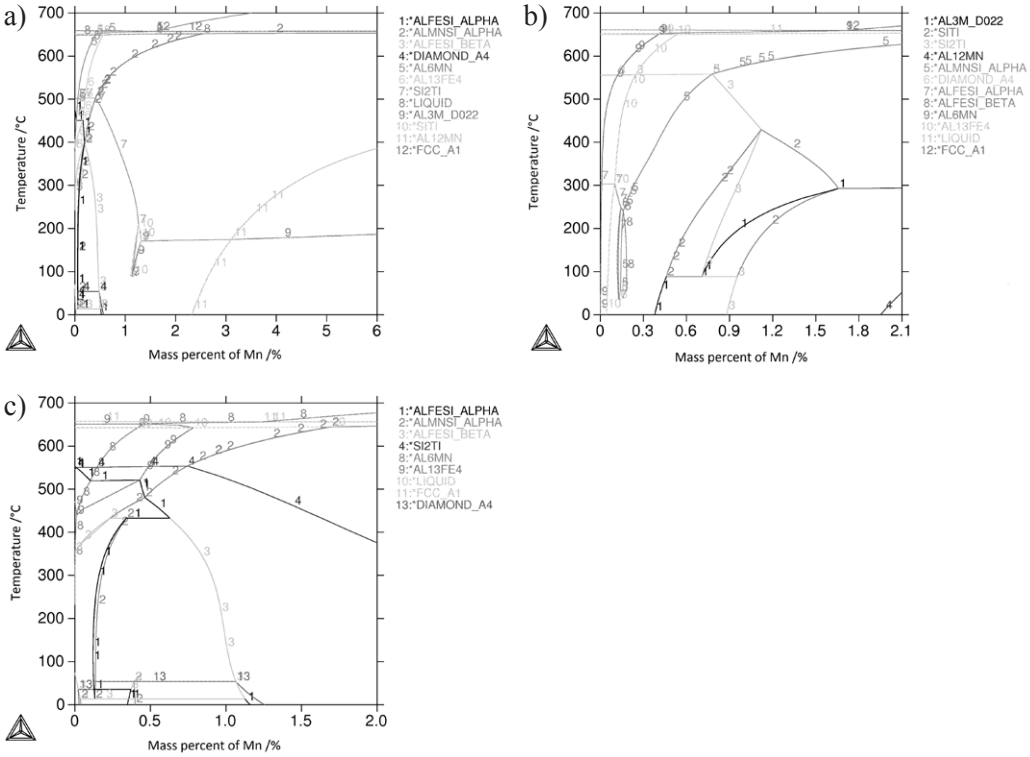

Figure 3. Isoplete equilibrium phase diagram of 1050 (a), 3002 (b) and 3003 (c) alloy

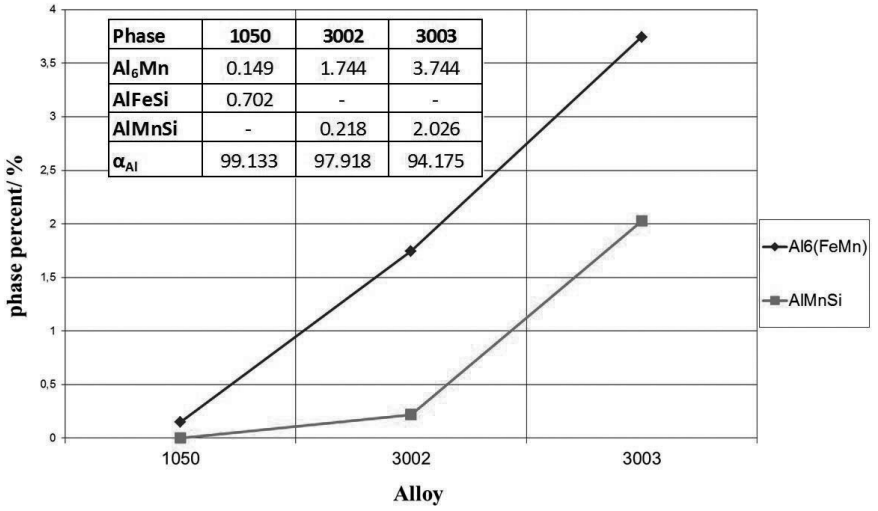

Figure 4. Portion of Al_6(FeMn) and AlMnSi phase in investigated alloys

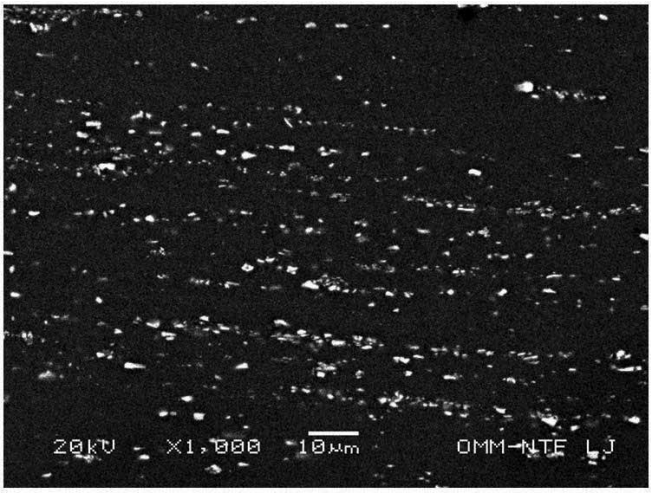

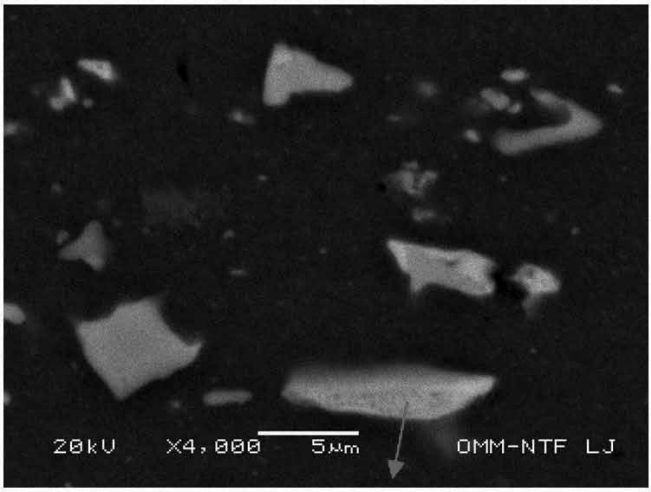

Elt.	Line	Intensity (c/s)	Error 2-sig	Atomic %	Conc		
Al	Ka	914.52	6.048	70.060	53.201	wt.%	
Si	Ka	0.19	0.088	0.021	0.017	wt.%	
Ti	Ka	2.17	0.294	0.112	0.151	wt.%	
Mn	Ka	146.24	2.419	9.944	15.375	wt.%	
Fe	Ka	258.24	3.214	19.723	30.999	wt.%	
Zn	Ka	0.98	0.198	0.140	0.257	wt.%	
				100.000	100.000	wt.%	Total

kV	20.0
Takeoff Angle	35.0°
Elapsed Livetime	100.0

Figure 5. Secondary-electron images of specimen C1 in longitudinal course and the inclusions with chemical analysis

Mn. For the 3002 alloy, the primary phase α_{Al} is also composed from 99.99 wt. % Al, Al_6(FeMn) phase is composed from 74.51 wt. % Al, 12.38 wt. % Fe and 13.11 wt. % Mn. Phase α_{Al} for the 3003 alloy is composed from 99.99 wt. % Al and phase Al_6(FeMn) is composed from 74.48 wt. % Al, 14.90 wt. % Fe and 10.6 wt. % Mn.

Analyses of inclusions

Samples C1 (cold forming) and C7 (final product) were examined with scanning electron microscope. In all samples, inclusions Al_6Mn composed of aluminium, iron and manganese were analysed. The inclusions were in longitudinal courses always longitudinal distributed (course of forming) and of polyedric shape (Figure 5).

Determination of portion and distribution of the inclusions

Metallographically prepared samples were observed at 500-times magnification (Figure 6), which was most representative for the analysis of the inclusion distribution. The inclusions were distributed at the grain boundaries which were most obviously seen at the unformed specimen with 1 wt. % Mn. The share of the inclusion increases with the increasing of Mn content. So at the input material for 1050 alloy, the surface fraction of the inclusions was 0.8 and for the alloy 3003 1.46 %. After the first stage of the cold forming, the inclusions become smaller and with its position do not indicate anymore the grain crystals, but are distributed along the forming course. Further six steps of forming have no further effect on the amount and distribution of the inclusions.

After microstructure analysis, the portion of the inclusions which appears in the investigated alloys was determined (Table 2). It can be observed that the surface portion of inclusions Al_6(FeMn) increases with the increasing of Mn content. Weight portion of inclusions was calculated from the surface portion using the density of Al_6(FeMn) inclusions (3.953 g/cm^3) which also contain some Fe.

The equilibrium, according to the Thermo-Calc program, shows bigger amount of the phase due to the equilibrium precipitation, which in the praxis is achieved only at a very slow cooling**.** The surface (Table 2) does not capture the whole amount of the inclusions. Phases captured at the analysis of surface portion could be intersected at the various cross-sections, so this can present only the comparison.

Microstructure analysis of the grains in polarized light

The samples from the slugs made from 1050, 3002 and 3003 alloys were grinded, polished and electrolytically etched in 5 % HF. From Figure 7 can be seen that at the bigger additions of Mn the crystal grains appear smaller. For the

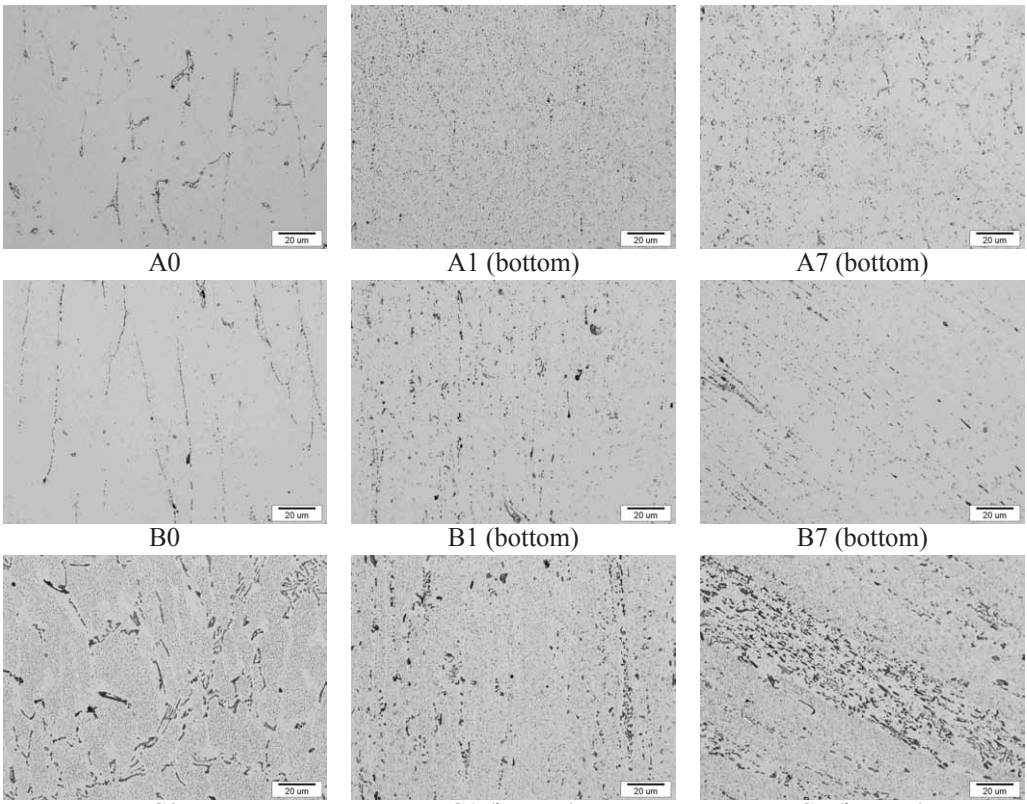

Figure 6. Micrographs of analysed samples

Table 2. Surface portion of the inclusions in investigated alloys

Alloy	Surface portion of inclusions			Portion of inclusions (wt. %)		
	(Pos.1)	(Pos.2)	(Pos.3)	(Pos.1)	(Pos.2)	(Pos.3)
1050	0.38	0.40	0.40	1.502	1.581	1.581
3002	0.60	0.42	0.45	2.372	1.660	1.779
3002	0.84	0.56	0.56	3.321	2.214	2.214

1050 alloy, the grains are 300–600 μm large. For the 3002 alloy, the grains are smaller, only 50–200 μm large and for the 3003 alloy a little bigger, 100–300 μm large. These changes in a grain size could be also consequence of the sampling, how the samples were taken from the slug regarding the impact extrusion respectively. The orientation and the size of the grains could be also a consequence of slug orientation, cut out of casted and formed sheets.

For the samples A1 (after cold forming), A7 (final forming of the pressure dose), C1 and C7 from Figure 8 can be

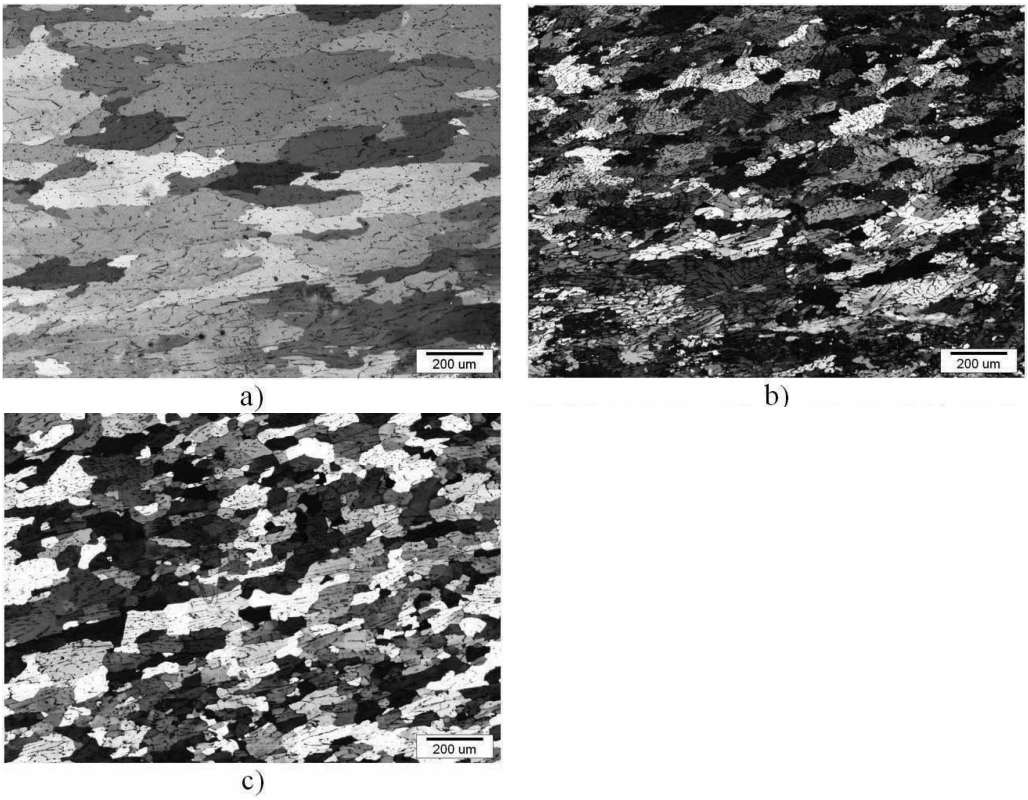

Figure 7. Micrographs of crystal grains in the polarized light: 1050 (a), 3002 (b) and 3003 (c) alloy.

observed that at the 200-times magnification, the crystal grains appear elongated (transformed) among which are equally distributed $Al_6(FeMn)$ inclusions. When the samples A and C are compared, the amount of the inclusions in the microstructure increases as the Mn content increases.

The results of Brinell hardness test are presented in Table 3 and the results of the pressure test in Table 4. Mechanical properties, mainly hardness of the input materials, with the increasing of Mn content increase. From Table 4, it is evident that the deformation pressure and crack pressure also increase with the increasing of Mn content in the alloy.

Table 3. Hardness of annealed alloys after Brinell

Alloy	Hardness HB
1050	20
3002	22
3003	30

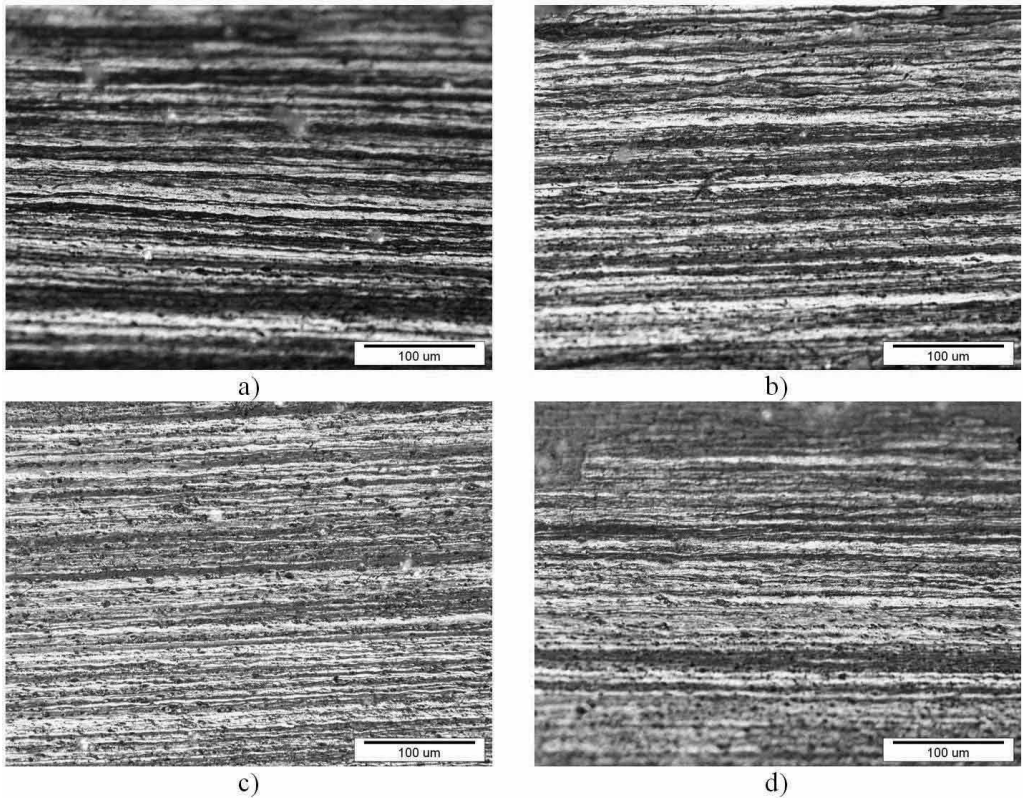

Figure 8. Micrographs of samples A1 (a), A7 (b), C1 (c) and C7 (d).

Table 4. Results from pressure test

Alloy	Wahl thickness [mm]	Bottom thickness [mm]	Deformation Pressure [bar]	Cracking pressure [bar]
1050	0.4	1.1	22	27
3002	0.4	1.1	25	29
3003	0.4	1.1	29	31

Conclusions

From the mentioned investigations, the following conclusions can be made:
Using the microstructure analysis and computer program Thermo-Calc, the amount of the inclusions in defined alloys was analysed. The amount of the inclusions increases from 0.4 % for the 1050 alloy to 0.45 % for the 3002 alloy and to 0.56 % for the 3003 alloy. According to the calculations with the Thermo-Calc program, the amount of the inclusions that could appear in

these alloys at equilibrium conditions was 0.15 % for the 1050 alloy, 1.74 % for the 3002 alloy and 3.74 % for the 3003 alloy.

The crystal grains of investigated alloys appear elongated (transformed) among which are equally distributed inclusions Al_6(FeMn). The concentration of those inclusions is bigger at the edge of the pressure dose and smaller at the middle of the pressure dose. When the specimens A, B and C were compared, it was established that the amount of the inclusions in the microstructure increases as the concentration of Mn in the alloys increases.

In all specimens, the inclusions Al_6(FeMn), composed from aluminium, iron and manganese, were analysed. In the longitudinal courses, the inclusions were always longitudinal distributed and of polyedric shape. At the bottom of the pressure dose (sample C9), the inclusions appear in bigger heaps.

The thickness of the bottom and wall of the pressure dose from various alloys is always the same. The deformation pressure was 22 bar for the 1050 alloy and it increases to 25 bar for the 3002 alloy and to 29 bar for the 3003 alloy. The crack pressure also increases when the concentration of Mn increases from 27 bar to 29 bar and finally to 31 bar.

References

[1] Engler, O. (2012): Control of texture and earing in aluminium alloy AA 3105 sheet for packaging applications, Materials Science and Engineering A, 538, pp. 69–80.

[2] Liu, J., Morris, J. G. (2003): Macro-, micro- and mesotexture evolutions of continuous cast and direct chill cast AA 3105 aluminum alloy during cold rolling, Materials and Engineering A, 357, pp. 277−296.

[3] Liu, W. C., Zhai, T., Morris, J. G. (2004): Texture evolution of continuous cast and direct chill cast AA 3003 aluminum alloys during cold rolling, Scripta Materialia 51, pp. 83–88.

[4] Mondolfo, L. F. (1962): Aluminium alloys: Structure and Properties, Butterworth Co., London.

[5] Martins, J. P., Carvalho, A. L. M., Padilha, A. F. (2009): Microstructure and texture assessment of Al–Mn–Fe–Si (3003) aluminum alloy produced by continuous and semicontinuous casting processes, J Mater Sci 44, pp. 2966–2976.

[6] http://www.talum.si/si/proizvodi/rondelice.php

[7] Liu, W. C., LI, Z., MAN, C. S., RAABE, D., MORRIS, J. G. (2006): Effect of precipitation on rolling texture evolution in continuous cast AA 3105 aluminum alloy, Materials Science and Engineering A, 434, pp. 105–113.

[8] Hatch, J. E. (1990): Aluminum, properties and physical metallurgy, ASM, Metals Park, Ohio.

[9] Li, Y. J., Muggerud, A. M. F., Olsen, A., Furu, T. (2012): Precipitation of partially coherent α-Al(Mn,Fe) Si dispersoids and their strengthening effect in AA 3003 alloy, Acta Materialia, 60, pp. 1004–1014.

[10] Zander, J., Sandstrom, R., Vitos, L. (2007): Modelling mechanical properties for non-hardenable aluminium alloys, Computational Materials Science, 41, pp. 86–95.

[11] Alexander, D. T. L., Greer, A. L. (2002): Solid-state intermetallic phase transformations in 3XXX aluminium alloys, Acta Materialia, 50, pp. 2571–2583.

[12] Li, Y. J., Arnberg, L. (2003): Quantitative study on the precipitation behavior of dispersoids in DC-cast AA3003 alloy during heating and homogenization, Acta Materialia, 51, pp. 3415–3428.

[13] Davis, J. R., Davis & Associates (April 2002): Aluminum and Aluminum Alloys, ASM Specialty handbook, the Materials Information Society, United States of America.

Structural research of Uzbekistan basalts

Strukturne raziskave Uzbekistanskih bazaltov

Abdirahim Ahmedovich Kurbanov[1, *]

[1]Navoi State Mining Institute, Faculty of Chemistry and Metallurgy, 27-a, Yujnaya Street, Navoi City, Uzbekistan

*Corresponding author. E-mail: bo_bosh@mail.ru

Received: March 28, 2012 **Accepted:** July 9, 2012

Abstract: In this article are cited the results of gamma spectrometer research and the structural analysis of basalts Northern Nurata, the West central Kyzylkum, the Tashkent area and Fergana valley of Uzbekistan. Technological parameters and specific features of mineralogical structure of basalt rock are established which define purpose and assortment of output are very important with the development of technology of their processing. Law of change of mineralogical structure with change of a deposit of basalts has been studied by sampling from «Aydarkul», «Asmansay» and «Gavasay» basalt deposits of Uzbekistan. Gamma spectrometry analysis has enabled to define activity of samples of the investigated rocks on unit of the area, and the structural analysis has allowed to estimate and enter criteria of mineralogical structure which determine a degree of suitability of basalts of Uzbekistan for their wider application.

Povzetek: V članku so prikazani rezultati gama spektrometrske raziskave in strukturne analize bazaltov severne Nurate, zahodno-osrednjega Kyzylkuma, taškentskega območja in Ferganske doline v Uzbekistanu. Opredeljeni so tehnološki parametri in lastnosti mineraloške zgradbe, ki določajo namen ter asortiment proizvodnje bazaltne kamnine in so pomembni za razvoj tehnologije njihove predelave. Zakonitosti spreminjanja mineraloške zgradbe v različnih nahajališčih so preučevali na vzorcih kamnine iz nahajališč bazalta Ajdarkul, Asmansaj in Gavasaj v Uzbekistanu. Z gama spektrometrsko analizo so določili aktivnost vzorcev preiskovanih kamnin na enoto površine, s strukturno analizo pa ocenili tiste lastnosti mineraloške zgradbe,

ki opredeljujejo primernost uzbekistanskih bazaltov za njihovo širšo uporabo.

Key words: basalt, mineralogical structure, structural analysis, acid-proof material, rocks specificity
Ključne besede: bazalt, mineraloška zgradba, strukturna analiza, odpornost materiala proti kislinam, posebne lastnosti kamnin

INTRODUCTION

It is considered, that the raw stock of basalts in Uzbekistan makes approximately more than 150 million tons. However, till now stocks of basalt rocks up to the end are not certain, including their structure is insufficiently investigated. According to the State Committee of Uzbekistan on geology the strip propagation of basalts in northern part of the country is stretched along northern a slope of mountains Northern Nurata, from settlement Chimkurgan in the east before the termination of the listed mountains and further proceeds up to Bukantau in the West - in Central Kyzilkum. Basalts of the Tashkent area basically in territory of area Ahangarinsk and Fergana valley basically are located in territory of the Namangan area, and also on frontier areas with the next states - Kirgizstan and Kazakhstan.[1–5] Data cited in the scientific and technical literature show, that purposes of basalt production depend from: chemical compound, physicomechanical properties, mineralogy-petrographic characteristics and structure of basalt rock, and also from the degree of salinity of ground of deposit. In practice, basaltprocessing the enterprises of Uzbekistan, basically special-purpose on release of basalt fibres which are used as heat-insulated material. This circumstance explained weakly investigated of chemical-mineralogical structure and properties of basalt rock, and also absence of effective methods of reception of basalt production. In this question results scale-spectrometer and the structural analysis of basalts in Uzbekistan can play an important role.

The further involving in production of basalt resource raw materials and their development will allow to raise industrial power and to expand assortment of production basaltprocessing enterprises that will promote economic development of our Republic.

On literary data basalts «Aydarkul» deposits on structure answer porphyritic and afirovodolerito to basalts with microdolerit, intersertal structures of basic mass and almonds stone structure.

On the zones most removed from the volcanic device they have glomeroparphyritic structure caused labrador phenocryst and pyroxene. The main mass often hyalopylite without dark-coloured minerals or intersertal. The texture quite often almond-shaped, but the size almonds and their quantity in these basalts noticeably is less 1–2 mm. Micro porphyritic basalts alternate with afiros differences with intersertal or toleyt structures of the main mass in which it is more plagioclase if they among basalts plagioclase , or it is less if among pyroxenes.[4–5]

It is established, that in Northern Nurata basalts are concentrated in reef zone covering Northern foothills - Pistalitau heights, the advanced ridge, Handbandytau, Egarbelitau, Bazaygor and Balyklytau. They are allocated as Chimkurgansk suite D1-D2 about the data established by researches of listed areas. The fullest section vulcanites of considered formation is in Asmansay and in Gavasay where in propagation vulcanites fragments of volcanic crater of the deposits[6] are found out.

Materials and methods

Scale-spectrometer the analysis of basalts

The scale-spectrometer the analysis allows to define activity radionuclids on unit of the area, volume or the sample of ground. For a statistical estimation of results of research have been taken any way on 15 samples rock of «Aydarkul» and «Asmansay» Kyzylkum deposits (basalts of Fergana valley are researched by employees of the center "Composite" of the Tashkent state technical university[7]). As now basalts of Uzbekistan it is extracted by the open cut were researched basically the samples of basalt rocks laying on a surface of the ground, on depth up to three meters. Researches were carried out by means of device Genie-2000, model S500.

In an initial stage definition of active specific efficiency of samples basalt rocks has been made. The analysis was carry out to three stages:

1. Weighing of test in quantity 100 g to Petri dish.
2. Calibration of the device on energy of efficiency with deducing factors, according to the maintenance instruction of the device.
3. Carrying out of the analysis. For this purpose Petri dish with t test establish in lead collimator the detector. After 3 600 s in a panel of the device displayable radionuclid structure rock in the form of spectrum proceeding from which, specific effective activity is defined. Then, start processing the received results.

Table 1. Results scale-spectrometer of basalt rock analysis

№	Place of selection test	Ordinal umbers of samples	K-40 Bq/kg	Ra-226 Bq/ kg	Th-232 Bq/kg	$A_{эфф}$ Bq/kg
1	Aydarkul	1*	2472	93	-	315.48
2	Asmansay	11	2423	28	51	312.91
3	Energy output		1 460.8 keV	609.3 keV	238.6 keV	

*Notice. Sample number 1, "Aydarkul" rocks and sample number 2, "Asmansay" rocks of deposits.

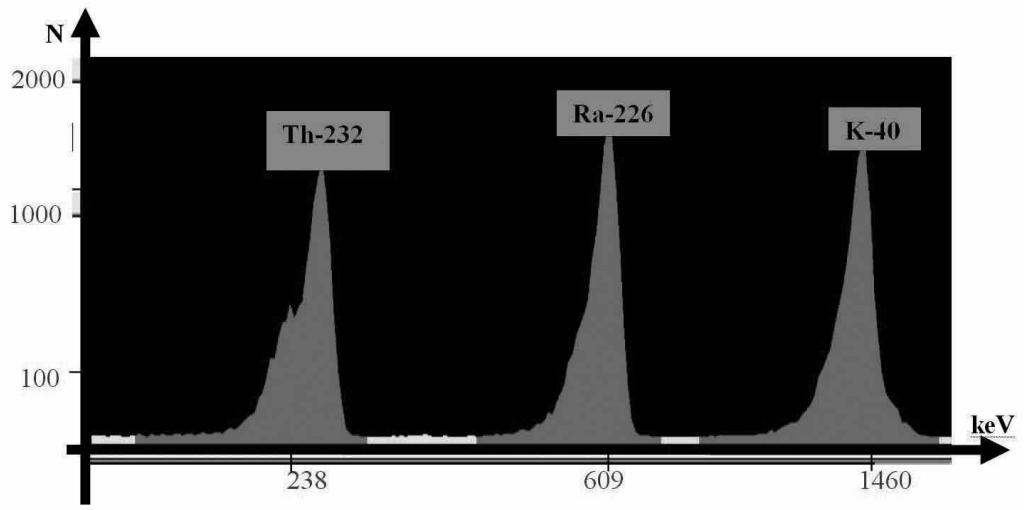

Figure 1. Spectrums natural radioactive nuclides with the image of output energy of nuclides basalts pairs of «Aydarkul» deposits

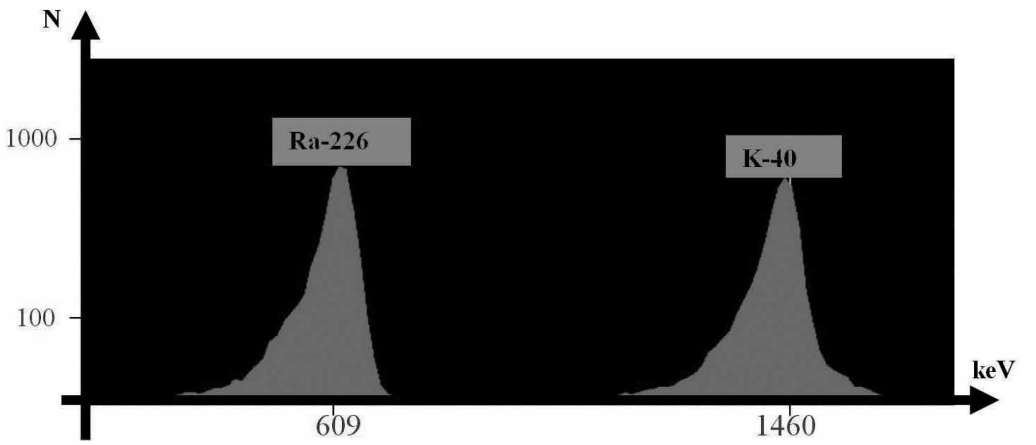

Figure 2. Spectrums natural radioactive nuclides with the image of output energy of nuclides basalts pairs of «Asmansayskoe» deposits

Readout of parameters was made as follows. First each test of rock mass 150 g is exposed to crushing. Then, the received crushed samples are passed through a sieve before reception of fractions in diameter no more than 0.5 mm. For weighing test were used scales VNC-VTI-10. After preparation of 15 tests calibration of device Genie-2000 on energy of efficiency with deducing coefficients, according to the operating instruction. For this purpose the gauge place in the buffer pH, chosen as the first calibrating buffer ***cal 1*** in the menu of the program. The buffer place in a volumetric glass, and after 2 s. displayable ***cal 1*** and procedure of calibration begins.

Results of the received analysis of parameters of test are resulted in table 1.

The result of calibration indications of instrument clearly recognized on corresponding normalized to parameters. The scale-spectrometer was exposed to the analysis each test separately. Activity of test on scale-spectrometry**,** on Bq/kg was defined. Results of research are resulted on Figures 1 and 2.

Results of an experimental research have shown, that the contents of natural radioactive elements in basalt correspond to sanitary norms SAN-PIN-00193-06 according to which the radio-activity of elements not should to exceed 370 Bq/kg. And, in samples of rock «Aydarkul» deposits quantity presence in basalt of element Th-232 was not revealed, that testifies to change of structure of basalts depending on this rock deposit.

Semiquantitative spectral analysis

After end scale-spectrometer analysis samples of basalt rock have undergone to semiquantitative spectral analysis which purpose was research of mineralogical structure of samples of rocks. This method is widely applied to the rock analysis by search and investigation of minerals and allows to study material rocks structure of of deposits.

For carrying out of experiment use special electrodes. The electrodes made from carbon of mark OSCh**-7** in diameter 6 mm, with depth and internal diameter of crater 3 mm, fill test, tineness 0.074 mm. On the working surface of the coal electrode with test dripped solution of a boric acid after that is dried up.[8–9]

Process of the analysis of samples of basalt rock was carry out on spectrograph ISP-30. First before an entrance spectrograph crack install a diaphragm with narrow inclined notch. Then an electrode with test place in an arc support. Evaporation of test and spectrum excitation carries out in an arch of an alternating current as follows.

Establish a diaphragm in position, optimum for allocation volatile elements. Thus, a current of an arch establish on instrument displayable equal 8 A, and the exposition made 30 s. Then a diaphragm move in spectral domain average-volatile elements. Thus constant burning an arch is provided, the size of a current of an arch rises up to 14 A, and the exposition increases up to 60 s. Then, under the same conditions, a diaphragm move in spectral area difficult-volatile elements, and increasing force of current of an arch up to 20 A, spend evaporation of test before its full burning out.

For full identification of spectral lines, after burning test, having established diaphragm in neutral position, photograph spectrum of the arch burning between iron and coal electrodes at force of current 8 A and expositions 10 s. An arc interval between the electrodes, equal 3 mm, support to constants during all experiment then start registration of a spectrum of tests on the photographic plate.

For realization of registration of the tests spectrum of on the photographic plate, last, with spectra of standard samples basalt rock of both deposits photograph separately. The photographic plate, after photographing spectra show, wash out, fix in current 8–10 min, wash out in flowing water 30 min and dry. Then start processing the received data. The given procedure begins with decoding the spectrogram.

Spectrograms were decoded on a spectro-projector. Presence of element in test of basalt rock, establish on the most sensitive lines of the received spectrum. Then it is possible to start an estimation percentage of the element by which it is usually carried out visually. For decoding spectrograms the atlas of spectral lines of making elements of samples basalt rock «Aydarkul» and «Asmansay» deposits was used. Thus the limit of detection of making elements of rock made $(n \times 10^{-4})$–$(n \times 10^{-3})$ %.

It is necessary to note, that comparison of spectral lines was made on intensity of standard lines samples of basalt breed and their tests. Semiquantitative spectra analysis results on revealing mineralogical structure of basalt rock samples are presented in tables 2 and 3. Research of tests was carried out in Central research laboratory of Navoi Mining Metallurgical Combine. For reception full representation about basalts structure of two listed deposits and carrying out of the comparative analysis with basalt rock «Gavasay» deposits have been the analysis of section basalts.

Table 2. Analysis results of basalt rock «Aydarkul» deposit (results × 10^{-3} %)*

№ п/п	Cu	Pb	Zn	Cd	Ag	Bi	Ge	Co	Ni	Tl	Sb	Cr	Mn	V	Ti	Mo	W	Sn	In	As	Yb	P	Ga	J	Sr
1	10	05	n/r	n/r	n/r	n/r	n/r	2	50	n/r	n/r	500	50	20	50	10	n/r	n/r	n/r	n/r	0.1	n/r	<0.2	n/r	20
2	5	05	B	n/r	<0.1	n/r	n/r	1	10	n/r	n/r	20	50	10	10	b	n/r	n/r	n/r	n/r	b	n/r	1	b	20
3	5	<0.5	n/r	n/r	<0.1	n/r	n/r	0.5	20	n/r	n/r	100	20	50	5	10	n/r	n/r	n/r	n/r	0.3	n/r	n/r	1	20
4	20	n/r	n/r	n/r	<0.1	n/r	n/r	5	50	n/r	n/r	10	50	10	20	0.5	n/r	n/r	n/r	n/r	0.1	n/r	5	n/r	20
5	5	b	B	n/r	<0.1	n/r	n/r	1	20	n/r	n/r	10	20	b	10	b	n/r	b	n/r	n/r	b	n/r	n/r	b	20
6	10	0.5	n/r	n/r	n/r	n/r	n/r	2	10	n/r	n/r	20	50	10	200	1	n/r	n/r	n/r	n/r	0.3	n/r	3	n/r	20
7	10	1	n/r	n/r	n/r	n/r	n/r	5	20	n/r	n/r	10	50	10	200	2	n/r	n/r	n/r	n/r	0.3	n/r	n/r	n/r	20
8	10	0.5	n/r	n/r	n/r	n/r	n/r	1	20	n/r	n/r	50	20	20	5	10	n/r	n/r	n/r	n/r	0.1	n/r	5	<1	20
9	10	1	n/r	n/r	n/r	n/r	n/r	5	20	n/r	n/r	100	20	10	200	2	n/r	n/r	n/r	n/r	0.1	n/r	5	n/r	20
10	10	n/r	n/r	n/r	n/r	n/r	n/r	5	20	n/r	n/r	10	50	10	200	1	n/r	n/r	n/r	n/r	0.3	n/r	5	n/r	20
11	10	n/r	n/r	n/r	n/r	n/r	n/r	5	20	n/r	n/r	20	50	10	200	1	n/r	n/r	n/r	n/r	0.3	n/r	3	1	20
12	10	n/r	n/r	n/r	n/r	n/r	n/r	5	20	n/r	n/r	50	20	10	50	1	n/r	n/r	n/r	n/r	0.3	n/r	3	n/r	20
13	10	n/r	n/r	n/r	n/r	n/r	n/r	5	20	n/r	n/r	20	20	10	100	0.5	n/r	n/r	n/r	n/r	0.3	n/r	3	n/r	20
14	10	0.5	n/r	n/r	n/r	n/r	n/r	5	20	n/r	n/r	20	50	10	100	0.5	n/r	n/r	n/r	n/r	0.3	n/r	3	n/r	20
15	5	1	n/r	n/r	n/r	n/r	n/r	2	10	n/r	n/r	20	50	10	200	5	n/r	n/r	n/r	n/r	0.3	n/r	5	n/r	20

* Notice: n/r – not revealed; b - to definition prevents a continuous background

Table 3. Analysis results of basalt rock «Asmansay» deposit (results × 10^{-3} %)*

№	Cu	Pb	Zn	Cd	Ag	Bi	Ge	Co	Ni	Tl	Sb	Cr	Mn	V	Ti	Mo	W	Sn	In	As	Ib	Li	P	Ga	I	Sr
1	3	0.4	<1	<1	<0.1	n/r	n/r	1	10	<1	<1	20	20	10	10	0.5	<0.1	<0.1	<1	<1	0.2	<1	<1	<0.2	n/r	20
2	5	0.5	B	n/r	<0.1	n/r	n/r	1	20	n/r	n/r	20	50	10	20	b	n/r	n/r	<0.1	<0.1	<1	<1	<0.2	<0.1	<0.1	50
3	5	0.4	<1	<1	<0.1	n/r	n/r	1	10	<1	<1	20	20	10	10	0.5	<0.1	<0.1	<1	<1	0.2	<1	<1	<0.2	n/r	20
4	4	0.5	B	n/r	<0.1	n/r	n/r	1	20	n/r	n/r	20	50	10	20	b	n/r	n/r	<0.1	<0.1	<1	<1	<0.2	<0.1	<0.1	50
5	3	0.4	<1	<1	<0.1	n/r	n/r	1	10	<1	<1	20	20	10	10	0.5	<0.1	<0.1	<1	<1	0.2	<1	<1	<0.2	n/r	20
6	10	1.0	<0.2	<1	<0.1	0.2	<0.1	<0.1	50	<1	<1	20	20	10	20	0.5	<0.1	<0.1	<1	<0.1	0.2	<1	<1	<0.2	n/r	50
7	5	0.5	B	n/r	<0.1	n/r	n/r	1	20	n/r	n/r	20	20	20	50	b	n/r	n/r	<0.1	<0.1	<1	<1	0.2	<0.1	<0.1	20
8	3	0.4	<1	<1	<0.1	n/r	n/r	1	10	<1	<1	20	20	10	10	0.5	<0.1	<0.1	<1	<1	0.2	<1	<1	<0.2	n/r	20
9	10	1.0	<0.2	<1	<0.1	0.2	<0.1	<0.1	50	<1	<1	20	20	10	20	0.5	<0.1	<0.1	<1	<0.1	0.2	<1	<1	<0.2	n/r	50
10	5	0.5	B	n/r	<0.1	n/r	n/r	1	20	n/r	n/r	20	20	20	50	b	n/r	n/r	<0.1	<0.1	<1	<1	0.2	<0.1	<0.1	20
11	3	0.4	<1	<1	<0.1	n/r	n/r	1	10	<1	<1	20	20	10	10	0.5	<0.1	<0.1	<1	<1	0.2	<1	<1	<0.2	n/r	20
12	10	1.0	<0.2	<1	<0.1	0.2	<0.1	<0.1	50	<1	<1	20	20	10	20	0.5	<0.1	<0.1	<1	<0.1	0.2	<1	<1	<0.2	n/r	50
13	5	0.5	B	n/r	<0.1	n/r	n/r	1	20	n/r	n/r	20	20	20	50	b	n/r	n/r	<0.1	<0.1	<1	<1	0.2	<0.1	<0.1	20
14	6	0.6	н/о	0.2	<1	<1	<0.2	n/r	50	n/r	n/r	10	10	20	50	0.5	<0.1	<0.1	<1	<0.1	0.5	n/r	n/r	3	n/r	10
15	5	1	<1	<1	<1	0.2	<0.1	<0.1	20	n/r	n/r	10	20	10	100	5	<0.1	<0.1	<1	<1	0.1	n/r	n/r	5	n/r	10

* Notice: n/r – not revealed; b - to definition prevents a continuous background

The structural analysis

As all rocks, basalts can be investigated by mineral-petrographic methods which basis make macro and macroscopical researches. To macroscopical studying of basalts of Uzbekistan enough quantity scientific of proceedings[1, 6, 7, 10, 11] literature practically there are no data about microscopic studying structure of section basalt rocks which will enable to receive a tentative estimation about a direction of processing and area of purpose basalts of this or that deposit of republic. In this connection, in this work microscopic studying basalt rocks has been carried out. In this case microscopic studying of section basalt rock includes:

- The description of mineralogical structure and its quantitative definition;
- The description of texture and structure;
- Definition of crystal constants;
- Quantitative definition rockforming minerals;
- The description impregnation and thin-scattered alloted.

Microscopic studying of basalts was carry out in accordance with GOST 30629-99 p.2, on transparent sections rock by the methods accepted in petrography. Thus the area investigated section should be not less than 400 mm^2, thickness - no more than 0.03 mm. The number sectionы should be sufficient for definition of mineralogical structure to within 1 %.

For carrying out of research from basalts rock (according to normative documents of GOST 16115, GOST 10110 and GOST 896) «Aydarkul» and «Asmansay» deposits have been cut out in three mutually perpendicular directions, six samples of the rectangular form (on two samples in each direction) by length 400 mm, width 250 mm and thickness 10 mm. In the beginning of research check of ability of basalts to polishing (with application milling-bound machine SMR-015 and glare-measurer type FB-2) has been carry out. Results of research were checked visually through a mineralogical magnifier.

Samples grind on grinding-and-polishing machine and lead up their surface up to glazed - smooth matte surface, without traces of processing at full revealing figure of the stone. Glazed surface of samples subject to the further polishing. Through everyone 10 mines of polishing measure reflective ability of a surface of the sample, preliminary having dried up and having cleared its dry flannel. Preliminary include glare-measurer type FB-2 in power circuit and warm up it during 30 min. On a measuring window impose the sample - the inorganic polished glass with reflective ability not less than 200 units. Manual updating bring an arrow of the microammeter in the position corresponding “200” and remove the sample, establish a measuring head on the

polished surface of the sample in nine points: through equal distances along four edges of the sample and one in the center of the sample. Polishing of the sample carried out until the measured value of limiting shine will differ from previous no more than on 1–2 %.

By results of measurements arithmetic-mean value of parameters was defined. Final results were compared to help data[12] and has been established, that basalt rocks «Aydarkul» and «Asmansay» deposits as well as basalts «Gavasay» deposits concern to IV category of polishing.

By results of microscopic research of basalt rock «Aydarkul» and «Asmansay» deposits the following is revealed.

On basalts «Aydarkul» *deposits***.** Seldom and small-porphyry rock with afiro, allotriomorphic granular structure. Consists approximately of equal quantity of absolutely wrong grains plagioclase and pyroxene on optical properties close to diopside - to augite C : Ng = 36–43 sizes of grains plagioclase do not exceed 0.01 mm in the bulk and 0.5–0.7 mm very rare porphyryarea.

Shape of crystals extended with not clear cutting, forming twisting gear, effuse-like borders. Crystals are braided, forming felt-like structures together with same xeromorphous grains of augite which sizes of grains in the bulk it is less, than plate of plagioclase. The contents anorthite a component to define it is impossible in view of bend of polysynthetic doubles. On width of individuals of doubles this plagioclases labrador structure is probable places going down up to andesine and rising up to bytownite. Crystals of augite more isometric in comparison with the extended grains plagioclase. They form fine tableting crystals, which sizes of the majority in the basic mass rock do not exceed 0.01 mm. But separate places in rock are borrowed by more integrated crystals of the augite forming fine porphyritic allocation in the size up to 0.5–0.7 mm. There are cases of formation such porphyritic allocation glomeroblastes, consisting of 3–5 individuals. The sizes of this glomeroblastes reach 1.0–1.5 mm. In them augite has precise prismatic cleavage, seldom meeting sections having 2 systems of cleavage cracks, crossed almost under a right angle (87°). Their structural features are shown on Figure 1.

The high relief, enough the big parameter of refraction to comparison with adjoining crystals plagioclase, bright enough light-yellow-brownish interference painting together with a big angle extinction, vacillating within the limits of 36–43° allow to consider structure pyroxene corresponding to

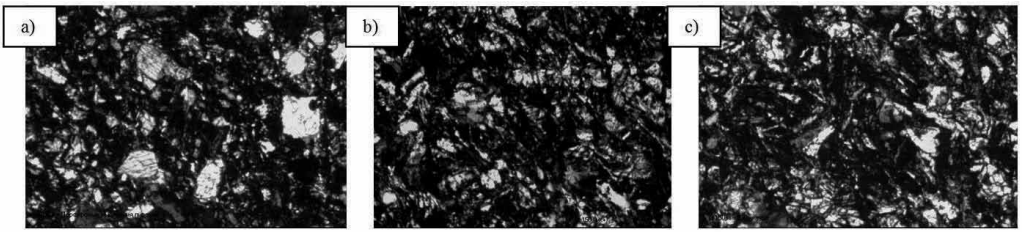

Figure 1. A microstructure of basalt Aydarkul deposit: a) small porphyry; b) afiros; c) braided structures (nicolies are crossed, increase 150-times)

transitive differences from diopside to augite. In crossed niccolies owing to interference painting easily diagnosed. Except for these two mineral phases in rock is available about 30 % of volume of glassy substance microgranular and implicational structures.

Described rock probably has undergone current of the grown lazy magma on a slope of volcano. About this testifies streak expansion of glassy substance focused in one direction. Rounding by glass separate crystals augite and crystals plagioclase creates figure ocellar structures of basic mass. The structure of glass on painting dark grey and almost black testifies about it's enough the big basicity.

Torsion crystals plagioclase and felt-like orientation of crystals of basic mass can specify on formation of rock in conditions of lava movement. Such rock also has the certain quantity of interstice. Interstice here are focused along a direction of current or the strips differing from each other by a parity of glass and crystal phases. Some strips contain glasses more than strips, witch adding prevail crystal grains. Everywhere interstices oblong, their length in a direction streakiness reaches 2.0 mm, at width 2–3 times smaller, than width of streakiness Sometimes streakiness are mutually informed narrow cord-like by cracks. Almost all large interstices here hollow, filled by the Canadian balsam. However in separate sites of rock there are fineer, rather isometric interstices filled chalcedony-like by quartz. Together with quartz in them there are pseudo-rocks not aggregated amorphous chlorite in very fine allotments which development on what minerals to define difficultly. Such finely afiro-porphyritic basalts to the north of mountains Severonuratinskiy have been studied by L. V. Shpotovoj and V. N. Ushakov. They consider as their product outpouring basalts Beltau-Kuramin structurally-formation zone.[1, 4]

On basalts «Amansay» deposits according to the results of research of

basalt samples «Amansay» deposits it is revealed that the structure of the rock is as follows: plagioclase (60 %), augite (40 %), secondary minerals: tiff, epidote, zoisite, sphen, chlorite, ore: magnetite, leucoxene; structure - gealopelit, places poikiloophite, intersertal. Rock fine-grained, finely and seldom porphyritic. Prevail leicestes and microlits plagioclase in which intervals meet fine crystal augite, conceding on a degree idiomorphic to plagioclase. The sizes plagioclase microlits up to 0.05–0.1 mm. The structure plagioclase in the basic mass sour, than in rare fine porphyritic allotment, on an angle of symmetric fading corresponds andesine. Is exposed partial albitization on edges of grains. Porphyritic allocation plagioclase do not exceed 1 mm. They usually represent prism, wafer formations slightly extended on ($\perp$001). The length of grains porphyritic allotment seldom exceeds width in 2–2.5-times. Their sizes, being gradually reduced, reach the sizes of microlits plagioclase from the basic mass. Only in separate places meet extended prismatic crystals which sizes are within the limits of 0.2–0.5 mm on length.

Microlits are focused randomly, mutually being crossed, and make intersertal structure. In intervals between microlits plagioclase are placed fine briefly prismatic allocation multiple-wedge pyroxene with an angle extinction on C : Ng = 38–41.

Together with pyroxene in intervals plagioclase microlits places keep glass microgranular aphanite structures, differing from crystals plagioclase by a low parameter of refraction and clear dispersive effect which is expressed by a weak golden shade of the surrounding weight combined by microlits plagioclase.

Because of insignificant quantity of glass and its distribution in the fragmentation intervals of crystals plagioclase microlits to notice dispersive effect are required careful crystal optics supervision. Character feature of the glass meeting in investments plagioclase of microlits, in this rock its saturapition ore minerals - magnetit which being allocated in common with glass in a significant part is in structure of glass in the form of solution microparticles firm. Microparticles dust mixed with glass, gives to the last dark grey painting with the spongy structure caused by non-uniform distribution of microparticles of ore mineral among glass. With it, connected change of intensity of black painting within the limits of microallotment the wrong form is with twisting edges.

However, among such mass are allocated black, dense, it is usual four and the triangular form the ore minerals representing fine grains of magnetit , allocated due to collective recristallisation in last stages of hardening of

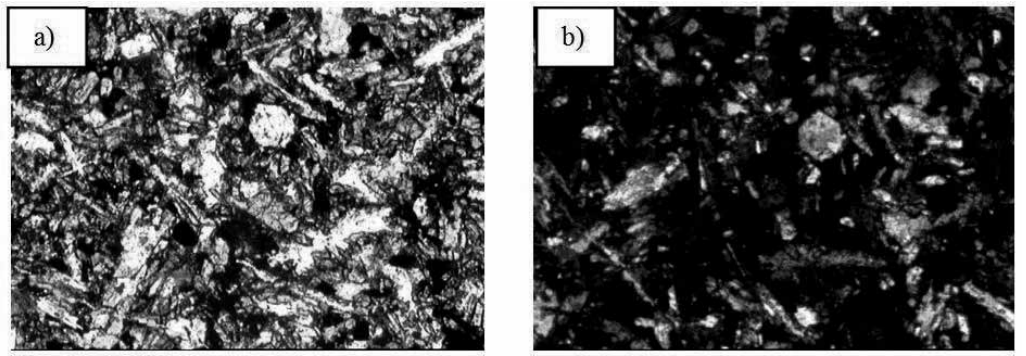

Figure 2. Microstructure of basalt «Asmansay» deposits: a) polarized; b) passing light (nicoles are crossed, increase 150-times)

basalt lava. Possibly, in structure of an ore mineral an appreciable role impurity of oxides of the titan, giving in the subsequent stages pigenetic changes of cloudy structure separation leucosen. In the rock in association with glass often meet wrong lenticular shape separation of epidote mixed with minerals of zoisite group. Among these minerals contain as well fine high-refractor, shapeless, sometimes rounded ellipse isometric grains of epidote, described with non-uniform distribution interference painting. Their structural features are shown on Figure 2.

The brightest feature of this basalt that it has almond-shaped structure. Almonds represent the various size the interstice filled by hysterogenic minerals among which overwhelming value has tiff, possible to note, that all times are completely filled tiff, forming well enough the developed crystals with polysynthetic doubles. They form in interstice glomer-blastes, consisting of several individuals which epitaxial growth from walls of interstice. Thus orientation of the crystal mineral lattice not monotonous, therefore crystals cause occurrence sectoral blackout. Together with tiff among them meet poikilit growth sour plagioclase - albite, sometimes forming nimbuses along contact tiff grains on wall border interstice. As inclusions among tiff, filling almonds meet also inclusions of epidote grain ,zoisiteand minerals of this group. Some inclusions among tiff form homo- axial pseudomorpus chlorite, developed, apparently, on relicts plagioclas**e**, remaining among tiff grains, i.e. grasped during their growth. Intensive filling interstice with carbonate accompanied by isolation tiff crystals with formation of proveins and socket among basalt matrix.

In this rock meets fragmental xenolith angular forms of wrong outline.

Around of these xenolith develops selvedge from ore substance of iron close to hydrooxides. On the entire area of fragments developed light green color afiros mass of chlorite. Places among xenolith meet the rests of glassy black-brown substance without the certain forms of allocation. The described rock can be named afiroleukobasalt.

Obviously, xenogeneic fragments have tufagenic the nature. Fragments of basalts of the previous impulse of eruption probably got in a fresh basalt lava. Thus the glassy material, having tested began thermal influence of a fresh lava distransition glass, allocating plagioclase growth which actually are observed among xenolithes, described above. Except for plagioclase growth among these xenolithes meet also micro allocation epidote, zoisite and sphenos. Being among heated melt these xenolithes, have been subjected devitrify with allocation specified growth, remaining as restitdevitrifiedti material. And the ore substance is migrated to edges xenolithes, forming similarity kelyphitic borders observed around of crystals of garnet, meeting in lamproits and diamondiferous kimberlite.

Conclusion

The analysis has shown, that specific effective activity of natural radioactive elements in basalt «Aydarkul» deposits 251 Bq/kg «Asmansay» 312 Bq/kg and «Gavasay» 202 Bq/kg, that corresponds to sanitary norms SanPIN-0193-06, according to which specific effective activity of natural elements not should to exceed 370 Bq/kg.

It is revealed, that mineralogical structure of basalt rock «Aydarkul» and «Asmansay» deposits have distinctive attributes. For example, in structure of basalt «Aydarkul» deposit are not found out such chemical elements as: Ib, Li, I and on the contrary in basalt «Asmansay» deposits contents Yb иJ has not been revealed.

In all investigated samples of basalt rock «Aydarkul» deposits have not been found out such chemical elements as: Zn, Cd, Ag, Bi, Ge, Ti, Sb, W, Sn, In, As and P. At that time, in basalt «Asmansay» deposits it is possible to notice the certain contents of the listed elements. Occurrence of similar elements in basalts «Gavasay» and «Asmansay» deposits are noticed. Thus, basalt rocks «Aydarkul» and «Asmansay» deposits on mineralogical structure noticeably differ from basalt rocks of other deposits.

In structure of basalt «Aydarkul» deposits it is found out: peridot within the limits of 13.7–18.7 %, pyroxene within the limits of 19.3–28 % and plagioclase within the limits of 346–53.3

%. Mmineralogical structure of basalt «Aydarkul» contains deposits: peridot within the limits of 11.7–18.7 %, pyroxene within the limits of 17.3–31 % and plagioclase within the limits of 31.6–50.1 %.

In turn by employees of the center "Composite" it is revealed, that in structure of «Gavasay» deposits is available: peridot 14.3–27.1 %, pyroxene 18.3–18.1 % and plagioclase 30.6–54.8 %. The basic part plagioclase borrows Si_2O (from 44 up to 67 %), and the smallest share makes Na_2O. According to experts high contents Si_2O in plagioclase just as at pyroxene promotes rise in temperature of basalt fusion.

It is revealed, that in basalts of our country the special place is borrowed with connections between Al, Fe, Mg, K, N, Ti and Si with oxygen. oxygen connection, with chemical elements of metals, forming oxides, makes a basis of silicate basalt as a whole. In such integral structure a lot of place is allocated flinty-oxygen connections as the basic part of basalt consists from SiO_2.

It is established, that the increase in the contents pyroxene in structure of basalts becomes one of the reasons of rise in temperature of basalts fusion. The temperature of peridot fusion is within the limits of 1 200–1 250 °C. Therefore producers for production basalt-fibrous materials often use basalt in structure which the basic place is allocated peridot. To date fusion temperature of basalts «Gavasay» deposits reaches 1 250–1 300 °C, that, «Asmansay» 1 350–1 450 °C and «Aydarkul»1 450–1 500 °C.

It is established, that on all beginnings described rock was generated as a product underwater (vend-paleozoic basalts of Paleo-Asian ocean from folded areas mountain Altai and east Kazakhstan and Central Asia, existed approximately 500–600 one million years ago) outpourings of the basic magma with characteristic almond-shaped texture, intersertal, in separate sites with poikilofit structure. From this follows, that on mineralogical structure basalt rocks «Aydarkul», «Asmansay» and «Gavasay» deposits noticeably differ from each other.

Thus, studying of basalt deposits of Uzbekistan has shown appreciable difference of this rocks in various deposits on mineralogical structure. In many cases the mineralogical structure of basalt promotes change temperature of fusion basalts. That, basalt-processing enterprises by selection of basalt rock can reduce the charge of power and fuel resources that will allow these enterprises to reconstruct the operative equipment and to carry out economy of financial assets.

References

[1] The State balance stocks of minerals РУз. «Raw material for manufacture of a mineral fibre ». Tash. 2010.

[2] Luchinskiy, V. I. (1949): Petrography. M.: Gosgeolizdat, 213–225.

[3] Lapinskaya L. A., Proshljakov, B. K. (1974): Bas of petrography. publishing house"Bowels", 30–36.

[4] Kurbanov, A. A., Abdurahmonov, S. A. & Turaev, A. S. (2010): Base of processing of basalts of Kyzyl Kum. The monography. publishing "Fan" AN RUz, 167.

[5] Dodis, G. M. & Kudinova, I. V. (2007): Structure melt from basaltofibrous rocks. Bulletin KGNU. Kyrgyzstan, 2–14.

[6] Iskandarove, Musaev, Hamraev, I. (1976): Experimental modelling of processes magmatogene make up rock- and ore. Tashkent: the Fan, 120 p.

[7] Salimsokov, J. A., Ibodullaev, A. S.:«know-how« of fibres from basalt rocks of Uzbekistan and composite materials on their basis. // Republican scientifically-технич. Konf. TashSU, 77.

[8] Kurbanov A. A. (2009): Specific of basalts featureof Kyzyl Kum. The monography.publishing. "Fan" RUz., 160 p.

[9] Dzhigaris D. D. & Mahova M. F. (2006): Base of basalt production fibres and products, 410 p.

[10] Safonova, I. JU. (2005): Geodynamic of conditions formation vendpaleozoic basalts Paleasiatic ocean from folded areas of mountain Altai and east Kazakhstan. Novosibirsk.

[11] Mahmudova, V. S. (2008): Development of technology reception low-temperature cements with use of basalt rock of Uzbekistan, Scientific degree, Tashkent.

[12] Muzafarov, V. G. (1979): Determinant of minerals, rocks and fossils. Reference manual M. Bowels, 328 p.

In-situ determination of the earth pressure at rest in overconsolidated clay

In-situ določanje mirnega zemeljskega tlaka v prekonsolidirani glini

Eszter Kalman[1, *]

[1]Canterbury Engineering Associates Ltd, 1036 Budapest, Hungary

*Corresponding author. E-mail: info@canterburyea.com

Received: March 19, 2012 **Accepted:** April 9, 2012

Abstract: In the paper, there is a study about the general genesis process of overconsolidated soils, as well as the effects of the overconsolidated ratio to structures. It will demonstrate the possible methods for the determination of the values of overconsolidated ratio and of earth pressure at rest; further, the processing of measurement results, through which the values of OCR (Overconsolidated ratio) and of λ_0 (Earth pressure at rest) in an overconsolidated clay have been determined.

Povzetek: V članku so opisani splošni proces nastanka prekonsolidiranih zemljin in učinki prekonsolidacijskega količnika na zgradbe. Prikazane so mogoče metode določanja vrednosti prekonsolidacijskega količnika in mirnega zemeljskega tlaka. Sledi razprava o rezultatih meritev, s katerimi so bile določene vrednosti prekonsolidacijskega količnika (OCR) in mirnega zemeljskega tlaka (λ_0) v prekonsolidirani kiscellijski glini.

Key words: coefficient of the earth pressure at rest, overconsolidated ratio, earth pressure cell, Borehole cell, Selfboring pressuremeter

Ključne besede: količnik mirnega zemeljskega tlaka, prekonsolidacijski količnik, celica zemeljskega tlaka, celica v vrtini, samouvrtalni presiometer

Review paper

INTRODUCTION

The need to utilise underground spaces was growing parallelly to fast expansion of large cities in the previous century, the growth-rate of which is further increasing these days. Building in underground spaces is supposed to be handled together with wider and wider exploration of soils and rock layers. The behaviour of overconsolidated soils is explored and investigated globally, because significant horizontal stresses emerging in overconsolidated soil- and rock-strata give rise to unproportionally high horizontal loads to structures.

In the process of the investigations the objective was to determine the natural horizontal and vertical stresses at rest in overconsolidated clay layer.

The stress condition at rest means a stress space free from human intervention, both in the rock- and in the soil-mechanical field. There are conditions used by both the soil- and rock-mechanics for the sake of simplification. These are for instance the homogeneity, the isotropicity and the elasticity of rock masses. The primary stress condition is the result of the dead-weight loads of rocks or soils but it can be changed by tectonic activities, desiccation or other physical influences. The determination of the coefficient of the earth pressure at rest differs significantly in the area of the classical soil-mechanics and in that of the classical rock-mechanics, which is demonstrated by Figure 1.[1, 2, 3]

In those cases, where the metamorphosis of soils to rock has already started, but the process has not yet been completed the rules of classical soil mechanics cannot be applied, but the rules of classical rock mechanics are not applicable either. They are in a transitionary condition, with its own specific rules and properties.[4, 16]

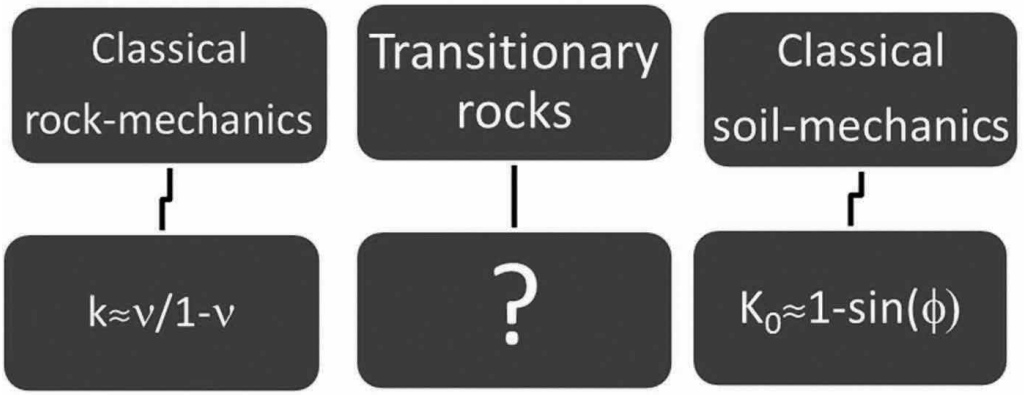

Figure 1. Coefficient of the earth pressure at rest

The laboratory tests are used for the soils and the rocks, the soil models are used for the soils[5] while the rock models are used for the rock masses. These models are not used for the transitionary rocks.

The best method to determine horizontal and vertical stresses is the use of local, in-situ investigations because these measurements have the least disturbing effects on the original stress conditions of a soil layer under test. The behaviour of the soils is determined by CPTu which is one of the world-wide best-known in-situ measurements[6] but horizontal earth pressure can be determined in indirect way.

Three different in-site investigations have been performed in order to determine the overconsolidated ratio and the earth pressure at rest: measurement with an earth-pressure cell; measurement with a borehole cell; and a measurement with a selfboring pressuremeter.

Geological, geotechnical environment

Place of the measurements

This study would like to show horizontal and vertical in-situ stress measurements around Budapest, Hungary. There are earth pressure cells around an SCL tunnel, one borehole cells sys-

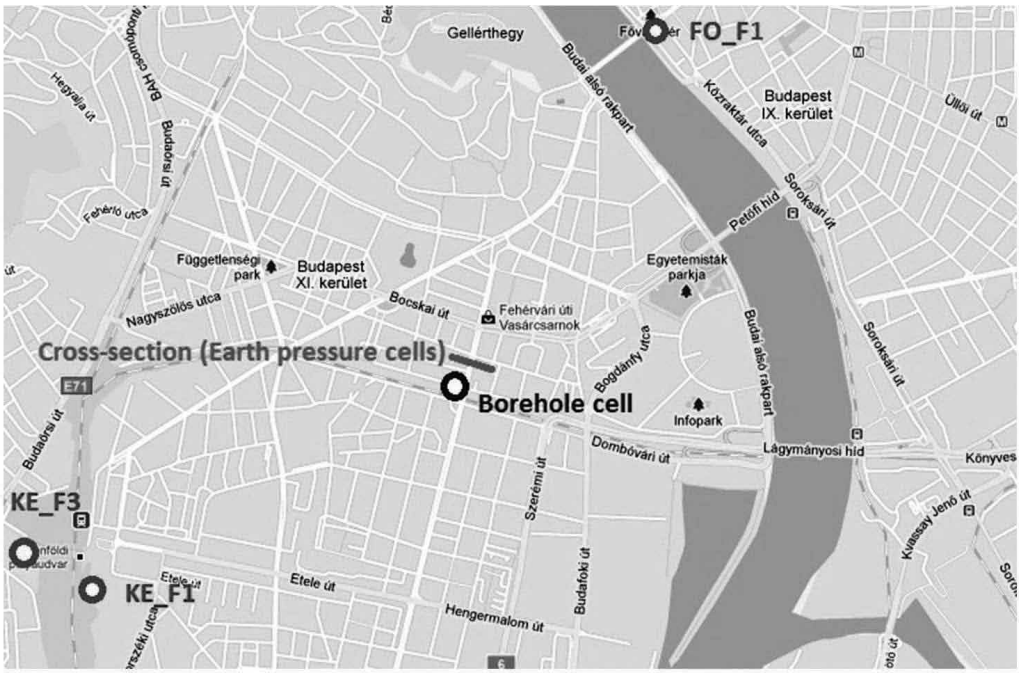

Figure 2. Place of the measurements

tem and three selfboring pressuremeter measurements.

In the map can show the place of the measurements. (Figure 2)

Geological environment

The rock layer of Kiscelli Clay Marl can be found beneath the major part of Budapest. It is situated on or near to the surface in the Buda-side of the city over a considerable area.

The thickness of the rock layer varies between 50 m and 500 m, but at certain spots it can reach even 1 000 m.

Kiscelli Clay was formed in the Cenozoic era of geohistory in the Tertiary period within that era.

The clay marl was depositing in the Oligocene, in its middle period when the location of the continents started to reach their today known location. Regarding the fauna of that period mammals were occupying an increasing area.

The Kiscelli Clay Marl is a marine deposit from the Middle-Oligocene. It was settling down among normal salty-water conditions in the Tethys-sea, which is considered to be the ancestor of the Mediterranean Sea of today.[7]

Geotechnical environment

Kiscelli Clay can be considered to be founding strata of the Quaternary period. After a rapid glance over geohistory it can be stated that Kiscelli Clay, after having deposited in the Oligocenic phase of the Tertiary period, became heavily consolidated later, upon the effects of soil layers deposited over it.[14, 15]

At the end of the Tertiary period of geohistory and in the Quaternary period the thick conglomerates lying over Kiscelli Clay underwent a significant erosion process. As a result of this major erosion vertical loads of Kiscelli Clay were removed and its upper layers became loose.

Table 1. The soil-physical properties of Kiscelli Clay

Soil type According to Msz. (14043-2-1979)	Bulk density of nat. State ρ_t/(t/m^3)	Angle of internal friction ϕ/°	Cohesion c/(kN/m^2)	Young modulus E_s/(kN/m^2)	Consistency index Ic	Void ratio e
Wethered zone of Kiscelli Clay	2.1	20–23	50–100	7–10	>1	0.4–0.68
Fissured zone of Kiscelli Clay	2.2	25–28	420	15–20	>1.2	0.32–0.4
Zone beyond the impact of expansion, Kiscelli Clay Marl	2.3	35–50	400–1000		>1.3	0.18–0.32

Kiscelli Clay cannot be considered as a homogenous layer: its vertical stratification must be taken into consideration both in the design and in the construction phase.

In general it can be broken down to three well-distinguishable zones:

- Weathered zone: This zone of Kiscelli Clay completely lost its properties characteristic of transitionary rocks during the process of losing its loads and now it is in a plastic or near-plastic condition.
- Fissured zone: The properties of the fissured zone are similar to those of the intact zone, no plasticity can be detected anymore. The fissures-textured rock bodies are in sound condition with high solidity.
- Intact rock mass zone, beyond the impact of expansion: the deeper layers of Kiscelli Clay were not exposed to the load-relief impacts of erosion, so this zone conserved the ancient soil-physical properties of clay. Obviously the highest load ever deposited over the clay layer before together with the resulting maximum consolidation have also been preserved in this zone. The impact of a formerly existing maximum load ever is called overconsolidation.

In-site investigations applied

Earth pressure cell

In the course of the investigations first-

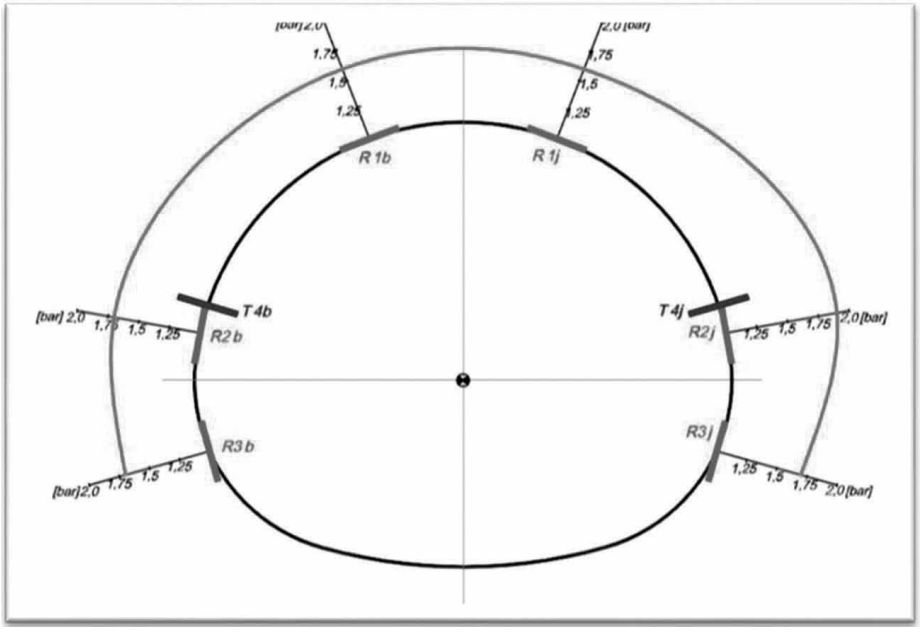

Figure 3. Points at which the earth pressure cells are located, and their alues

ly earth pressure cells (Figure 3) were used to determine the stresses to the tunnel being built in the Kiscelli Clay.[15] During the investigation radial and tangential cells made by company Glötzl have been installed. These cells determined the value of the normal force emerging in the shotcrete wall, as well as the value of the force exercised by the rock environment to the shotcrete wall. Six radial cells and two tangential cells were installed in the system.

Processing the measurement results it was outlined that the value of horizontal and vertical stresses in the neighbourhood of the completed tunnel are nearly the same.[9]

Borehole cell

An earth pressure cell system installed into a borehole called Stress Monitoring System (Figure 4) was installed during the investigations. Similarly to the pressure cells, the borehole cell is also made in Germany, by the firm Glötzl.[11]

The name borehole cell refers to the place of the installation: the cell system is installed into a borehole. The borehole cell means a system of individual cells always compiled in accordance with individual needs. The system used here is made up of five cells, but obviously either more or less cells could also be combined together.

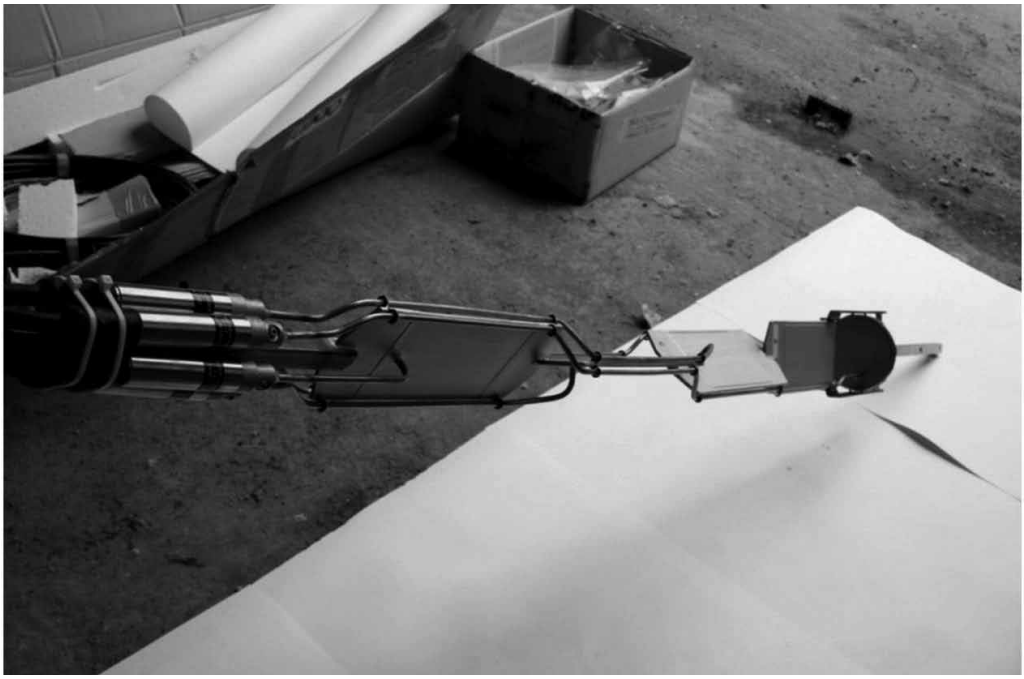

Figure 4. Borehole cell (Glötzl Ltd)

The purpose of the investigation was to determine the value of horizontal and vertical stresses in the overconsolidated Kiscelli Clay.

The borehole cell was installed in a stress-free area in a depth of 15 m. The installation depth was selected with regard to the RQD indices. The instrument was installed in the zone of the intact rock environment.

The borehole cell system was installed on 19 May 2008 and keeps performing its measurement tasks until today after appropriate reconstruction and protection.

In the first 7 months there were two reading per day. Subsequently to the first 7-month period the number of readings reduced to one per day until the end of the first year. In the second year the number of readings could be further reduced to once a week, while after the first eighteen months following the installation of the instrument, the number of readings was decreased to once in two weeks.

Selfboring pressuremeter (SBP)

During the research there was a big chance to take part in investigations carried out with selfboring pressuremeter at several locations in the city.[12, 13] The investigations were targeted at defining the overconsolidated ratio of the overconsolidated clay (Kiscelli Clay). Since the measurement results could be used for scientific purposes the research group had the opportunity to investigate the Kiscelli Clay at various sites.

In the case of a selfboring pressuremeter the rock environment cannot expand after the borehole had been completed as it is continuously supported until the completion of the investigation process. This device allows us to determine the real, in-situ stresses in any cases.[11]

SBP is a special device combining the tooling required for boring and the pressuremeter instrument. The device is 1.2 m long with a diameter of 83 mm ending in a boring crown head. (Figure 5).

The pressuremeter itself is a 0.5 m long polyurethane membrane, protected with a stainless steel mantle. Inside the membrane there is a six-branch displacement meter measuring the displacements in the wall of the borehole. The six-branch displacement meter makes it possible to determine also the main direction of the horizontal stress, in addition to the size of stresses measured in the process. With the help of the horizontal stress instrument the research group was able to measure the total horizontal stress. If groundwater or strata-water is present this device measures not the horizontal stress accumulated in the layer but the horizon-

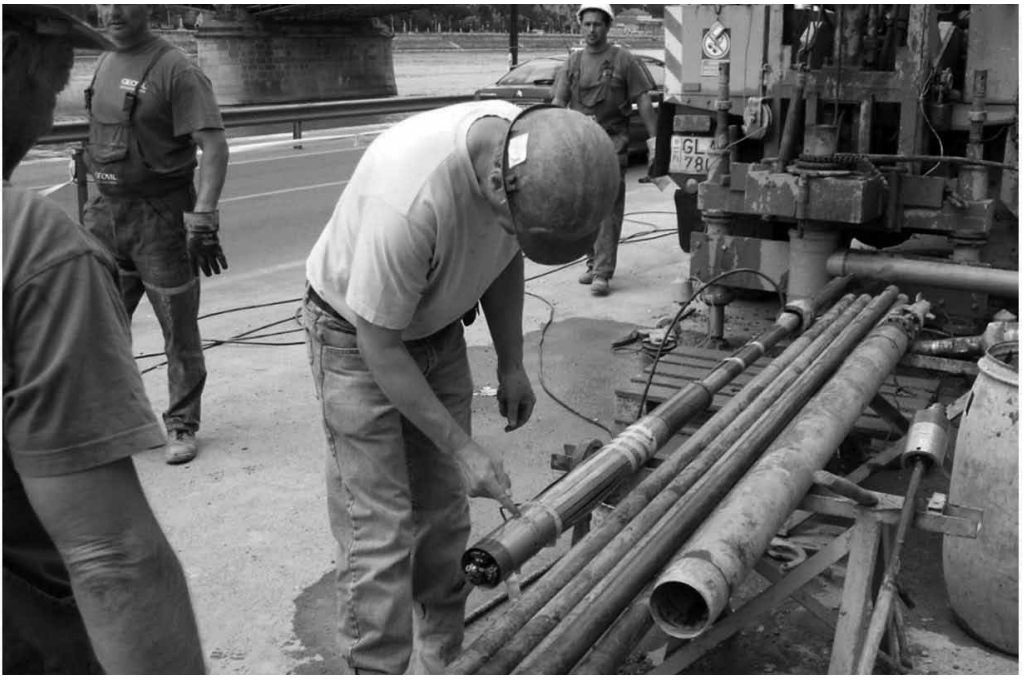

Figure 5. Selfboring pressuremeter

tal stress of the layer and the stress of the water in the layer. In order to enable the device to measure the effective stress of the soil/rock layer two cells are also installed outside the membrane to measure the pore-water pressure, the purpose of which is to determine the value of the neutral stress due to water pressure in the layer. If the total horizontal pressure and the neutral stress is known the effective horizontal stress can be determined.

MEASUREMENT RESULTS

In-situ measurements were carried out in the course of the investigations for more than two years to establish the overconsolidation ratio of the Kiscelli Clay caused by a preliminary loading, and the value of the resulting horizontal stress.

With the investigations performed to determine the overconsolidated ratio of Kiscelli Clay the research group established that the Kiscelli Clay, after its settling down, consolidated under the effect of a nearly 400-meter thick covering layer, and developed to its currently known condition. We were carrying out measurements through the installation of a borehole cell for more than two years, in order to establish the overconsolidated ratio. Then we processed the results of the measurements

with a selfboring pressuremeter performed at three additional sites in four different depths to determine the OCR value (Figure 6). The Figure 6 shows the results of measurements. The blue and red lines (name of the measurements are KE_F1 and KE_F3) were made on Kelenföld station (Figure 2) where the ground is typical Kiscelli Clay. The measurement FO_F1 was made in the Fövam station where the ground is mix. There are Kiscelli Clay but it hasN't got the typical parameters.

The Kiscelli Clay Marl is heavily overconsolidated, its overconsolidation ratio varies between 10 and 16 depending on depth.[7]

To determine the horizontal stress at rest the group used the results of the series of measurements of more than two years with the borehole cell as well as those of the selfboring pressuremeter investigations. The place of the borehole cells can be seen on the Figure 2. The results of the borehole cell were depicted in a time/pressure graph (Figure 8). It was established that the values of the horizontal stress at rest were varying along an ellipse, and the maximum value of the stress in the intact rock mass zone of Kiscelli Clay is 4.62 bar.

As the result of the measurements with the selfboring pressuremeter we established that the value of the horizontal stress at rest varied between 270 kPa and 1 100 kPa depending on depth (Figure 7).

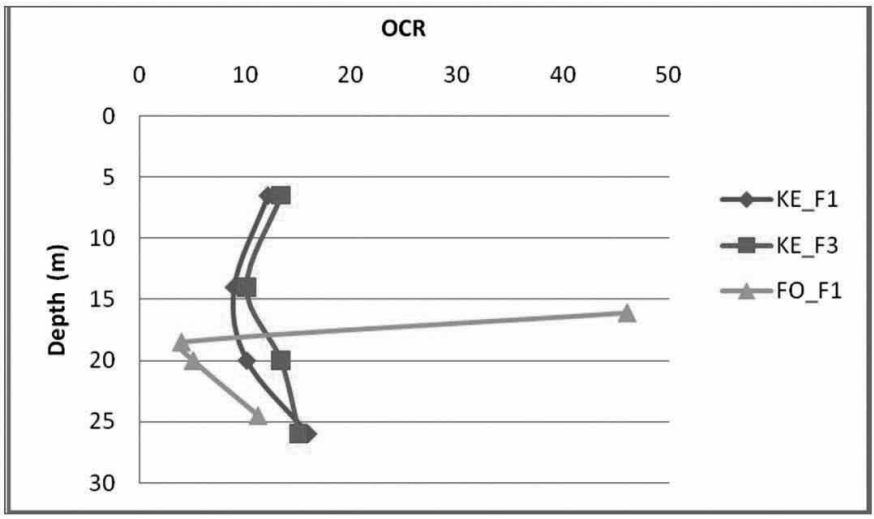

Figure 6. OCR value versus depth value E_F1; KE_F3; FO_F1- name of the measurments

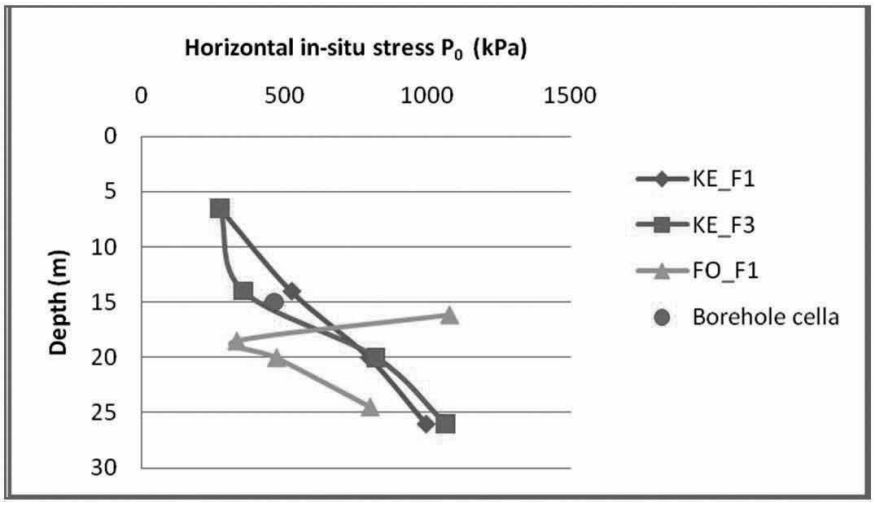

Figure 7. Horizontal stress values versus depth values, Borehole cella = Borehole cell

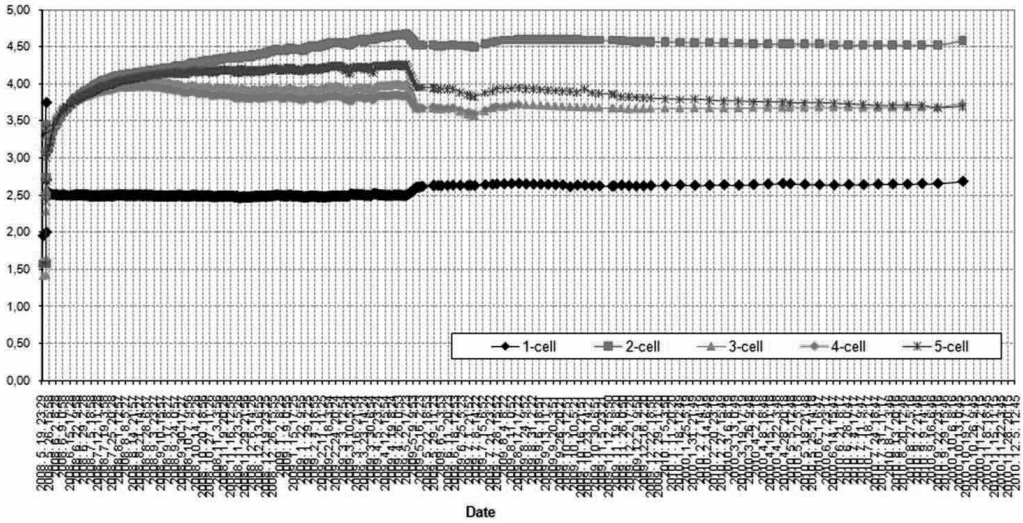

Figure 8. Borehole-cell-measurement values in a time/pressure diagram-
1cell- vertical cell;
2cell, 3cell, 4cell, 5cell-name of the horizontal earth pressure cells

We used to determine the value of the coefficient of the earth pressure at rest the measurement results provided by the borehole cell and by the selfboring pressuremeter investigations. In the course of these investigations we determined not only the value of the coefficient of the earth pressure at rest

but the research group investigated its evolution in depth too.

The value of the coefficient of the earth pressure ($K_0 = \lambda_0$) at rest in Kiscelli Clay varies between 1.2 and 2.5 in the function of depth. (Figure 9).

To determine the guidedness of the horizontal stress, first it had to be considered that the value of stress in a plain is constant, that is its value is the same in every direction of the plain, or if could such a case occur where it is not constant. In that case, when the uniform stress distribution developed during the deposition process gets modified upon the effect of any external force, them this amount will not be constant any more, bur the maximum values of the horizontal stresses will be carried along an ellipse in a plain (Figure 10). The measurements right after the installation and until today verify the theory that the values of horizontal stresses have a guided character. The results of the series of investigations carried out by the selfboring pressuremeter have yielded the same output. I was able to determine the values of the horizontal stress in 4 different directions. It can be shown on the Figure 4. The Figure 8 shows the values of the 4 horizontal cells and 1 vertical sell during the research and the Figure 10 shows the values of the maximum hori-

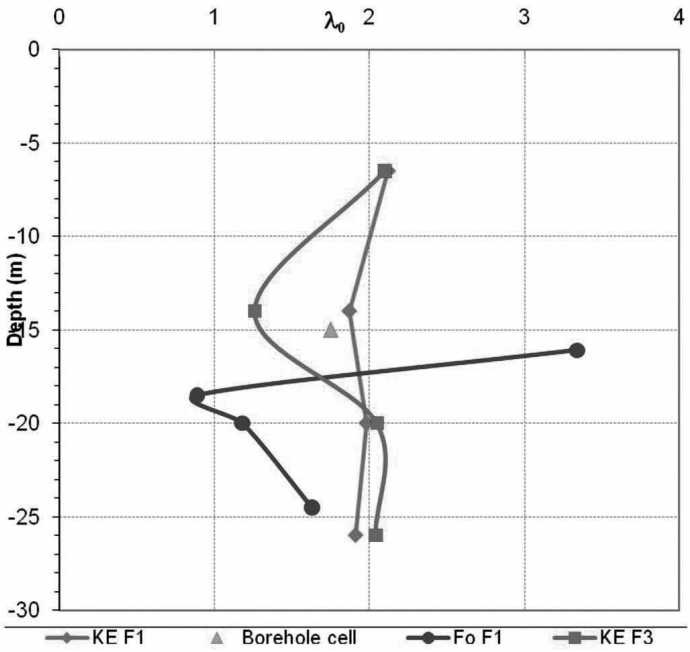

Figure 9. Changes of the value of the coefficient of earth pressure at rest in the function of depth

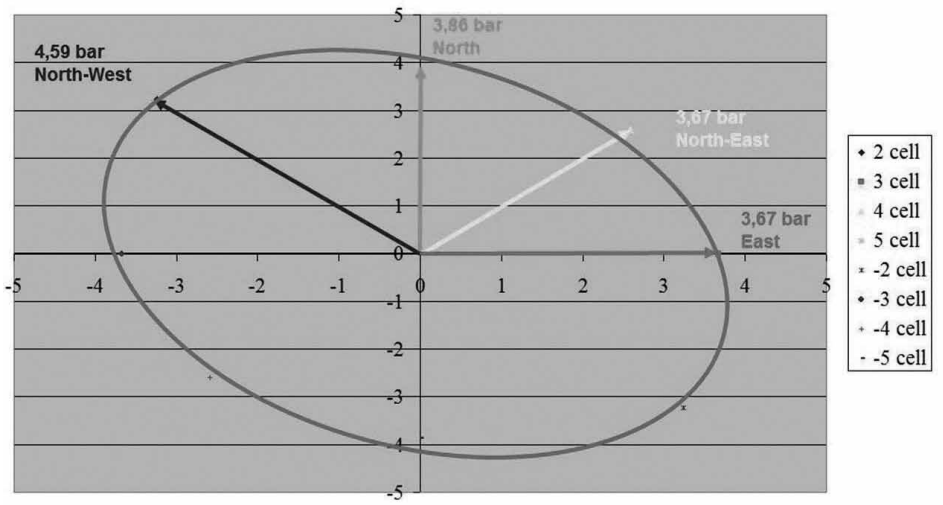

Figure 10. Ellipse of the horizontal earth pressure from the borehole cells system

zontal stress in the horizontal section. When I drew the ellipse I had used the theory of horizontal stress of Glötzl Company.

CONCLUSIONS

It can be established through the investigations that the method applied by classical soil mechanics and classical rock mechanics for the determination of the value of earth pressure at rest cannot be applied in the case of overconsolidated soils. In those situations where the stress values at rest for an overconsolidated soil must be determined, not even approaching calculations are recommended with the application of the rules of classical soil mechanics or classical rock mechanics. The most accurate results for the determination of primary stresses are provided by in-site investigations. From among the scale of in-site investigations the measurements recommended for use are where the rock environment to be tested cannot expand.

People could measure the values of the horizontal stress, the coefficient of the earth pressure at rest (λ_0) and the OCR but sometimes this information are not enough because the direction of the measurements is indispensable.

In the course of the research work we demonstrated that the Kiscelli Clay is heavily overconsolidated and consequently the value of the horizontal stress is 1.5 to 2 times higher than the value of the vertical stress.

This result highly influences the statical force impacts of the structures that are going to be built in the overconsolidated clay layer.

References

[1] Terzaghi, V. K. (1943): Theoretical Soil Mechanics; John Wiley and Sons, Inc., New York, USA.

[2] Jáky, J. (1944): Talajmechanika; Egyetemi Nyomda, Budapest, Magyarország.

[3] Jáky, J. (1948): New theory of earth pressure; Proceedings of the 2nd ICSMFE, Rotterdam, Hollandia.

[4] Szechy, K. (1961): The art of Tunnelling; Tankönyvkiadó, Budapest, Magyarország.

[5] Varga, G., Czap, Z. (2004): Soil models; safety factor and settlements; *Periodica Polytechnica Civil Engineering*, 48/1-2 pp. 53-63 HU ISSN 0553-6626.

[6] Mahler, Szendefy (2009): Estimation of CPT resistance based on DPH results; *Periodica Polytechnica Civil Engineering,* 53/2 (2009) 101-106 DOI: 10.3311/pp.ci.2009-2.06.

[7] Kalman, E. (2007): Geotechnical monitoring of the tunnel constructed in Kiscelli clay in Budapest; Proceedings of The 2nd Symposium of Underground Excavations for Transportation, pp. 509–516, Istanbul, Törökország.

[8] Kalman, E. (2009): Determination of the coefficient of the earth pressure at rest in overconsolidated clay; Proceedings of 9th International Conference on Tunnel Construction and Underground Structures pp. 99–104, Ljubliana, Slovenia.

[9] Kalman, E. (2007): Alagútbeli geotechnikai mérési tapasztalatok a Budapest 4. metró Bocskai úti állomás szellőző alagút építésénél, Geotechnikai Konferencia, 2007, Ráckeve.

[10] Schnaid, F. (2009): In Situ Testing in Geomechanics; Taylor & Francis Group, London, UK and New York, USA.

[11] Clarke, B. G. (1995): Pressuremeters in Geotechnical Design; Department of Civil Engineering, University of Newcastle upon Tyne, Blackie Academic & Professional, an imprint of Chapman &Hall, Glasgow, UK.

[12] GEOVIL LTD & CAMBRIDGE INSITU LTD (2008): Budapest Metro Line 4 Kelenföld Junction Station & Reversing Facility, Additional Site Investigation; Volume 1 and 2.

[13] GEOVIL LTD & CAMBRIDGE INSITU LTD (2008): Budapest Metro Line 4 Fovam ter Station, Additional Site Investigation; Volume 1 and 2.

[14] Horváth, T. (2005): Expert opinion on the geotechnical, engineering geological and hydrogeological issues regarding the Kelenföld Junction Station, Budapest.

[15] Horváth, T. (2005): Expert opinion on the geotechnical, engineering geological and hydrogeological issues regarding the Bocskai Street Station, Budapest.

[16] Hudson, J. A. (2009): Stresses in rock masses; a review of key points; Eurock Conference, Dubrovnik Croatia.

Author`s Index, Vol. 59, No. 1

Adamović Dragan	
Godicelj Tomaž	
Gupta S. K.	
Kalman Eszter	info@canterburyea.com
Kores Stanislav	stanislav.kores@ntf.uni-lj.si
Kovačič Miha	miha.kovacic@store-steel.si
Kurbanov Abdirahim Ahmedovich	bo_bosh@mail.ru
Mandić Vesna	mandic@kg.ac.rs
Medved Jožef	jozef.medved@omm.ntf.uni-lj.si
Mrvar Primož	primoz.mrvar@omm.ntf.uni-lj.si
Sharma Ashok	ashok.mnit12@gmail.com
Srikanth Madhulika	
Stefanović Milentije	stefan@kg.ac.rs
Šarler Božidar	bozidar.sarler@ung.si
Terčelj Milan	milan.tercelj@omm.ntf.uni-lj.si
Vončina Maja	maja.voncina@omm.ntf.uni-lj.si
Živković Miroslav	

INSTRUCTIONS TO AUTHORS

RMZ-MATERIALS & GEOENVIRONMENT (RMZ- Materiali in geookolje) is a periodical publication with four issues per year (established 1952 and renamed to RMZ-M&G in 1998). The main topics of contents are Mining and Geotechnology, Metallurgy and Materials, Geology and Geoenvironment.

RMZ-M&G publishes original Scientific articles, Review papers, Preliminary notes, Professional papers **in English**. In addition, evaluations of other publications (books, monographs,...), In memoriam, Professional remarks and reviews are welcome. The Title, Abstract and Key words in Slovene will be included by the author(s) or will be provided by the referee or the Editorial Office.

**** Additional information and remarks for Slovenian authors:***
Only Professional papers, Publications notes, Events notes, Discussion of papers and In memoriam, will be exceptionally published in the Slovenian language.

Authorship and originality of the contributions. Authors are responsible for originality of presented data, ideas and conclusions as well as for correct citation of data adopted from other sources. The publication in RMZ-M&G obligate authors that the article will not be published anywhere else in the same form.

Specification of Contributions

RMZ-M&G will publish papers of the following categories:

Full papers (optimal number of pages is 7 to 15, longer articles should be discussed with Editor prior to submission). An abstract is required.

- **Original scientific papers** represent unpublished results of original research.
- **Review papers** summarize previously published scientific, research and/or expertise articles on the new scientific level and can contain also other cited sources, which are not mainly result of author(s).

- **Preliminary notes** represent preliminary research findings, which should be published rapidly.
- **Professional paper**s are the result of technological research achievements, application research results and information about achievements in practice and industry.

Short papers (the number of pages is limited to 1 for Discussion of papers and 2 pages for Publication note, Event note and In Memoriam). No abstract is required for short papers.

- **Publication notes** contain author's opinion on new published books, monographs, textbooks, or other published material. A figure of cover page is expected.
- **Event notes** in which descriptions of a scientific or professional event are given.
- **Discussion of papers (Comments)** where only professional disagreements can be discussed. Normally the source author(s) reply the remarks in the same issue.
- **In memoriam** (a photo is expected).

Supervision and review of manuscripts. All manuscripts will be supervised. The referees evaluate manuscripts and can ask authors to change particular segments, and propose to the Editor the acceptability of submitted articles. Authors can suggest the referee but Editor has a right to choose another. **The name of the referee remains anonymous.** The technical corrections will be done too and authors can be asked to correct missing items. The final decision whether the manuscript will be published is made by the Editor in Chief.

The Form of the Manuscript

The manuscript should be submitted as a complete hard copy including figures and tables. The figures should also be enclosed separately, both charts and photos in the original version. In addition, all material should also be provided in electronic form on a diskette or a CD. The necessary information can conveniently also be delivered by E-mail.

Composition of manuscript is defined in the attached Template

The original file of Template is available on RMZ-Materials and Geoenvironment Home page address:

http://www.rmz-mg.com

References - can be arranged in two ways:
- first possibility: alphabetic arrangement of first authors - in text: (Borgne, 1955), or
- second possibility: [1] numerated in the same order as cited in the text: example[1]

Format of papers in journals:

Le Borgne, E. (1955): Susceptibilite magnetic anomale du sol superficiel. *Annales de Geophysique*, 11, pp. 399–419.

Format of books:

Roberts, J. L. (1989): Geological structures, *MacMillan*, *London*, 250 p.

Text on the hard print copy can be prepared with any text-processor. The electronic version on the diskette, CD or E-mail transfer should be in MS Word or ASCII format.
Captions of figures and tables should be enclosed separately.
Figures (graphs and photos) and tables should be original and sent separately in addition to text. They can be prepared on paper or computer designed (MSExcel, Corel, Acad).
Format. Electronic figures are recommended to be in CDR, Al, EPS, TIF or JPG formats. Resolution of bitmap graphics (TIF, JPG) should be at least 300 dpi. Text in vector graphics (CDR, Al, EPS) must be in MSWord Times typography or converted in curves.
Color prints. Authors will be charged for color prints of figures and photos.
Labeling of the additionally provided material for the manuscript should be very clear and must contain at least the lead author's name, address, the beginning of the title and the date of delivery of the manuscript. In case of an E-mail transfer the exact message with above asked data must accompany the attachment with the file containing the manuscript.

Information about RMZ-M&G:
Editor in Chief prof. dr. Peter Fajfar (phone: ++386 1 2000451) or
Secretary Barbara Bohar Bobnar, univ. dipl. ing. geol. (phone: ++386 1 4704-630),
Aškerčeva 12, 1000 Ljubljana, Slovenia
or at E-mail addresses:
peter.fajfar@omm.ntf.uni-lj.si,
barbara.bohar@geo.ntf.uni-lj.si

Sending of manuscripts. Manuscripts can be sent by mail to the **Editorial Office** address:

- RMZ-Materials & Geoenvironment
  Aškerčeva 12,
  1000 Ljubljana, Slovenia

or delivered to:

- **Reception** of the Faculty of Natural Science and Engineering (for RMZ-M&G)
  Aškerčeva 12,
  1000 Ljubljana, Slovenia
- E-mail - addresses of Editor and Secretary
- You can also contact them on their phone numbers.

These instructions are valid from August 2009

NAVODILA AVTORJEM

RMZ-MATERIALS AND GEOENVIRONMENT (RMZ- Materiali in geookolje) – kratica RMZ-M&G - je revija (ustanovljena kot zbornik 1952 in preimenovana v revijo RMZ-M&G 1998), ki izhaja vsako leto v štirih zvezkih. V reviji objavljamo prispevke s področja rudarstva, geotehnologije, materialov, metalurgije, geologije in geookolja.

RMZ- M&G objavlja izvirne znanstvene, pregledne in strokovne članke ter predhodne objave samo v angleškem jeziku. Strokovni članki so lahko izjemoma napisani v slovenskem jeziku. Kot dodatek so zaželene recenzije drugih publikacij (knjig, monografij …), nekrologi In Memoriam, predstavitve znanstvenih in strokovnih dogodkov, kratke objave in strokovne replike na članke objavljene v RMZ-M&G v slovenskem ali angleškem jeziku. Prispevki naj bodo kratki in jasni.

Avtorstvo in izvirnost prispevkov. Avtorji so odgovorni za izvirnost podatkov, idej in sklepov v predloženem prispevku oziroma za pravilno citiranje privzetih podatkov. Z objavo v RMZ-M&G se tudi obvežejo, da ne bodo nikjer drugje objavili enakega prispevka.

Vrste prispevkov

Optimalno število strani je 7 do 15, za daljše članke je potrebno soglasje glavnega urednika.
Izvirni znanstveni članki opisujejo še neobjavljene rezultate lastnih raziskav.
Pregledni članki povzemajo že objavljene znanstvene, raziskovalne ali strokovne dosežke na novem znanstvenem nivoju in lahko vsebujejo tudi druge (citirane) vire, ki niso večinsko rezultat dela avtorjev.
Predhodna objava povzema izsledke raziskave, ki je v teku in zahteva hitro objavo.
Strokovni članki vsebujejo rezultate tehnoloških dosežkov, razvojnih projektov in druge informacije iz prakse.
Recenzije publikacij zajemajo ocene novih knjig, monografij, učbenikov, razstav …(do dve strani; zaželena slika naslovnice in kratka navedba osnovnih podatkov - izkaznica).

In memoriam (do dve strani, zaželena slika).
Strokovne pripombe na objavljene članke ne smejo presegati ene strani in opozarjajo izključno na strokovne nedoslednosti objavljenih člankov v prejšnjih številkah RMZ-M&G. Praviloma že v isti številki avtorji prvotnega članka napišejo odgovor na pripombe.
Poljudni članki, ki povzemajo znanstvene in strokovne dogodke (do dve strani).

Recenzije. Vsi prispevki bodo predloženi v recenzijo. Recenzent oceni primernost prispevka za objavo in lahko predlaga kot pogoj za objavo dopolnilo k prispevku. Recenzenta izbere Uredništvo med strokovnjaki, ki so dejavni na sorodnih področjih, kot jih obravnava prispevek. Avtorji lahko sami predlagajo recenzenta, vendar si uredništvo pridržuje pravico, da izbere drugega recenzenta. **Recenzent ostane anonimen**. Prispevki bodo tudi tehnično ocenjeni in avtorji so dolžni popraviti pomanjkljivosti. Končno odločitev za objavo da glavni in odgovorni urednik.

Oblika prispevka

Prispevek predložite v tiskanem oštevilčenem izvodu (po možnosti z vključenimi slikami in tabelami) ter na disketi ali CD, lahko pa ga pošljete tudi prek E-maila. Slike in grafe je možno poslati tudi risane na papirju, fotografije naj bodo originalne.

Razčlenitev prispevka:

Predloga za pisanje članka se nahaja na spletni strani:

http://www.rmz-mg.com/predloga.htm

Seznam literature je lahko urejen na dva načina:
-po abecednem zaporedju prvih avtorjev ali
-po [1]vrstnem zaporedju citiranosti v prispevku.

Oblika je za oba načina enaka:
Članki:

> Le Borgne, E. (1955): Susceptibilite magnetic anomale du sol superficiel. *Annales de Geophysique*; Vol. 11, pp. 399–419.

Knjige:

ROBERTS, J. L. (1989): Geological structures, *MacMillan*, *London*, 250 p.

Tekst izpisanega izvoda je lahko pripravljen v kateremkoli urejevalniku. Na disketi, CD ali v elektronskem prenosu pa mora biti v MS Word ali v ASCII obliki.
Naslovi slik in tabel naj bodo priloženi posebej. Naslove slik, tabel in celotno besedilo, ki se pojavlja na slikah in tabelah, je potrebno navesti v angleškem in slovenskem jeziku.
Slike (ilustracije in fotografije) in tabele morajo biti izvirne in priložene posebej. Njihov položaj v besedilu mora biti jasen iz priloženega kompletnega izvoda. Narejene so lahko na papirju ali pa v računalniški obliki (MS Excel, Corel, Acad).
Format elektronskih slik naj bo v EPS, TIF ali JPG obliki z ločljivostjo okrog 300 dpi. Tekst v grafiki naj bo v Times tipografiji.
Barvne slike. Objavo barvnih slik sofinancirajo avtorji
Označenost poslanega materiala. Izpisan izvod, disketa ali CD morajo biti jasno označeni – vsaj z imenom prvega avtorja, začetkom naslova in datumom izročitve uredništvu RMZ-M&G. Elektronski prenos mora biti pospremljen z jasnim sporočilom in z enakimi podatki kot velja za ostale načine posredovanja.

Informacije o RMZ-M&G: urednik prof. dr. Peter Fajfar, univ. dipl. ing. metal. (tel. ++386 1 2000451) ali tajnica Barbara Bohar Bobnar, univ. dipl. ing. geol. (tel. ++386 1 4704630), Aškerčeva 12, 1000 Ljubljana
ali na E-mail naslovih:
peter.fajfar@omm.ntf.uni-lj.si
barbara.bohar@geo.ntf.uni-lj.si

Pošiljanje prispevkov. Prispevke pošljite priporočeno na naslov **Uredništva:**

- RMZ-Materials and Geoenvironment
  Aškerčeva 12,
  1000 Ljubljana, Slovenija

oziroma jih oddajte v

- **Recepciji** Naravoslovnotehniške fakultete (pritličje) (za RMZ-M&G)
  Aškerčeva 12,
  1000 Ljubljana, Slovenija
- Možna je tudi oddaja pri uredniku oziroma pri tajnici.

Navodila veljajo od avgusta 2009.

TEMPLATE

The title of the manuscript should be written in bold letters (Times New Roman, 14, Center)

Naslov članka (Times New Roman, 14, Center)

Name Surname[1], …. , & Name Surname[X] (Times New Roman, 12, Center)

[x] University of ..., Faculty of ..., Address…, Country ... (Times New Roman, 11, Center)

*Corresponding author. E-mail: ... (Times New Roman, 11, Center)

Abstract (Times New Roman, Normal, 11): The abstract should be concise and should present the aim of the work, essential results and conclusion. It should be typed in font size 11, single-spaced. Except for the first line, the text should be indented from the left margin by 10 mm. The length should not exceed fifteen (15) lines (10 are recommended).

Izvleček (Times New Roman, navadno, 11): Kratek izvleček namena članka ter ključnih rezultatov in ugotovitev. Razen prve vrstice naj bo tekst zamaknjen z levega roba za 10 mm. Dolžina naj ne presega petnajst (15) vrstic (10 je priporočeno).

Key words: a list of up to 5 key words (3 to 5) that will be useful for indexing or searching. Use the same styling as for abstract.
Ključne besede: seznam največ 5 ključnih besed (3–5) za pomoč pri indeksiranju ali iskanju. Uporabite enako obliko kot za izvleček.

Introduction (Times New Roman, Bold, 12)

Two lines below the keywords begin the introduction. Use Times New Roman, font size 12, Justify alignment.

There are two (2) admissible methods of citing references in text:

1. by stating the first author and the year of publication of the reference in the parenthesis at the appropriate place in the text and arranging the reference list in the alphabetic order of first authors; e.g.:
   "Detailed information about geohistorical development of this zone can be found in: Antonijević (1957), Grubić (1962), ..."
   "… the method was described previously (Hoefs, 1996)"
2. by consecutive Arabic numerals in square brackets, superscripted at the appropriate place in the text and arranging the reference list at the end of the text in the like manner; e.g.:
   "... while the portal was made in Zope environment. [3]"

Materials and methods (Times New Roman, Bold, 12)

This section describes the available data and procedure of work and therefore provides enough information to allow the interpretation of the results, obtained by the used methods.

Results and discussion (Times New Roman, Bold, 12)

Tables, figures, pictures, and schemes should be incorporated in the text at the appropriate place and should fit on one page. Break larger schemes and tables into smaller parts to prevent extending over more than one page.

Conclusions (Times New Roman, Bold, 12)

This paragraph summarizes the results and draws conclusions.

Acknowledgements (Times New Roman, Bold, 12, Center - optional)

This work was supported by the ****.

References (Times New Roman, Bold, 12)

In regard to the method used in the text, the styling, punctuation and capitalization should conform to the following:

FIRST OPTION - in alphabetical order

Casati, P., Jadoul, F., Nicora, A., Marinelli, M., Fantini-Sestini, N. & Fois, E. (1981): Geologia della Valle del'Anisici e dei gruppi M. Popera - Tre Cime di Lavaredo (Dolomiti Orientali). *Riv. Ital. Paleont.*; Vol. 87, No. 3, pp. 391–400, Milano.

Folk, R. L. (1959): Practical petrographic classification of limestones. *Amer. Ass. Petrol. Geol. Bull.;* Vol. 43, No. 1, pp. 1–38, Tulsa.

SECOND OPTION - in numerical order

[1] Trček, B. (2001): *Solute transport monitoring in the unsaturated zone of the karst aquifer by natural tracers.* Ph. D. Thesis. Ljubljana: University of Ljubljana 2001; 125 p.

[2] Higashitani, K., Iseri, H., Okuhara, K., Hatade, S. (1995): Magnetic Effects on Zeta Potential and Diffusivity of Nonmagnetic Particles. *Journal of Colloid and Interface Science, 172*, pp. 383–388.

Citing the Internet site:

CASREACT-Chemical reactions database [online]. Chemical Abstracts Service, 2000, updated 2. 2. 2000 [cited 3. 2. 2000]. Accessible on Internet: http://www.cas.org/CASFILES/casreact.html.

Texts in Slovene (title, abstract and key words) can be written by the author(s) or will be provided by the referee or by the Editorial Board.

PREDLOGA ZA SLOVENSKE ČLANKE

Naslov članka (Times New Roman, 14, Na sredino)

The title of the manuscript should be written in bold letters (Times New Roman, 14, Center)

Ime Priimek[1], …, Ime Priimek[X] (Times New Roman, 12, Na sredino)

[X]Univerza…, Fakulteta…, Naslov…, Država… (Times New Roman, 11, Center)

*Korespondenčni avtor. E-mail: ... (Times New Roman, 11, Center)

Izvleček (Times New Roman, Navadno, 11): Kratek izvleček namena članka ter ključnih rezultatov in ugotovitev. Razen prve j bo tekst zamaknjen z levega roba za 10 mm. Dolžina naj ne presega petnajst (15) vrstic (10 je priporočeno).

Abstract (Times New Roman, Normal, 11): The abstract should be concise and should present the aim of the work, essential results and conclusion. It should be typed in font size 11, single-spaced. Except for the first line, the text should be indented from the left margin by 10 mm. The length should not exceed fifteen (15) lines (10 are recommended).

Ključne besede: seznam največ 5 ključnih besed (3–5) za pomoč pri indeksiranju ali iskanju. Uporabite enako obliko kot za izvleček.
Key words: a list of up to 5 key words (3 to 5) that will be useful for indexing or searching. Use the same styling as for abstract.

Uvod (Times New Roman, Krepko, 12)

Dve vrstici pod ključnimi besedami se začne Uvod. Uporabite pisavo Times New Roman, velikost črk 12, z obojestransko poravnavo. Naslovi slik in tabel (vključno z besedilom v slikah) morajo biti v slovenskem jeziku.

Slika (Tabela) X. Pripadajoče besedilo k sliki (tabeli)

Obstajata dve sprejemljivi metodi navajanja referenc:

1. z navedbo prvega avtorja in letnice objave reference v oklepaju na ustreznem mestu v tekstu in z ureditvijo seznama referenc po abecednem zaporedju prvih avtorjev; npr.:

"Detailed information about geohistorical development of this zone can be found in: Antonijević (1957), Grubić (1962), ..."

"… the method was described previously (Hoefs, 1996)"

ali

2. z zaporednimi arabskimi številkami v oglatih oklepajih na ustreznem mestu v tekstu in z ureditvijo seznama referenc v številčnem zaporedju navajanja; npr.;

"... while the portal was made in Zope[3] environment."

Materiali in metode (Times New Roman, Krepko, 12)

Ta del opisuje razpoložljive podatke, metode in način dela ter omogoča zadostno količino informacij, da lahko z opisanimi metodami delo ponovimo.

Rezultati in razprava (Times New Roman, Krepko, 12)

Tabele, sheme in slike je treba vnesti (z ukazom Insert, ne Paste) v tekst na ustreznem mestu. Večje sheme in tabele je po treba ločiti na manjše dele, da ne presegajo ene strani.

Sklepi (Times New Roman, Krepko, 12)

Povzetek rezultatov in sklepi.

Zahvale (Times New Roman, Krepko, 12, Na sredino - opcija)

Izvedbo tega dela je omogočilo ……

Viri (Times New Roman, Krepko, 12)

Glede na uporabljeno metodo citiranja referenc v tekstu upoštevajte eno od naslednjih oblik:

PRVA MOŽNOST (priporočena) - v abecednem zaporedju

Casati, P., Jadoul, F., Nicora, A., Marinelli, M., Fantini-Sestini, N. & Fois, E. (1981): Geologia della Valle del'Anisici e dei gruppi M. Popera – Tre Cime di Lavaredo (Dolomiti Orientali). *Riv. Ital. Paleont.*; Vol. 87, No. 3, pp. 391–400, Milano.

Folk, R. L. (1959): Practical petrographic classification of limestones. *Amer. Ass. Petrol. Geol. Bull.;* Vol. 43, No. 1, pp. 1–38, Tulsa.

DRUGA MOŽNOST - v numeričnem zaporedju

[1] Trček, B. (2001): *Solute transport monitoring in the unsaturated zone of the karst aquifer by natural tracers.* Ph. D. Thesis. Ljubljana: University of Ljubljana 2001; 125 p.

[2] Higashitani, K., Iseri, H., Okuhara, K., Hatade, S. (1995): Magnetic Effects on Zeta Potential and Diffusivity of Nonmagnetic Particles. *Journal of Colloid and Interface Science, 172*, pp. 383–388.

Citiranje spletne strani:

CASREACT-Chemical reactions database [online]. Chemical Abstracts Service, 2000, obnovljeno 2. 2. 2000 [citirano 3. 2. 2000]. Dostopno na svetovnem spletu: http://www.cas.org/CASFILES/casreact.html.

Znanstveni, pregledni in strokovni članki ter predhodne objave se objavijo v angleškem jeziku. Izjemoma se strokovni članek objavi v slovenskem jeziku.

Skupina GEN

PREMOGOVNIK VELENJE

PREMOGOVNIK VELENJE

je pomemben in zanesljiv člen
v oskrbi Slovenije
z električno energijo.

Zavedamo se odgovornosti do
lastnikov, zaposlenih in okolja.

ČUT ZA PRIHODNOST

Slovenčeva 93
SI 1000 Ljubljana

tel.: +386 (1) 560 36 00
fax: +386 (1) 534 16 80
www.irgo.si

IRGO

Inženirska geologija
Hidrogeologija
Geomehanika
Projektiranje
Tehnologije za okolje
Svetovanje in nadzor